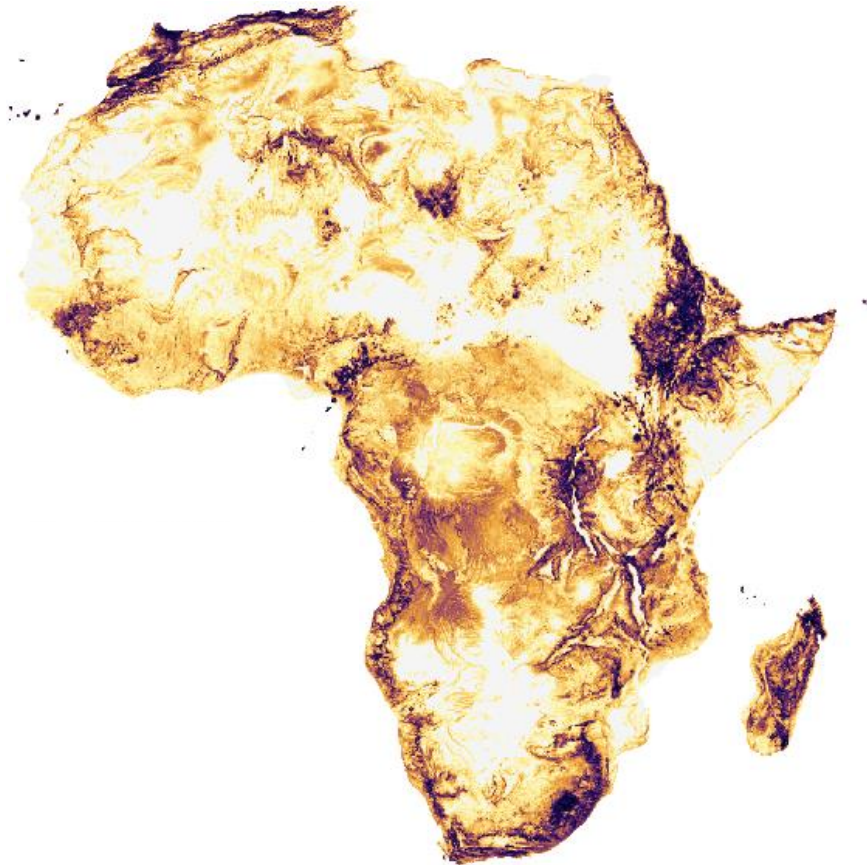


Chair of hydrology
University of Freiburg

Carolin Winter

Africa's groundwater resources

The impact of regolith hydraulic properties on large-scale
groundwater modelling for Africa



Master thesis under the supervision of Asst. Prof. Dr. Inge E.M. de Graaf

Freiburg i. Br., August 2018

Chair of hydrology
University of Freiburg

Carolin Winter

Africa's groundwater resources

The impact of regolith hydraulic properties on large-scale
groundwater modelling for Africa

1. Supervisor Asst. Prof. Inge E. M. de Graaf
2. Supervisor JProf. Dr. Andreas Hartmann

Master thesis under the supervision of Asst. Prof. Dr. Inge E.M. de Graaf

Freiburg i. Br., August 2018

Acknowledgements

My cordial thanks goes to Inge de Graaf for having me as her first Master student and for her close support during all steps of this work. I acknowledge the funding through the German Academic Exchange Service (DAAD), especially for supporting the exchange with hydrogeology experts from the IGE Grenoble (France) that contributed to this work with their excellent field knowledge on groundwater and regolith in western sub-Saharan Africa. In this context, I especially want to thank Basile Hector and Amelie Herzog for sharing their knowledge and for further support. Last but not least, I want to thank Florian Schnabel and Birgit Müller for correction reading and especially Florian Schnabel for constructive criticism and for mental support at all stages of this work.

Table of contents

Abstract.....	1
Zusammenfassung	2
1 Introduction.....	5
1.1 The role of groundwater	5
1.2 Large-scale groundwater estimates	6
1.3 Crystalline basement aquifers and regolith	8
1.4 Problem stating, research questions and hypothesis	10
2 Pre-analysis - Global datasets for aquifer parametrization	13
2.1 Global datasets of aquifer thickness	13
2.2 Global dataset of aquifer permeability	16
2.3 Best available datasets for aquifer parametrization	18
3 Methods	21
3.1 Regolith permeability and thickness in Africa – A literature review	21
3.2 Groundwater modelling	21
3.3 Model setup and parametrization.....	22
3.3.1 Aquifer thickness and parametrization of regolith	22
3.3.2 Permeability	25
3.3.3 Boundary conditions	26
3.3.4 Recharge	28
3.4 Sensitivity analysis.....	28
3.5 Validation	29
3.6 Software and programming language.....	30
4 Results	31
4.1 Regolith permeability and thickness in Africa – A literature review	31
4.2 Model parametrization – Regolith layer	32
4.3 Sensitivity Analysis	34
4.4 Validation of simulated groundwater heads.....	35
4.5 Simulated groundwater depth and ground- and surface water interactions	39

5 Discussion	43
5.1 The global groundwater model PCR-GLOBWB-MODFLOW	43
5.2 Aquifer parametrization	43
5.2.1 Regolith layer.....	45
5.3 Impact of regolith parametrization on simulated groundwater depth.....	46
5.3.1 Sensitivity	46
5.3.2 Validation	47
5.3.3 Simulated groundwater depth	50
5.4 Simulated groundwater drainage and river infiltration	51
6 Conclusion and Outlook	53
References.....	55
Appendix	59
Supplement to chapter 3.....	59
References - Regolith permeability and thickness in Africa	61
Supplement to chapter 4.....	64
List of abbreviations	65
Ehrenwörtliche Erklärung.....	69

List of figures

Fig. 1: Global map of the proportion of population per country with at least basic drinking water service in 2015, derived from the WHO and UNICEF (2017).	6
Fig. 2: The distribution of Precambrian crystalline bedrock in Africa; data derived from the United States Geological Survey (USGS, 2000).	8
Fig. 3: Structure, relative permeability and relative porosity of a stereotype regolith overlying crystalline bedrock, adapted from Chilton and Foster (1995).	9
Fig. 4: Overview of the most up to date global datasets of aquifer thickness, selected for Africa and for a regional example in western sub-Saharan Africa.	14
Fig. 5: The spatial and relative distribution of permeability estimates ($\log(k)$ in m^2) for Africa, taken from (a) GLHYMPS (Gleeson et al. 2014) and (b) GLHYMPS 2.0 (Huscroft et al. 2018).	18
Fig. 6: Schematic construction of the grid-based global hydrological model PCR-GLOBWB-MODFLOW with two horizontal layers implemented in MODFLOW.	22
Fig. 7: Digital elevation model (DEM) of Africa derived from HydroSHEDS.	23
Fig. 8: Schematic construction of aquifer layers (not true to scale) with different scenarios for the regolith layer with (a) the topography scenario (b) the average scenario, both developed in this study and (c) the permanent water table (PWT) scenario developed by Pelletier et al. (2016).	24
Fig. 9: Long-term average naturalized river discharge (Q_{av}), obtained from PCR-GLOBWB, used to calculate the channel dimensions that were passed on to MODFLOW.	26
Fig. 10: Average daily groundwater recharge, calculated from PCR-GLOBWB, used to calculate input groundwater recharge that was passed on to MODFLOW.	28
Fig. 11: Observed groundwater depth data from Fan et al. (2013) used for the model validation.	30
Fig. 12: Number of studies per African country that were found during the literature review.	31
Fig. 13: Summarized regolith permeability and thickness values from the literature review for (a) all lower range, average and upper range values and (b) the total of all values.	32
Fig. 14: Thickness of the two layers for the aquifer parametrization, with (a) the sediment/crystalline layer representing extensive deeper aquifer and crystalline basement underlying regolith and (b) the upper regolith layer, representing local regolith over crystalline basement, exemplified for the topography scenario with average thickness.	32
Fig. 15: Relative thickness distribution for the regolith layer that was calculated according to the topography scenario with minimum (D_{min}), average (D_{mean}) and maximum thickness (D_{max}). ...	33
Fig. 16: Transmissivity over Africa where (a) includes a regolith layer that was calculated according to the topography scenario with average permeability and thickness from literature (<i>Topography-$D_{mean}-\log(k)_{mean}$</i>), and where (b) was simulated without a regolith layer (<i>No-Regolith</i>).	34

Fig. 17: Spatial distribution of the simulated groundwater depth sensitivity if (a) varying regolith transmissivity or (b) the regolith scenario (topography, average and permanent water table scenario). Sensitivity is expressed by the coefficient of variation (CV).	35
Fig. 18: De- and increase of groundwater depth (m) simulated with a regolith layer, compared to the simulation without a regolith layer (<i>No-Regolith</i>).	36
Fig. 19: Observed groundwater table heads against simulated ones from the most promising model run (<i>Average-D_{min}-log(k)$_{min}$</i>), separated into regions covered by a regolith layer and regions without regolith coverage.....	38
Fig. 20: Digital elevation map (DEM) of Africa with residuals (observed (ho) - simulated heads (hs)) for the groundwater head simulation according to the most promising model run (<i>Average-D_{min}-log(k)$_{min}$</i>). Subfigures (a-c) are close-up maps of the regions with the highest frequencies of observation data points.	38
Fig. 21: Residuals (observed (ho) - simulated heads (hs)) for Africa, with (a) the relative distribution of residuals and (b) the residuals in dependency to observed groundwater depth, colored for their specific origin, which is marked in the Africa map at the top right corner (c).	39
Fig. 22: Depth to groundwater in meters below the ground level (mbgl), simulated with the most promising regolith layer from this study (<i>Average-D_{min}-log(k)$_{min}$</i>) included into the aquifer parametrization.....	40
Fig. 23: Histogram of simulated depth to groundwater for the model runs with the most promising regolith layer (<i>Average-D_{min}-log(k)$_{min}$</i>) and the one without a regolith layer (<i>No-Regolith</i>).....	40
Fig. 24: Simulated groundwater drainage (Qb negative) or river infiltration (Qb positive), with (a) the simulation integrating the most promising regolith layer (<i>Average-D_{min}-log(k)$_{min}$</i>) and (b) the simulation without a regolith layer (<i>No-Regolith</i>).	41
Fig. 25: Histogram of depth to groundwater for the model run that was simulated with the most promising regolith layer (<i>Average-D_{min}-log(k)$_{min}$</i>) and the one without a regolith layer (<i>No-Regolith</i>).	41
Fig. 26: Quantitative groundwater maps (a) of the aquifer saturated thickness from Bonsor and MacDonald et al. (2011) and (b) of the estimated depth to groundwater in meters below the ground level (mbgl) from MacDonald et al. (2012) (maps derived from the British geological survey © NERC 2011).	44
Fig. 27: Maps and histograms of estimated depth to groundwater from (a) this study, (b) the study from de Graaf et al. (2017), (c) the study from Fan et al. (2013) and the study from MacDonald et al. (2012).	51

List of tables

Tab. 1: Average, minimum and maximum aquifer thickness (m) compiled for the three most up to date datasets on aquifer thickness for Africa and a regional example in western sub-Saharan Africa.	15
Tab. 2: Geometric mean of aquifer permeability ($\log(k)$ in m^2) for all hydrolithological classes and subclasses taken from Gleeson et al. (2014), Börker et al. (2018) and Huscroft et al. (2018). ..	17
Tab. 3: All constellations of regolith parametrizations that were run in an extensive sensitivity analysis, varying either the regolith scenario, its thickness (D) or its permeability ($\log(k)$).	29
Tab. 4: Average regolith layer thickness with standard deviation and the absolute minimum and maximum regolith layer thickness of the topography scenario, calculated with average (D_{mean}), minimum (D_{min}) and maximum thickness (D_{mean}) from literature.	33
Tab. 5: Coefficient of determination (R^2) for the model validation of all regolith layer variations included into the simulation of groundwater heads for Africa.	37

List of figures in Appendix

Fig. S 1: Matrix of weights, created for the purpose of this study to smooth aquifer thickness.	64
Fig. S 2: Transmissivity over Africa simulated with an additional regolith layer that was calculated according to (a) the average scenario with average transmissivity from literature (<i>Average-$D_{mean}-\log(k)_{mean}$</i>) and (b) the permanent water table scenario with average permeability from literature (<i>PWT-$\log(k)_{mean}$</i>).	64
Fig. S 3: Proportion of regolith that was simulated to hold groundwater and of regolith where groundwater was simulated below the regolith layer.	65

List of tables in Appendix

Tab. S 1: Confidence levels and their respective criteria, assigned to studies of regolith thickness and permeability in Africa	59
Tab. S 2: Database of regolith thickness and permeability in Africa including the source of data, the respective confidence level, the country where the study was conducted, methods used and sample size.	59
Tab. S 3: Average transmissivity (T) over Africa for all tested regolith layers alone, combined with the underlying sediment/crystalline layer and the relative increase through the integration of the respective Regolith layer.	64

Abstract

Groundwater is estimated to be by far the largest freshwater resource of Africa, buffering climate extremes and supplying a vital resource for the local population and environmental cycles. However, increasing droughts and abstractions due to a rapidly growing population threaten this vital resource. A continent-wide assessment of Africa's groundwater resources is, therefore, needed to estimate their potential for sustainable usage. In this context, large-scale groundwater models hold the opportunity to extrapolate their simulations over data scarce regions, such as Africa. Differences between global datasets of aquifer parameters, however, are huge and a detailed comparison on their suitability to represent Africa's aquifers is missing. In sub-Saharan Africa, where the population is among the poorest of the world and heavily dependent on groundwater, low productive crystalline basement aquifers are ubiquitous. In these regions, most groundwater occurs in an overlying weathering mantle – the regolith. Regolith, however, is typically neglected in global datasets or related to high uncertainties, which is assumed to lead to high model inaccuracies if simulating Africa's groundwater resources.

Therefore, in this study, global datasets of aquifer thickness and permeability were compared to select the best available parameters that represent aquifer characteristics apart from regolith. To represent regolith, a literature review on regolith thickness and permeability in Africa was conducted and the resulting estimates were used to parametrize three different regolith layer scenarios. With these regolith scenarios and parameters, the global groundwater model PCR-GLOBWB-MODFLOW was run (steady state, 5' resolution, natural conditions) in an extensive sensitivity analysis to assess the impact of regolith on groundwater modelling. Finally, simulated groundwater heads were validated against a set of observed heads.

The most reliable representation of aquifers, apart from regolith, was a topography-based algorithm that estimated the thickest aquifers at valley bottoms, based on estimates of aquifer thickness for Africa. The most promising regolith representation was the scenario with a constant average thickness of approximately 10 m and a log permeability of -13.1 m², which were the lower bound estimates from literature. However, the sensitivity of simulated groundwater depth to the regolith parametrization was small with a coefficient of variation <0.15. Highest sensitivity was found at deeper groundwater tables. All simulated groundwater heads compared well to observed ones (R² 0.919 – 0.930) but model runs with a regolith layer showed only a slightly better performance than without regolith. Importantly, simulated ground- and surface water interactions occurred at shallow water tables, which have a higher relevance for humans and environmental cycles than deeper ones. However, due to a lack of validation data these interactions could not be validated.

This study provides a first overview on the impact of regolith hydraulic properties on groundwater modelling in Africa. Based on the presented results, complex approaches for regolith compilation are not significantly better than simplistic approaches like a constant average and might, therefore, be overrated. Finally, regolith could not be confirmed as a major driving source for large-scale model uncertainties, but its influence on ground- and surface waters might be significant and should be further investigated.

Key words: groundwater, Africa, regolith, crystalline bedrock, large-scale modelling, PCR-GLOBWB-MODFLOW, aquifer parametrization

Zusammenfassung

Grundwasser ist nach Schätzungen die mit Abstand größte Süßwasserressource Afrikas. Es bildet einen natürlichen Schutz gegen Klimaextreme und ist Lebensgrundlage für einen Großteil der lokalen Bevölkerung sowie der Tier- und Pflanzenwelt. Zunehmende Dürren und Grundwasserentnahmen einer schnell-wachsenden Bevölkerung gefährden jedoch diese lebenserhaltende Ressource. Eine kontinentweite Abschätzung von Afrikas Grundwasserressourcen ist daher unabdingbar um deren nachhaltige Nutzung zu gewährleisten. Großskalige Grundwasser-Modelle sind dafür besonders geeignet, da sie Ergebnisse über Regionen mit spärlicher Informationsdichte (wie z.B. Afrika) extrapolieren können. Globale Datensätze zur Parametrisierung von Aquiferen weisen jedoch große Unterschiede auf und wurden, bis heute, nicht auf ihre Tauglichkeit hinsichtlich afrikanischer Aquifere verglichen. In Subsahara Afrika, wo die Bevölkerung zu den ärmsten der Welt zählt und stark vom Grundwasser abhängt, sind gering produktive kristalline Festgesteins-Aquifere weit verbreitet. In diesen Regionen halten aufliegende Verwitterungsdecken, sogenannter Regolith, einen Großteil des Grundwassers. Regolith wird jedoch in den meisten globalen Datensätzen nicht berücksichtigt oder ist mit großen Unsicherheiten behaftet, was als wesentlicher Grund für Modellungenauigkeiten angenommen wird.

In dieser Studie wurden daher Datensätze globaler Aquifermächtigkeiten und Permeabilitäten verglichen, um die repräsentativsten Aquiferparameter, abgesehen von Regolith, für Afrika zu bestimmen. Für Regolith wurde zusätzlich Literatur nach Afrika-spezifischen Regolithmächtigkeiten und Permeabilitäten durchsucht, die anschließend verwendet wurden, um drei verschiedene Regolith Szenarien zu parametrisieren. Mit diesen Szenarien und Parametern wurde das Grundwasser-Modell PCR-GLOBWB-MODFLOW in einer umfangreichen Sensitivitätsanalyse angewendet (stationärer Zustand, 5'Auflösung, natürliche Bedingungen), um den Einfluss von Regolith auf die Modellierung von Grundwasser zu testen. Abschließend wurden modellierte und gemessene Grundwasserspiegelhöhen miteinander verglichen, um die Ergebnisse zu validieren.

Die repräsentativste Parametrisierung von Aquiferen, Regolith ausgenommen, war ein Topographie-basierter Algorithmus mit maximalen Aquifermächtigkeiten unter Talböden, basierend auf Afrika-spezifischen Aquifermächtigkeiten. Die vielversprechendste Darstellung von Regolith ergab sich aus dem Szenario einer konstanten mittleren Mächtigkeit von ungefähr 10 m und einer logarithmischen Permeabilität von -13.1 m^2 , entsprechend der niedrigsten Werte aus der Literatur. Die Sensitivität modellierter Grundwasserstände auf die Parametrisierung von Regolith war mit einem Variationskoeffizienten von >0.15 gering. Der stärkste Einfluss wurde an tiefen Grundwasserständen gefunden. Insgesamt, stimmten alle modellierten Grundwasserspiegelhöhen gut mit den beobachteten überein ($R^2 \text{ } 0.919 - 0.930$), jedoch konnte nur eine leichte Verbesserung durch die Integration von Regolith verzeichnet werden. Im Gegensatz dazu waren die modellierten Grund- und Oberflächenwasser Interaktionen von höherer Relevanz, da hier Veränderungen speziell an oberflächennahen Grundwasser verzeichnet wurden, welches einen deutlich größeren Einfluss auf Mensch und Umwelt hat als tiefes Grundwasser. Aufgrund mangelnder Validierungsdaten konnten diese Interaktionen jedoch nicht bestätigt werden.

Zusammenfassend bietet diese Studie einen ersten Überblick über den Einfluss von Regolith und seinen hydraulischen Eigenschaften auf die Modellierung von Grundwasser in Afrika. Auf Grundlage der hier präsentierten Resultate sind komplexe Modell-Ansätze für die Integration von Regolith nicht eindeutig besser als einfache Ansätze wie ein konstanter Mittelwert. Diese komplexen Ansätze sind daher wohlmöglich überbewertet. Weiterhin konnte Regolith nicht als Hauptfaktor für großskalige

Modellungenauigkeiten bestätigt werden. Einflüsse von Regolith auf die Interaktion von Grund- und Oberflächenwasser könnten jedoch signifikant sein und sollten weitergehend untersucht werden.

Stichwörter: Grundwasser, Afrika, Regolith, kristallines Festgestein, großskalige Modellierung, PCR-GLOBWB-MODFLOW, Aquiferparametrisierung

1 Introduction

1.1 The role of groundwater

Groundwater plays a crucial role in the global hydrologic cycle and is estimated to be the second greatest source of fresh water on earth after snow and ice (Gleick, 2003). It is a life-sustaining resource for billions of people in form of drinking and irrigation water (Oki and Kanae, 2006).

In arid regions, groundwater is often the only reliable freshwater resource. It can buffer the impacts of climate extremes, such as droughts, which are predicted to increase substantially due to climate change in some regions of the world (Dai, 2013; IPCC, 2014). As groundwater is naturally protected against pathogenic contamination, it also likely remains the only reliable freshwater resource, if surface water is contaminated due to a lack of wastewater treatment. Except for some local geogenic contaminations such as elevated arsenic or fluoride concentrations, groundwater, moreover, is generally of good quality, which substantially reduces treatment costs in comparison to surface water (MacDonald and Davies, 2000). Finally, shallow groundwater is vital for environmental cycles, sustaining the base flow of rivers and lakes, wetlands and, if located within the rooting zone, providing vital water storage for the vegetation, especially during droughts (Fan et al., 2013; Giordano, 2009; Miguez-Macho and Fan, 2012).

In Africa, groundwater is estimated to be by far the largest freshwater resource (MacDonald et al., 2012). However, groundwater resources are distributed highly unevenly within the continent. While the greatest groundwater volumes are found in the sandstone aquifers of the sparsely populated Saharan desert, wide regions of the more densely populated sub-Saharan Africa are covered by low productive crystalline basement aquifers (Chilton and Foster, 1995). In the Sahara, although groundwater storage can reach up to $75 \text{ mio m}^3 \text{ km}^{-2}$ (MacDonald et al., 2012), most groundwater is not actively recharged, as the water originates from wetter periods in the late Pleistocene and the Holocene (Thornton, 1948). Its abstraction is, therefore, not sustainable in the present. Furthermore, groundwater tables are mainly located deeper than 100 m underneath the land surface, which significantly increases the drilling costs for groundwater abstraction (MacDonald et al., 2012). In contrary, the groundwater resources of sub-Saharan Africa are presently recharged and the vast majority of water tables depth is shallower than 50 m (MacDonald et al., 2012). However, it is sub-Saharan Africa, where the save access to drinking water is not assured for around 40% of the population, one of the greatest percentages worldwide. This can be attributed to the fact that a large share of the population is amongst the poorest and most vulnerable of the world (Fig. 1, World Health Organization and UNICEF, 2017).

The greatest part of sub-Saharan Africa is covered by crystalline basement aquifers, with more than 220 million people of Africa's rural population living upon and depending on their low well yield, which is generally sufficient for domestic supplies and livestock watering (MacDonald and Davies, 2000; Wright, 1992). On the one hand, water supplying infrastructure in these rural areas is often poorly developed, thus providing an opportunity for further, but careful, development of groundwater abstraction aimed at extensive use which could substantially contribute to poverty alleviation (e.g. Vörösmarty et al., 2005; Burney and Naylor, 2012; Pavelic et al., 2013). On the other hand, both the rapidly increasing demand for urban water supply and the growing interest in groundwater use for more intense agricultural irrigation are threatening this vital resource (Foster et al., 2012). Climate change further intensifies these problems, being projected to cause higher frequencies as well as expansions of droughts and consequently increased water stress and reduced yields from rain-fed agriculture (IPCC, 2014, 2007).

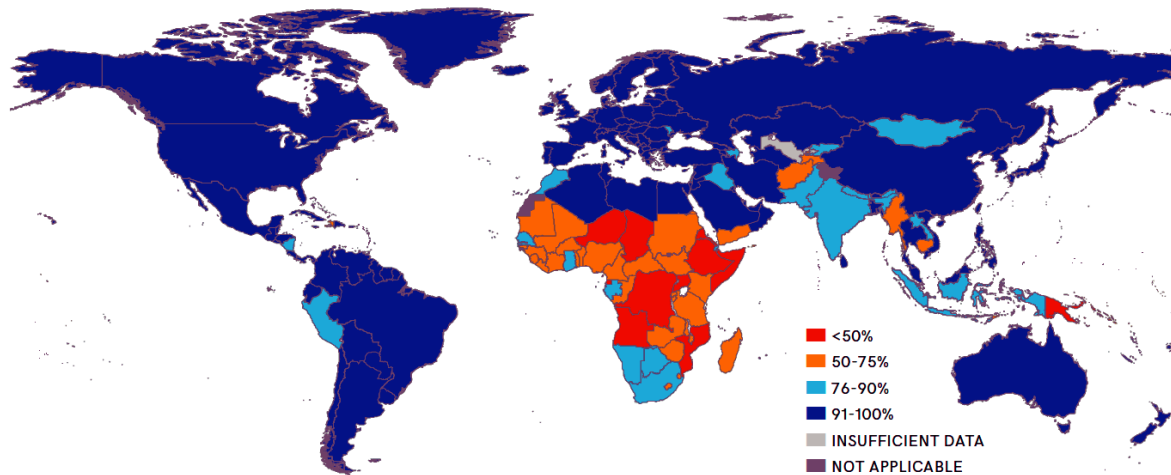


Fig. 1: Global map of the proportion of population per country with at least basic drinking water service in 2015, derived from the WHO and UNICEF (2017).

Finding a balance between satisfying the water demand of a growing population, increasing living standards and buffering climate change impacts on the one hand and avoiding overexploitation, water stress and associated environmental impacts on the other hand, is a highly challenging task. It is, however, an indispensable task, which should be addressed on a local, regional as well as on a continental scale. Focusing on the continental scale, I aim to contribute towards an assessment of the potential of Africa's groundwater resources, which in a further step could enable the development of sustainable management strategies that maintain the described balance.

1.2 Large-scale groundwater estimates

The first assessment of Africa's groundwater resources on a continental scale was done by MacDonald et al. (2012), who developed the first quantitative maps of groundwater in Africa. In this context, three principal maps of (1) groundwater depth, (2) groundwater storage and (3) and aquifer productivity (as a proxy for aquifer transmissivity) were compiled, based on available literature and expert knowledge over Africa. These maps provide an overview on the unequal distribution of groundwater resources over the continent and allow for a first, but rough, estimate of total groundwater volumes available on the continent. They give, therefore, a good and reliable estimate for the spatial patterns of aquifer characteristics in Africa at the current state. Still, the groundwater maps are relatively coarse, as they only differentiate between six quantitative classes of respective groundwater depth, storage or productivity. Furthermore, without an underlying model approach, no scenario analyze on growing demand and/or climate variability is possible, as it would be with process-based models.

Besides the quantitative maps of MacDonald et al. (2012), continent-wide data on aquifer properties is still scarce, especially in Africa. Therefore, it remains challenging to assess its groundwater resources at a high resolution or predict possible changes in the water availability through human induced abstraction or climate change. Still, global high- or hyper- (0.1-1 km (Bierkens et al., 2015)) resolution models provide the opportunity to extrapolate hydrogeological information over data scarce regions on the base of general processes that are derived from continents that are more intensively covered by data, such as Europe and the U.S. (e.g. de Graaf et al., 2017; Pelletier et al., 2016; Huscroft et al., 2018). With this approach, Africa's aquifers and groundwater resources can be estimated on a broad scale, but an adaption of global hydraulic parameters towards Africa specific ones, is believed to significantly improve the assessment of Africa's groundwater resources. Therefore, combining both, the knowledge from literature and experts compiled in maps from MacDonald et al. (2012) with large-scale

groundwater modelling that enables to upscale resolution and integrate different scenarios is a very promising approach to access Africa's groundwater resources most accurately.

The first global groundwater modelling approach on a hyper resolution (30'', ~1×1 km at the equator) was developed by Fan et al. (2013), who simulated groundwater table depths globally, focusing especially on shallow groundwater. Although a pioneer work in groundwater modelling, this approach is limited to water tables in unconfined aquifers only and hydrogeological parameters such as the aquifer hydraulic conductivity and thickness were not integrated. Instead, soil porosity was used, and thickness was estimated by soil-porosity declining with depth, which leads to an underestimation of deeper groundwater tables. Also, according to the modelling approach, groundwater can only drain when it rises above the surface elevation, which does not represent real-world ground- and surface water interactions. These interactions however, are an important control on groundwater levels, especially in humid regions (de Graaf et al., 2015). Neglecting groundwater drainage into rivers that occur below the surface elevation of a grid cell, consequently leads to an overestimation of shallow groundwater tables. Furthermore, as the simulation is applied on steady state, it is not suitable for the simulation of storage changes under climate change or abstraction scenarios.

To address these shortcomings, de Graaf et al. (2015) coupled the global hydrological model PCR-GLOBWB (van Beek and Bierkens, 2009) to the hydrogeological model MODFLOW (Harbaugh et al., 2000), which enables to parametrize aquifers based on hydrogeological information. Accordingly, the aquifer parametrization from de Graaf et al. (2015) is based on global lithological maps (Hartmann and Moosdorf, 2012), a therefrom developed database of global permeability (Gleeson et al., 2014) and a further estimate on global aquifer thickness based on topography, assuming productive aquifers to occur in sedimentary deposits underneath valley bottoms. Besides the aquifer thickness estimate from de Graaf et al. (2017, 2015), there are other global estimates that represent possible alternatives to the current aquifer parametrization (Pelletier et al., 2016; Shangguan et al., 2017). However, a detailed comparison regarding their suitability for the parametrization of aquifers for groundwater models is missing, both globally and for Africa.

Besides the hydrogeological parametrization of aquifers, the interactions of ground- and surface water in form of groundwater drainage and river infiltration can be simulated via MODFLOW following a groundwater head gradient. Consequently, in the approach from de Graaf et al. (2015) groundwater can drain from below the surface elevation of a grid cell (depending on the respective drainage level), which leads to more realistic estimates on shallow groundwater than the ones from Fan et al. (2013). These interactions of ground- and surface water play an important role for transient simulations, especially when simulating abstractions and environmental impacts on groundwater sustaining river baseflow and wetlands. A further advantage is the simulation of lateral flow between cells, which becomes especially important at higher resolutions and when modelling large abstractions with their drawdown expanding over neighboring cells. In the further process, de Graaf et al. (2017) added a confined layer to the aquifer parametrization and modelled global groundwater table heads transiently, which enables to simulate scenarios of global groundwater depletion. Due to these improvements, model results were very promising when validated with groundwater head data from Europe and the U.S., especially for sedimentary basins (coefficient of determination (R^2): 0.98). In conclusion, the global hydrological model PCR-GLOBWB-MODFLOW is believed to be currently the best option if simulating groundwater depth and ground- and surface water interactions for Africa.

However, it is unclear which global aquifer estimates are the most suitable for groundwater modelling over Africa and how they might be adapted towards more Africa specific ones. Especially the occurrence of deeply weathered crystalline basement aquifers and their hydraulic properties are not explicitly

included into the models parametrization yet, due to a lack of global datasets containing information about their weathered overburden (Gleeson et al., 2014; Pelletier et al., 2016). Consequently, it remains unclear how accurate model outcomes for Africa are if they integrate current aquifer estimates, or whether groundwater resources in the crystalline basement aquifers of sub-Saharan Africa are substantially under- or overestimated. To address this shortcoming, it is crucial to understand these aquifer systems and to compile existing knowledge and data on their occurrence and hydraulic properties to more accurately simulate Africa's groundwater resources, especially in the sensitive zones of sub-Saharan Africa.

1.3 Crystalline basement aquifers and regolith

Crystalline basement aquifers cover around 40% of sub-Saharan Africa (MacDonald and Davies, 2000; Vouillamoz et al., 2015) (Fig. 2). They developed in the Precambrian (>5mio years) and typically have a weathered residual overburden of varying thickness – so called regolith (e.g. Chilton and Foster, 1995; Chilton and Smith-Carington, 1984; Foster, 2012; Wright, 1992) (Fig. 3). It is especially the regolith that provides an important, if not the most important aquifer of sub-Saharan Africa, making up for the low transmissivity of the underlying crystalline bedrock, where groundwater can only be stored within fissures and fractures (Chilton and Foster, 1995; Tindimugaya, 1995; Wright, 1992) (Fig. 3).

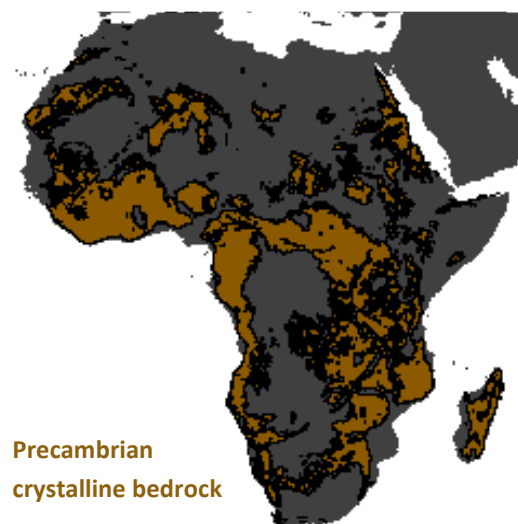


Fig. 2: The distribution of Precambrian crystalline bedrock in Africa; data derived from the United States Geological Survey (USGS, 2000).

Besides sub-Saharan Africa, regolith is also commonly reported as an important aquifer in other regions of the world, such as Australia (Wilford et al., 2016), India (Dewandel et al., 2006), Scandinavia (Karlsson et al., 2014), the Amazon basin (da Costa et al., 2014) or the Southern Sierra (Holbrook et al., 2014).

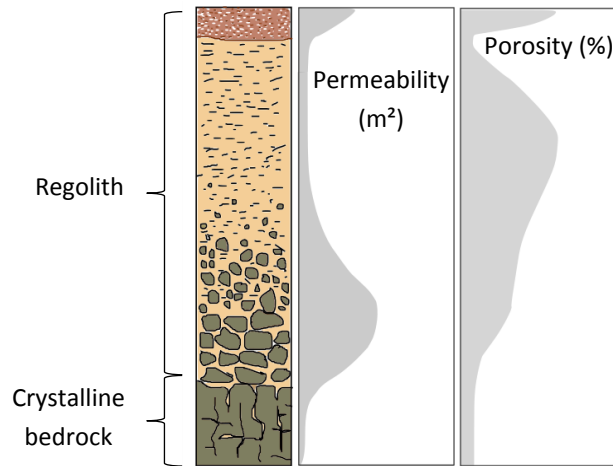


Fig. 3: Structure, relative permeability and relative porosity of a stereotype regolith overlying crystalline bedrock, adapted from Chilton and Foster (1995).

Besides the general occurrence of regolith, its thickness is considered to be the most important factor for well success and yield (Foster, 2012; Wright, 1992). Until today, however, the factors controlling the thickness of regolith are poorly understood (Holbrook et al., 2014; Pelletier et al., 2016). Wright (1992) mentioned controlling factors such as (1) bedrock characteristics, (2) climate, (3) age of the land surface and 4) relief; but no significant correlation could be found. This finding is confirmed by experts from the *Institut des Géosciences de l'Environnement* (IGE, Grenoble) that work on crystalline basement aquifers in West Africa and cannot report any significant correlation between regolith and one of the factors mentioned above (personal communication, May 2018). However, some approaches exist that claim to predict regolith occurrence and/or thickness, which are presented in the following:

Rempe and Dietrich (2014) established a modelling approach that predicts regolith thickness based on the assumption that weathering is controlled bottom up by the permanent water table. Accordingly, Regolith thickness increases with lower water tables and is consequently thicker at mountain ridges and thinner at valley bottoms. Although promising, this approach was only validated on very limited data (Rempe and Dietrich, 2014). It is assumed that relevant factors are missing, especially in arid areas, where the permanent water table tends to be rather deep, leading to thick regolith layer predictions (Pelletier et al., 2016). This contrasts with most findings in the related literature, which report thickest regolith in the humid tropics (e.g. Aizebeokhai and Oyeyemi, 2018; Chilton and Foster, 1995; Foster, 2012). Nevertheless, based on the model of Rempe and Dietrich (2014), Pelletier et al. (2016) built the first global dataset of aquifer thickness which includes a regolith layer, acknowledging its great importance for groundwater flow and storage. This dataset gives first-ever global estimates on regolith occurrence and thickness on a hyper resolution (30'', equal to approximately 1×1km at the equator), therefore adding valuable information to global groundwater modelling. However, model predictions for this layer are influenced by all above mentioned uncertainties, especially if they are applied on a global scale with varying climatic conditions. Pelletier et al. (2016), therefore, did not include this layer into an overall aquifer thickness layer, stating their estimated regolith thickness to be the least confidential of all their datasets (thickness of soil, sedimentary deposits and regolith). Nevertheless, the regolith estimate was not yet tested hydrologically, and its potential is therefore unassessed.

St. Clair et al. (2015), suggests that tectonic stress leads to higher fracture density and consequently to a deeper weathering front. This finding again, implies thicker regolith on mountain ridges, where the topographic stress is higher, and thinner regolith at valley bottoms, but in this case independent from

the permanent water table. In accordance to the finding of St. Clair et al. (2015) and assumptions from Rempe and Dietrich (2014), the general pattern of thicker regolith on mountain ridges and thinner regolith at valley bottoms finds widespread confirmation in the literature (e.g. Parsekian et al., 2015; Pavich et al., 1989; Ruddock, 1967; Thomas, 1966). Although contested by the struggle to find significant correlations (Wright, 1992, see above), topography is therefore assumed to be a possible predictor on regolith thickness, at least at a broader scale, that is worth being tested in a hydrological model.

Nevertheless, the study from Braun et al. (2016) challenges the general applicability of the theory that regolith thickness is steadily larger at topographic highs. The authors state that whether regolith is thicker at mountain ridges or valley bottoms depends on the local surface slope, the aquifer permeability and local precipitation and is therefore locally variable. A further option for implementing regolith occurrence and thickness into large-scale groundwater models would thus be to simply apply an average regolith thickness upon crystalline basements that compensates the high local variation of regolith thickness that might not be caught by the models' resolution.

The permeability of regolith, although quantitatively highly variable, is better understood in its theory than its thickness-distribution (Chilton and Foster, 1995; Foster, 2012; MacDonald and Davies, 2000). Chilton and Smith-Carington (1984) build up the first sketch of a permeability- and porosity-gradient in a stereotype regolith profile, which was improved by Chilton and Foster (1995), adapted by a large number of following studies (e.g. Deyassa et al., 2014; Foster, 2012; MacDonald and Davies, 2000) and not significantly modified until today (comp. Fig. 3). According to this sketch, crystalline basement aquifers are most permeable at the transition zone between the fractured bedrock and the regolith, where the material is relatively coarse. Upwards in the regolith, with continued weathering, the material gets gradually finer and the clay content increases, reducing the permeability of the aquifer. In contrast to the permeability, porosity and consequently storage capacity of the aquifer increases upwards in the regolith with increasing clay content (Chilton and Foster, 1995). However, both permeability and porosity of regolith are in general believed to exceed the ones from the underlying fresh bedrock by about one or two orders of magnitude (Tindimugaya, 1995).

This theory of a consistent gradient of permeability and porosity (in relative numbers) within each regolith profile was confirmed by many following studies (e.g. Bakundukize et al., 2016; Deyassa et al., 2014; Taylor and Howard, 2000) and was not refuted until today. Although understood in theory, quantitative data on regolith permeability on a continental scale for Africa is missing. For this reason, global datasets on aquifer permeability tend to neglect these layers, assuming only crystalline basement aquifers and the properties of fractured crystalline bedrock (Gleeson et al., 2011). As a first approach, Gleeson et al. (2014) integrated deeply weathered soil layers into the global permeability map GLHYMPS, realizing their great importance for groundwater modelling. This approach, however, is still related to high uncertainties and lacks further validation. Furthermore, the assumption of regolith occurring underneath lateritic soils lacks further lithologic information and does not cover all regions in Africa where regolith on crystalline basement has been reported (e.g. Akanmu and Adewumi, 2016; Courtois et al., 2010; Tessema et al., 2014).

1.4 Problem stating, research questions and hypothesis

Current estimates on global aquifer properties often lack testing via the integration into a hydrological model and a critical reflection on their suitability to do so. They are furthermore, seldomly focused on Africa, which calls for an adaption of current global estimates towards continent-specific ones. Furthermore, the complete neglect of and high uncertainties on regolith layer properties in global

aquifer estimates are believed to lead to severe miscalculations when modelling groundwater in Africa, especially in the sensitive rural areas of sub-Saharan Africa. An assessment of current available regolith data and information is therefore crucial.

Based on a comparison and Africa-specific adaption of current global aquifer estimates and a compilation of the best available knowledge and data on regolith in Africa, this study aims to assess the above-mentioned research gap. Focus of this study lays on the impact of the integration of regolith hydraulic parameters on groundwater modelling outcomes for Africa and the potential model improvement through the integrating of regolith into groundwater modelling.

Specifically, (1) the most up-to-date global datasets of aquifer permeability and thickness were compared in regard to their suitability for the simulation of Africa's groundwater in order to improve current estimates on aquifer parametrization. This was done as a pre-analysis to this study, building the base of the further methods applied. After deciding on the general model parametrization, (2) A further literature search for reported values of regolith hydraulic properties (thickness and permeability) in Africa was conducted to integrate regolith hydraulic parameters into the best available aquifer estimates from the pre-analysis (step 1) and to adapt current aquifer estimates. Based on this research, (3) the high resolution groundwater model PCR-GLOBWB MODFLOW (de Graaf et al., 2015, 2017) was run for Africa in an extensive sensitivity analysis, integrating a regolith layer with best available parameters from global datasets and further literature (step 1 and 2) in order to assess the sensitivity of simulations to the integration of a regolith layer and its hydraulic properties. Finally (4) the model outcome was validated with available, observed groundwater head data to quantify the possible improvement of simulations through integrating regolith and to identify the most promising approach to parametrize regolith in large-scale modelling. With this, the study aims to quantify an important share of the uncertainty related to simulations of Africa's groundwater resources. Nonetheless, it is stressed that high model uncertainties are likely to remain as data on aquifer properties in Africa is still sparse.

The main research question asked in this work was, how the model parametrization of Africa's aquifers can be improved in order to access the groundwater resources of the continent through large-scale modelling. Further, is regolith a mayor driving factor for current model uncertainties and if so, is there enough data and knowledge available to address these uncertainties?

Regarding the model parametrization, the following specific research questions were asked:

- (1) Which are the most reliable global datasets on aquifer thickness and permeability for aquifer parametrization and groundwater modeling for Africa?
- (2) What is the best estimation of regolith occurrence, thickness and permeability that can be integrated into groundwater modelling for Africa?

Beyond the model parametrization, looking at the model outcome, the hypothesizes were:

- (1) The simulation of groundwater depth in Africa is highly sensitive to the integration of a regolith layer and its hydraulic parameters.
- (2) The integration of regolith into groundwater modelling clearly improves the resulting model outcome.

2 Pre-analysis - Global datasets for aquifer parametrization

With the aim to find the best available datasets and calculation methods for the parametrization of aquifers in Africa, a pre-analysis on global of aquifer thickness and permeability was conducted. In total, three global datasets of aquifer thickness and two datasets of permeability were found and compared amongst each other. The comparison focused on the method of compilation, the range and spatial distribution of data and the main advantages and limitations of the specific dataset for large-scale groundwater modelling over Africa. Based on the comparison, the most promising datasets were chosen and incorporated into the aquifer parametrization of this study.

For the comparison of aquifer thickness, a smaller example in West Africa (Lon: -5.425, 0.583; Lat: 6.517, 9.35), which is dominated by crystalline basement aquifers, was additionally selected to compare patterns at the regional scale and in an area that was expected to have a large percentage of regolith coverage. In total, the aquifer thickness comparison consisted of three datasets that comprised four maps:

(1) “Aquifer thickness” from De Graaf et al. (2017, 2015), (2) “Depth to bedrock” from Shangguan et al. (2017), (3a) “Average soil and sedimentary deposit thickness” from Pelletier et al. (2016) and (3b) “Upland hillslope regolith thickness” also from Pelletier et al. (2016).

Although described by different designations, all these datasets describe the thickness of geologic layers that are permeable and/or porous enough to store and transmit significant amounts of groundwater. They can, therefore, be summarized under the term aquifer thickness and compared amongst each other equally.

Only one global dataset on aquifer permeability existed that was first published by Gleeson et al. (2011). Later on, this dataset was updated two times. The second version was the GLHYMPS dataset (Gleeson et al., 2014) and the latest version GLHYMPS 2.0 that was published during the development of this study (Huscroft et al., 2018). To avoid repetition, only the two latest versions of GLHYMPS (2014 and 2018) were compared amongst each other.

2.1 Global datasets of aquifer thickness

In the following, all above mention global datasets of aquifer thickness are described according to their methods of compilation and the range and spatial distribution of aquifer thickness over Africa.

1) Aquifer thickness – de Graaf et al. (2017, 2015)

Method: Global aquifer thickness was calculated at a 5' resolution under the assumption that thickness is log-normally distributed and that productive aquifers coincide with sedimentary deposits and sediments below river valleys. Therefore, aquifers were divided into valleys of deeper productive aquifers and into mountain ranges with negligible aquifer thickness, according to the surface elevation. Based on thickness data of sedimentary deposits in the U.S., an algorithm was developed, producing a global likelihood of aquifer thickness. Additionally, a confining layer for confined aquifers was added (de Graaf et al. 2017).

Range & Spatial distribution: Following to the calculation method, deepest aquifers in Africa occurred in its large sedimentary basins, such as the upper Nile basin, the Chad basin, the Kalahari basin and the Taoudeni basin in West Africa, reaching up to more than 1000 m thickness. Shallower aquifer thickness was found at higher elevations especially in sub-Saharan Africa, everywhere where crystalline basement aquifers are mapped (Fig. 4, a). In Tab. 1, the minimum, maximum and average thickness of aquifers for the whole African continent and for the regional extent in western sub-Saharan Africa are reported.

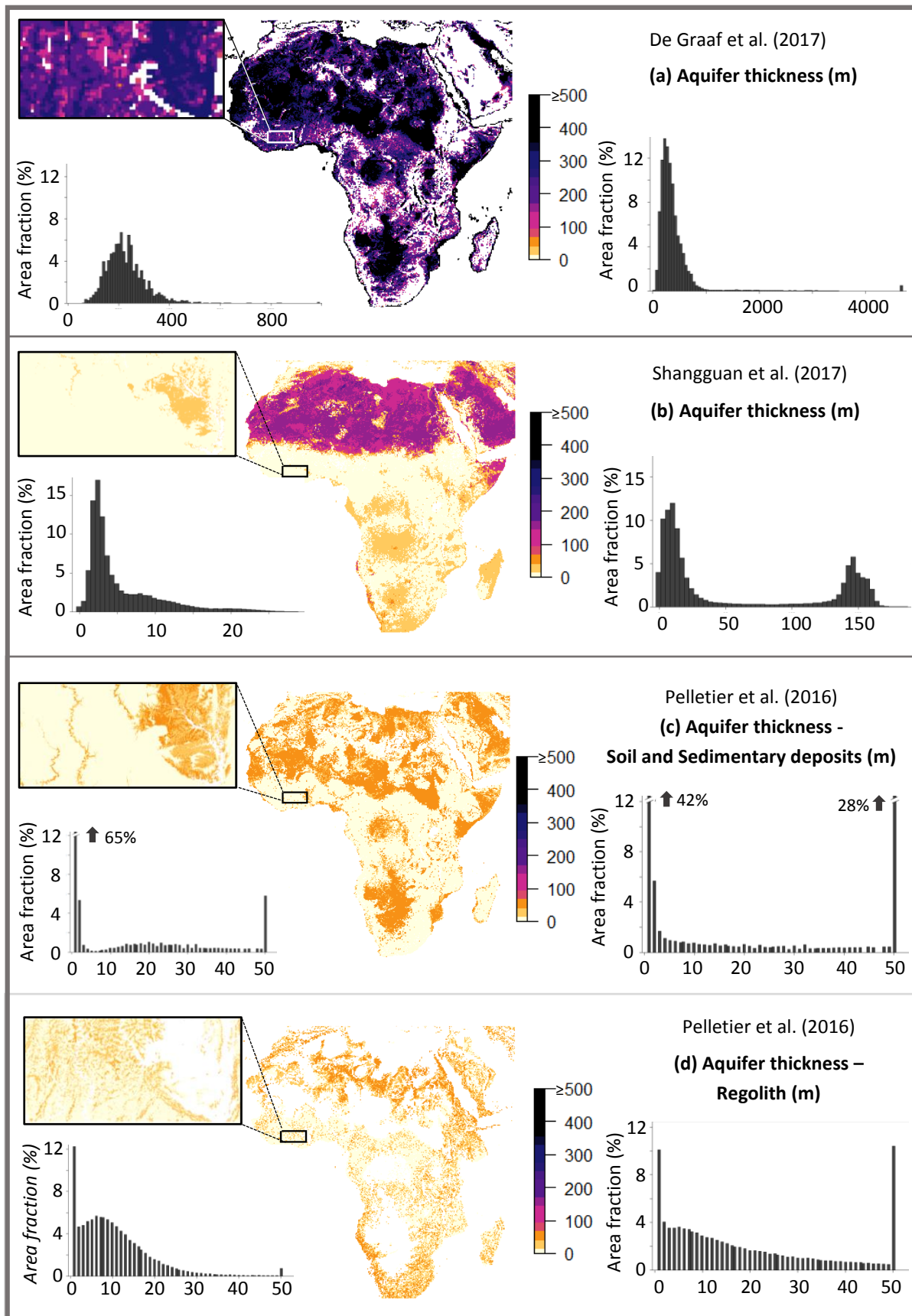


Fig. 4: Overview of the most up to date global datasets of aquifer thickness, selected for Africa and for a regional example in western sub-Saharan Africa.

Tab. 1: Average, minimum and maximum aquifer thickness (m) compiled for the three most up to date datasets on aquifer thickness for Africa and a regional example in western sub-Saharan Africa.

	Aquifer thickness - Africa (m)			Aquifer thickness - regional (m)		
	average	min	max	average	min	max
De Graaf et al. (2017)	406.2	16.6	4665.2	228.8	62.2	985.3
Shangguan et al. (2017)	57.8	0.01	383.8	5.4	0.01	62.5
Pelletier et al. (2016)						
Regolith	18.9	1	50	10.3	1	50
Average Soil & Sedimentary deposits	18.5	1	50	9.5	1	50

Aquifer thickness, calculated by de Graaf et al. (2017, 2015), was more than one order of magnitude higher than values from the other datasets compared at both the whole continent and on the regional scale that represented crystalline basement aquifers in sub-Saharan Africa. In total, approximately 89% of the African land surface was covered by the estimated aquifers.

2) Depth to bedrock – Shangguan et al. (2017)

Method: Depth to bedrock, equivalent to the thickness of productive aquifers, was calculated on a hyper resolution of 250 m and based on a purely statistical approach using random forests and gradient Boosting Tree algorithms. A number of 155 covariates (including soil, sedimentary deposit and regolith thickness from Pelletier et al. (2016)) was included in the modelling process and three types of training data sources were used for the spatial prediction of depth to bedrock, which were (1) soil profile data, (2) borehole drilling logs and (3) pseudo observations. Pseudo observations are simulated data points based on remote sensing for shifting sand and outcrops or on literature values without specific coordinates. For Africa, no borehole drilling data was compiled and aquifer thickness was highly extrapolated over the African continent (Shangguan et al., 2017).

Range & Spatial extent: Africa can be divided into two regions of differing training data sources: On the one hand the Sahara, which was covered by Pseudo observations, mainly randomly located data points of 150 m depth, based on the reported average depth to bedrock of 150 m by Dregne (2011). On the other hand, sub-Saharan Africa, which was mainly covered by soil observations that were limited to a few meters of depth and therefore biased towards shallower aquifers. Calculated aquifer thickness covered the whole continent and values clearly reflect the two different sources of training data (Table x and (Fig. 4, b). Over the Sahara, values varied around 150 m of thickness and for sub-Saharan Africa average thickness showed the lowest value of all datasets, mainly between 1-20m of depth, which can also be observed at the regional scale in Fig. 4, b.

3) Aquifer thickness– Pelletier et al. (2016)

Method: Pelletier et al. (2016) developed one dataset with two complementary maps of aquifer thickness, which were (1) average soil and sedimentary thickness and (2) intact regolith thickness. Both maps were calculated on a 30'' resolution, based on topography and limited to 50 m of thickness. Values equal to 50 m should therefore be interpreted as 50 m or thicker.

3a) Average soil and sedimentary deposit thickness

Method: Average soil and sedimentary deposit thickness covered the whole continent but was calculated separately for soils at upland hillslopes and for sedimentary deposits at upland valley bottoms and at

lowlands (Fig. 4, c). In upland valley bottoms, sedimentary deposit thickness was calculated on the assumption that bedrock in valley bottoms continues in a U or V shape underneath the sedimentary deposits. Sedimentary deposits in lowlands were predicted from the topography using an empirical model, calibrated and validated with well data from the U.S. Additionally, soil thickness was calculated on upland hillslopes as the long-term balance between soil production and erosion, so that finally all three datasets were combined to an average soil and sedimentary deposit layer.

Range & Spatial extent: Average soil and sedimentary thickness was spatially relatively similar distributed as the one from de Graaf et al. (2017, 2015), thus it was deepest at the large sedimentary basins of Africa. The main difference was the limitation to 50 m of depth and a high accumulation of thickness values at 1 m and 50 m. Furthermore, the simulated aquifer thickness was more than one order of magnitude thinner than the one from de Graaf et al. (2015, 2017), both on the continental and on the regional scale.

3b) Intact regolith thickness

Method: Intact regolith thickness was limited to upland hillslopes, which covered approximately half of Africa's land surface area. It was calculated with the quantitative model from Rempe and Dietrich (2014) for the prediction of the vertical extent of weathered rock underlying soil-mantled hillslopes. The model is a bottom up approach assuming that the weathered front of regolith is controlled by the permanent water table. For this purpose, the equilibrium water table depth, simulated by Fan et al. (2013), was taken as a proxy for the permanent water table. Additionally, this water table depth was divided by two to account for shallow water tables that are not captured by the 30'' resolution. Following this equilibrium water table, the model predicted thicker regolith at (semi-)arid regions with deep groundwater tables and thinner regolith in the tropics, where groundwater tables are generally shallow (Fig. 4, d). Simulated regolith thickness, furthermore, went along with the topography, as permanent water tables tend to be deeper at mountain ridges and shallower at valley bottoms (e.g. Rempe and Dietrich, 2014; Schaller and Fan, 2009).

Range & Spatial extent: Similar to the average soil and sedimentary deposit layer, the regolith thickness showed a high accumulation of regolith thickness at 1 m and 50 m, only this time with shallow values at upland valley bottoms and lowlands and maximum thickness at desert regions of Africa, especially at the Sahara and the Namib Desert where the water table is generally deep. The average thickness was comparable to the one for average soil and sedimentary deposits and more than an order of magnitude thinner than the aquifer thickness dataset from de Graaf et al. (2017, 2015). It was also thinner than the depth to bedrock from Shangguan et al. (2017) for the Sahara but thicker at sub-Saharan Africa, as can also be observed at the regional scale (Fig. 4, c).

2.2 Global dataset of aquifer permeability

The global hydrogeology maps of permeability and porosity (GLHYMPS, Fig. 5) provide the only available global dataset for aquifer permeability in current research. For the compilation of the permeability map, the high resolution global lithological map (GLiM) from Hartmann and Moosdorf (2012) (an expansion from Dürr et al., 2005) was merged into 5 hydrolithological classes of largely similar hydrogeological characteristics. Subclasses, based on coarse or fine grain size, were compiled for siliciclastic sedimentary and for unconsolidated sediments (Tab. 2). Gleeson et al. (2011) found that the permeability of each hydrolithological class or subclass can be characterized by its geometric mean, which is representative also on the larger scale, except for carbonate, most likely due to karstification. Consequently, geometric means of permeability were assigned to every hydrolithological class or

subclass. The GLHYMPS database was freely available in the form of a shapefile with permeability values $\log(k)$ (m^2).

The main achievement for Africa, if comparing GLHYMPS to the first version from 2011, was that deeply weathered soils in the tropics (lateritic soils) were reassigned from the hydrogeological class of *crystalline* to *mixed unconsolidated sediments* with a permeability approximately one order of magnitude higher, assuming that lateritic soils dominate the aquifer permeability instead of the underlying lower permeable crystalline basement.

The latest version, GLHYMPS 2.0, divided global permeability into two layers: (1) the underlying hydrogeology, represented by the GLHYMPS dataset (Gleeson et al., 2014) and (2) an upper layer with thickness values derived from the depth to bedrock dataset from Shangguan et al. (2017) and with a reclassified permeability for unconsolidated sediments, derived from the global unconsolidated sediments map database (GUM) from Börker et al. (2018). In the GUM database, unconsolidated sediments were separated into 6 classes of permeability, according to their grainsize distribution. The most striking change in the upper layer permeability for Africa was, therefore, a shift from mixed unconsolidated sediments towards *Sand+* (Tab. 1) with a permeability more than two orders of magnitude higher than permeability from the previously assigned mixed unconsolidated sediments (Fig.5).

However, no adaption was made for areas of crystalline basement and lateritic soils (described by the permeability of mixed unconsolidated sediments), but the GLHYMPS permeability values were adopted unchanged also to the upper layer of GLHYMPS 2.0 (Fig. 5, b).

Tab. 2: Geometric mean of aquifer permeability ($\log(k)$ in m^2) for all hydrogeological classes and subclasses taken from Gleeson et al. (2014), Börker et al. (2018) and Huscroft et al. (2018).

Hydrogeology	Permeability $\log(k)$ (m^2)	Permeability $\log(k)$ σ (m^2)	Source
Unconsolidated (mixed)	-13.00	2.0	GLHYMPS
c.g. unconsolidated	-10.90	1.2	GLHYMPS
f.g. unconsolidated	-14.00	1.8	GLHYMPS
Sand+	-10.52	1.6	GUM / GLHYMPS 2.0
Sand/Silt	-11.94	1.7	GUM / GLHYMPS 2.0
Sand/Clay	-11.35	1.3	GUM / GLHYMPS 2.0
Silt	-14.13	1.4	GUM / GLHYMPS 2.0
Silt/Clay	-14.95	2.6	GUM / GLHYMPS 2.0
Clay	-15.77	2.1	GUM / GLHYMPS 2.0
Sil. Sedimentary	-15.20	2.5	GLHYMPS
c.g. sil. Sedimentary	-12.50	0.9	GLHYMPS
f.g. sil. Sedimentary	-16.50	1.7	GLHYMPS
Carbonate	-11.80	1.5	GLHYMPS
Crystalline	-14.10	1.5	GLHYMPS
Volcanic	-12.50	1.8	GLHYMPS

Note: f.g.: fine grained; c.g.: coarse grained; Sand+: sand and coarser grain sizes; sil.: sedimentary is siliciclastic. GLHYMPS: global hydrogeology maps (Gleeson et al., 2014), GUM: global unconsolidated sediments map (Börker et al., 2018), GLHYMPS 2.0: global hydrogeology maps 2.0 (Huscroft et al., 2018).

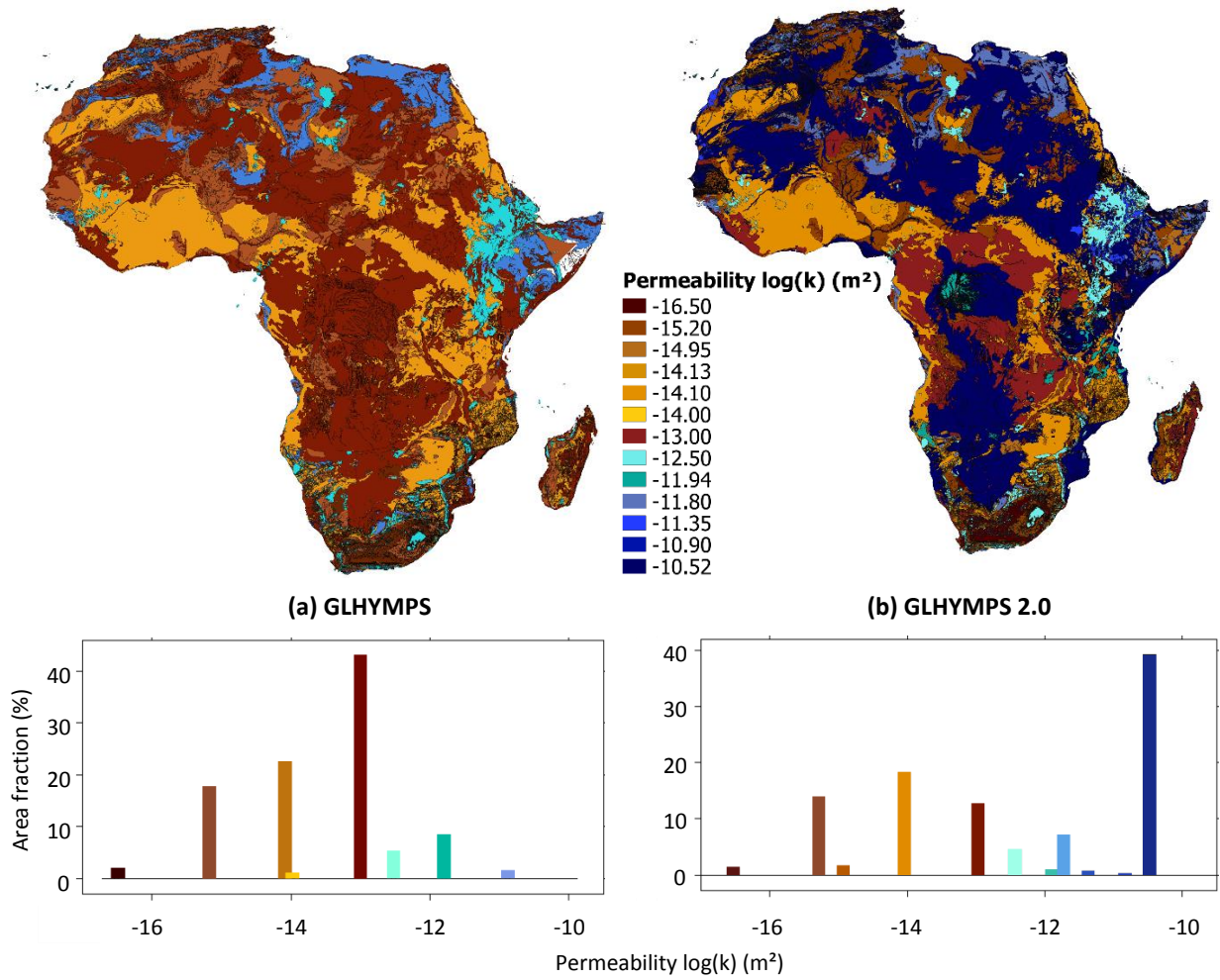


Fig. 5: The spatial and relative distribution of permeability estimates ($\log(k)$ in m^2) for Africa, taken from (a) GLHYMPS (Gleeson et al. 2014) and (b) GLHYMPS 2.0 (Huscroft et al. 2018).

2.3 Best available datasets for aquifer parametrization

All aquifer thickness datasets showed huge differences in the way they were compiled and in their respective range and spatial distribution of data, while only one main dataset of aquifer permeability existed. For this study, the aquifer thickness from de Graaf et al. (2015, 2017) and the permeability dataset GLHYMPS (Gleeson et al., 2014) were chosen as the most promising parametrization of deep extensive aquifers over Africa with the following argumentation:

Statistical models, as used by Shangguan et al. (2017), have the advantage to allow for the inclusion of several covariates. Therefore, Shangguan et al. (2017) created more accurate results at interpolated areas such as the U.S. and Europe (Shangguan et al., 2017). On the contrary, aquifer thickness was heavily extrapolated in data-sparse regions such as Africa. In this case, process-based models like the ones from de Graaf et al. (2015, 2017) and Pelletier et al. (2016) show more robust results as they rely on a few general assumptions (Shangguan et al., 2017). The two different training data sources in the dataset of Shangguan et al. (2017) (pseudo observations in the Sahara, soils data in sub-Saharan Africa), further intensified the extrapolation-uncertainties as they led to the simulation of two very distinct classes of aquifer thickness that were biased towards the respective training data source. Therefore, the dataset from Shangguan et al. (2017) is not the best choice for the parametrization of Africa's aquifers.

The average soil and sedimentary deposit thickness from Pelletier et al. (2016) was limited to 50 m of depth. The high accumulation of values at 50 m in the dataset shows that a high percentage of aquifers is not represented within the range from 1-50 m. Furthermore, the dataset was spatially limited to lowlands and upland valley bottoms, while upland hillslopes were covered by soil thickness only. In the context of this study, the average soil and sedimentary deposit thickness was, therefore, not found to be suitable for the parametrization of aquifers in Africa.

The aquifer thickness from de Graaf et al. (2017, 2015) was process based and therefore more robust on extrapolation than the aquifer thickness from Shangguan et al. (2017). It was, furthermore, neither limited in height nor in spatial extent, as was the estimate from Pelletier et al. (2016). Consequently, it was found to be the most suitable for the parametrization of extensive aquifers in Africa. Nevertheless, the aquifer thickness from de Graaf et al. (2017, 2015) showed the coarsest resolution of all datasets. Therefore, an improvement through a recalculation at a hyper resolution would be recommendable. Furthermore, global estimates that were based on aquifer thickness in the U.S. need adjustment towards African-characteristic aquifer thickness, for example with maps of MacDonald et al. (2012). Last but not least, regolith was not represented by the extensive aquifers from de Graaf et al. (2017, 2015) but requires the additional implementation of a second layer that is separately parametrized.

The regolith thickness estimate from Pelletier et al. (2016) was the first estimate of this kind. According to the authors, it still holds great uncertainties, but the impact of these uncertainties on the outcome of groundwater modelling remains unclear as long as it has not been hydrologically tested. In this study, the regolith estimate was, therefore, integrated into groundwater modelling, as one possible scenario for the occurrence and thickness of regolith among other scenarios that were developed in this study.

For the parametrization of aquifer permeability in Africa, GHLYMPS was chosen as the best suitable dataset to be assigned to deep extensive aquifers whose thickness was calculated according to de Graaf et al. (2017, 2015). GLHYMPS also represented the underlying permeability of GLHYMPS 2.0 and was therefore the only permeability dataset that is suitable for the parametrization of deeper aquifers that include the crystalline basement underneath of regolith, while regolith itself required a separated parametrization. The upper layer with updated sediment permeability (GLHYMPS 2.0) was not included in the aquifer parametrization of this study. This was decided because the focus of this study lay on the parametrization of crystalline basement aquifers and regolith, which were not accounted for in GLHYMPS 2.0. Furthermore, the aquifer thickness from Shangguan et al. (2017), which was used for the upper layer thickness of updated sediment permeabilities in GLHYMPS 2.0, constitutes a further uncertainty factor for Africa's aquifer parametrization due to the above-mentioned reasons. It is thus up to future studies to focus on the improvement of the parametrization of unconsolidated sediment aquifers in Africa and to find reliable estimates of upper sediment thickness to test the upper permeability layer from GLHYMPS 2.0 hydrologically.

3 Methods

3.1 Regolith permeability and thickness in Africa – A literature review

Extensive datasets on regolith permeability and thickness estimates are scarce. The only estimates found that covered the African continent were the global regolith thickness from Pelletier et al. (2016) and permeability approximated by mixed unconsolidated sediments from Gleeson et al. (2014). Therefore, a literature review on regolith thickness and permeability was conducted to derive new and more comprehensive estimates of regolith permeability and thickness for Africa. All studies appearing in Google Scholar under the search terms “Africa”, “regolith”, “hydraulic conductivity” and “thickness” were selected and scanned for values of regolith thickness and regolith hydraulic conductivity. Google Scholar was used as it includes also non-ISI listed publications. The search was conducted under the condition that (1) the appearing study was conducted in Africa, (2) it was conducted fully or partly on crystalline basement aquifers and that (3) the study was freely available for the University of Freiburg. A confidence level from 1 (lowest confidence) to 5 (highest confidence) was assigned to each study according to the methods used, the sample size, the quality of the journal (peer-reviewed or not) and the age of the respective study. A more detailed explanation on the confidence level is shown in the Appendix (Tab. S1).

To be able to compare hydraulic conductivity values from the literature with the global permeability values from GLHYMPS (Gleeson et al., 2014), values of hydraulic conductivity were transformed into permeability values $\log(k)$, according to the following equation:

$$\log(k) = \log\left(\frac{K}{\rho \cdot \frac{g}{\mu}}\right) \quad (1)$$

where $\log(k)$ is the log-scaled permeability in m^2 , ρ is the density of a fluid, approximated by 1000 kg m^{-3} for normal water, g is the acceleration due to gravity on earth with 9.81 m s^{-2} and μ is the viscosity of a fluid, $0.001 \text{ kg m}^{-1} \text{ s}^{-1}$ for normal water.

For the parametrization of regolith, the arithmetic mean of all thickness values (D_{mean}) and the geometric mean of all permeability values ($\log(k)_{\text{mean}}$) was calculated. Furthermore, a lower bound estimate was calculated as the arithmetic and geometric mean from all lower range values for thickness (D_{min}) and permeability ($\log(k)_{\text{min}}$), respectively. An upper bound estimate was similarly calculated from all upper range values (D_{max} and $\log(k)_{\text{max}}$). In the following, the calculated means were used to parametrize regolith layers for groundwater modelling.

This literature review had no claim for completeness, as this was beyond the scope of this study. Nevertheless, it served as a first and reliable approximation of regolith hydraulic parameters.

3.2 Groundwater modelling

Groundwater depth in Africa was modelled with the high-resolution global-scale groundwater model PCR-GLOBWB-MODFLOW (de Graaf et al., 2015) (Fig. 6) assuming steady state and natural conditions. The model consists of two different models that were coupled offline for this study: (1) the global hydrological model PCR-GLOBWB for the simulation of water storage and fluxes within and between two soil stores, forced by atmospheric data (for a more detailed description see Sutanudjaja et al., 2018; or Van Beek et al., 2011) and (2) the groundwater model MODFLOW, which replaces the linear groundwater store of PCR-GLOBWB.

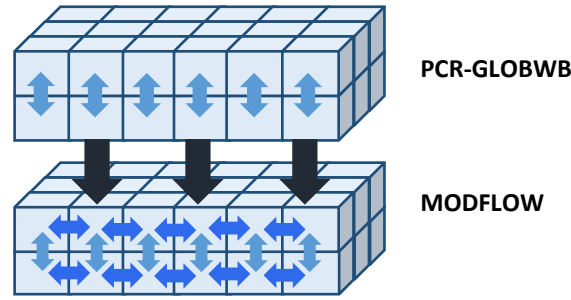


Fig. 6: Schematic construction of the grid-based global hydrological model PCR-GLOBWB-MODFLOW with two horizontal layers implemented in MODFLOW.

MODFLOW is a grid-based calculation method, written by the United States Geological Survey (USGS). It solves 3D groundwater flow through a porous medium (aquifer) after Darcy's law, using the finite-differences method, which leads to a partial-differential equation solving the distribution of hydraulic heads as follows (McDonald and Harbaugh, 1988):

$$\frac{\partial}{\partial x} \left[K_{xx} \frac{\partial h}{\partial x} \right] + \frac{\partial}{\partial y} \left[K_{yy} \frac{\partial h}{\partial y} \right] + \frac{\partial}{\partial z} \left[K_{zz} \frac{\partial h}{\partial z} \right] + Q = S_s \frac{\partial h}{\partial t} \quad (2)$$

where K_{xx} , K_{yy} and K_{zz} are the values of hydraulic conductivity (K in m d^{-1}) in x , y and z direction along the coordinate axis (3D). h (m) is the potentiometric groundwater head, Q ($\text{m}^3 \text{d}^{-1}$) the volumetric groundwater flux, S_s (m) the specific storage, depending on the aquifer porosity, and t the time in days.

In contrast to the linear groundwater store from PCR-GLOBWB, MODFLOW enables to simulate groundwater heads with a lateral flow component between cells and allows for interactions between ground- and surface water. Furthermore, MODFLOW allows for the implementation of multiple horizontal layers and therefore enabled to implement separated parametrizations for regolith and the underlying crystalline basement.

Offline coupling of these two models means that, as a first step, PCR-GLOBWB was run independently and that the results in the form of groundwater recharge and river discharge were consequently passed on to MODFLOW. On the contrary, results from MODFLOW were not returned to PCR-GLOBWB, hence the model was only coupled one-way.

3.3 Model setup and parametrization

3.3.1 Aquifer thickness and parametrization of regolith

To improve the hydraulic model parametrization for Africa, two layers were calculated that form the aquifer's spatial extent and thickness: (1) an extensive deeper layer, called sediment/crystalline layer from here on for simplicity reasons, which represented all aquifers besides regolith and the crystalline basement underneath of regolith and (2) a regolith layer with a higher permeability than the underlying, lower permeable crystalline basement. This second layer was integrated to improve the accuracy and the level of detail covered by the aquifer parametrization at the local occurrence of crystalline basement aquifers, especially in sub-Saharan Africa.

Both layers were calculated on a $30''$ resolution, on the base of the digital elevation model (DEM) from HydroSHEDS at $30''$ (Fig. 7). The hyper resolution allowed to include smaller topographic variations than a high resolution of $5'$ and consequently led to a higher and more precise coverage of aquifers over the continent. However, model runs were conducted at a high resolution of $5'$ due to limitations in

computational power. Consequently, both hyper resolution layers were aggregated for the model runs via averaging to match 5'.

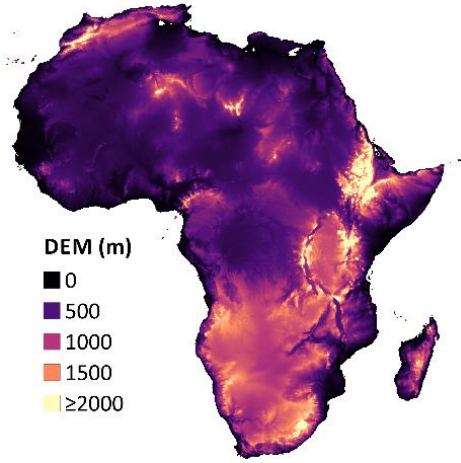


Fig. 7: Digital elevation model (DEM) of Africa derived from HydroSHEDS.

Sediment/crystalline layer

The deeper and more extensive sediment/crystalline layer was calculated following the methodology of de Graaf et al. (2017, 2015) as a result from the comparison of available aquifer thickness datasets (see chapter 2.3). Adaptions of the methodology were the calculation on 30'' instead of 5' to achieve a better coverage and the change from the global scale towards Africa specific aquifer thickness, with the help of the map of aquifer saturated thickness from Bonsor and MacDonald (2011) and depth to groundwater from MacDonald et al. (2012).

According to the methodology of de Graaf et al. (2017, 2015), aquifers occurred within valleys up until a surface level elevation of 50 m above the floodplain elevation. It was assumed that the higher the surface elevation is relative to the floodplain, the thinner is the assigned aquifer (Fig. 8). Relative elevation within a valley was therefore standardized to define a log-normally distributed aquifer thickness, assuming thickness to be non-negative and positively skewed.

As a first step, a measure for the relative difference between the surface elevation and the floodplain was calculated for each cell, leading to a thinning layer towards the edges of the valley with a maximum thickness at the valley bottom:

$$F'(x) = 1 - \frac{F(x) - F_{\min}}{F_{\max} - F_{\min}} \quad (3)$$

with $F()$ standing for the difference between the surface and floodplain elevation at cell x . And F_{\min} and F_{\max} are the minimal and maximal elevation value.

Secondly, the associated z-score ($Z()$) was calculated. The z-score is a measure of deviation between a single thickness value (x) and the mean of total thickness values, given in number of standard deviations and was calculated as follows:

$$Z(x) = G^{-1}(F'(x)) \quad (4)$$

with $G^{-1}()$ standing for the inverse of the standard normal distribution.

For the final generation of a spatial aquifer thickness distribution map, an average thickness (D_{sc}) and a coefficient of Variation (CV_{sc}) were needed. Values were chosen to match the range of saturated

thickness of the map from Bonsor and MacDonald (2011) plus the depth to groundwater of the map from MacDonald et al. (2012), which range between <25 and >500 m.

De Graaf et al. (2015) found that groundwater depth, simulated with PCR-GLOBWB-MODFLOW, is relatively insensitive to a change in aquifer thickness compared to a change in permeability, which can vary more than an order of magnitude within one hydrogeological class. Therefore, and as the focus of this study lay on the parametrization of a regolith layer, D_{sc} and CV_{sc} (eq. 5) were fixed accordingly for the sediment/crystalline layer and not further adapted. With this, a spatial distribution of aquifer thickness was generated, based on the topography of each delineated basin:

$$D_{sc}(x) = e^{\overline{\ln D_{sc}}(1 + CV_{sc} \overline{\ln D_{sc}} Z(x))} \quad (5)$$

Finally, the layer was smoothened to reduce the effect of isolated outliers with the help of a moving window in form of a matrix of weights (Appendix, Fig. S1). All cells covered by the window were multiplied by their respective weight and the sum of cells was written into the centered cell. This window was applied for each single cell in the raster.

Regolith layer

For the regolith layer, three scenarios were applied:

- 1) *Topography scenario*: Regolith thickness depends on the topography; hence it is thickest on mountain ridges and thinner towards valley bottoms, exactly opposite to the deeper sediment/crystalline layer (Fig. 8, a).
- 2) *Average scenario*: The average thickness of regolith is assumed everywhere where regolith occurs, with the spatial extent equal to scenario (Fig. 8, b).
- 3) *Permanent water table (PWT) scenario*: Regolith thickness from Pelletier et al. (2016), where regolith is limited by the permanent water table (Fig. 8, c; for a more detailed description see chapter 2.1)

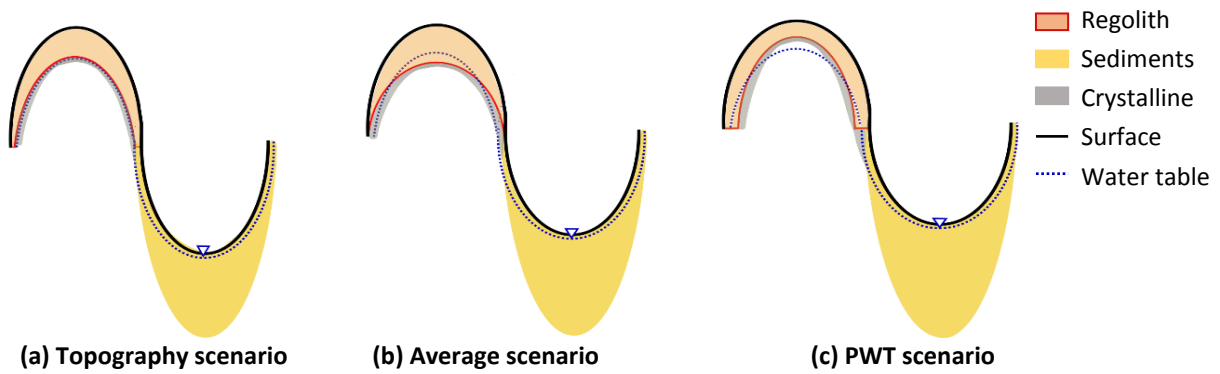


Fig. 8: Schematic construction of aquifer layers (not true to scale) with different scenarios for the regolith layer with (a) the topography scenario (b) the average scenario, both developed in this study and (c) the permanent water table (PWT) scenario developed by Pelletier et al. (2016).

1) *Topography scenario*

Regolith was assumed to be thinner at valley bottoms and thicker at mountain ridges, an observation frequently reported among critical zone scientists (e.g. Clair et al., 2015; Holbrook et al., 2014; Pavich et al., 1989; Rempe and Dietrich, 2014). Following this assumption, the above described estimation of

the sediment/crystalline layer was reversed: Only cells with a surface elevation 50 m *above* the floodplain were considered and the measure of expressing the relative difference between surface elevation and floodplain was modified to a thinning layer towards valley bottoms with the maximum thickness at mountain ridges:

$$F_{reg}'(x) = \frac{F_{reg}(x) - F_{reg,min}}{F_{reg,max} - F_{reg,min}} \quad (6)$$

The z-score (eq. 4) was consequently calculated with the new measure ($F'_{reg}()$) at all cells (x):

$$Z_{reg}(x) = G^{-1}(F_{reg}'(x)) \quad (7)$$

An average thickness (D) and coefficient of variation (CV_{reg}) were chosen to fit the range of regolith thickness values reported in the literature. To account for a thickness reduction due to subsequent smoothing, D was multiplied by an empirically determined factor of 4. With this, the final spatial distribution of regolith thickness was calculated accordingly, following eq. 5:

$$D(x) = e^{\frac{\ln(4 \times D)}{1 + CV_{reg}} Z_{reg}(x)} \quad (8)$$

This final regolith layer was also smoothened with the moving window (Appendix, Fig. S1) to reduce the effect of isolated outliers.

2) Average scenario

For the second scenario, the spatial distribution of the topography scenario was kept, but a constant averaged thickness (D) was applied. The average scenario was developed after personal communication with hydrogeology experts from the IGE (Grenoble, May 2018) that work mainly in western sub-Saharan Africa. The average scenario followed the assumption that the variation of regolith thickness happens on a local scale, which is not accurately captured on a 5' - 30'' resolution and that regolith thickness might therefore, be best described by an average thickness.

3.3.2 Permeability

Transmissivity, which was required as an input parameter for MODFLOW, is the driving factor for groundwater flow. It is the product of aquifer thickness and hydraulic conductivity, which was, in turn, calculated from the permeability. For the sediment/crystalline layer, permeability was derived from the global hydrogeology map GLHYMPS (Gleeson et al., 2014) as it resulted to be the best available permeability dataset for the purpose of this study (see chapter 2.3). GLHYMPS was freely available with global permeability data mapped as polygons and stored in a shape file. To be compatible to MODFLOW, this shapefile was consequently clipped to the extent of Africa, rasterized and permeability values were transformed into hydraulic conductivities ($m\ d^{-1}$) (see eq. 1).

In contrast to the underlying sediment/crystalline layer, solely the geometric mean from permeability values derived from the literature review (D_{mean} , D_{min} or D_{max} , see chapter 3.1) was assigned to the upper regolith layer. The only exception to this assignment was made when the permeability from the overlaying regolith was lower than the underlying permeability for the sediment/crystalline layer. In this case, the same permeability as for the sediment/crystalline layer was assigned to the upper layer:

$$K_{layer1} = \begin{cases} K_{reg} & \text{if } K_{reg} \geq K_{sed} \\ K_{sed} & \text{if } K_{reg} < K_{sed} \end{cases} \quad (9)$$

where K_{layer1} is the hydraulic conductivity, assigned to the upper layer ($m\ d^{-1}$) and K_{reg} and K_{sed} are the hydraulic conductivities, calculated from the permeability of regolith and from the permeability of GLHYMPS, respectively.

This exception was made under the rational that in the GLHYMPS database, a higher permeability than regolith occurred only for carbonates and unconsolidated sediments, which are typically not overlain by regolith (Bonsor and MacDonald, 2011; Chilton and Foster, 1995). Therefore, in these areas, regolith was believed to be erroneously estimated and was, consequently, replaced by the underlying lithology according to Gleeson et al. (2014).

3.3.3 Boundary conditions

All cells representing the ocean or large lakes were set to a constant head boundary condition, with the ocean set to 0m and large lakes set to their respective elevation, provided by the DEM from HydroSHEDS.

Rivers and drains

To incorporate the interaction of surface- and groundwater (groundwater drainage and river infiltration), the MODFLOW river package (RIV) and the drain package (DRN) were used, following the methodology from De Graaf et al. (2017, 2015). Surface water interactions were divided into three categories that were based on Sutanudjaja et al. (2011): (1) larger rivers, with a width $\geq 10m$, (2) rivers and streams $< 10m$ and (3) smaller springs and streams up in the mountains.

Category 1 (Larger rivers)

The RIV package was used for all larger rivers, where river bottoms (Riv_{bottom}) and heads (Riv_{head}) are needed as an input to MODFLOW. Consequently, channel dimensions were calculated from the long-term averaged naturalized river discharge from 1960-2000 (Q_{av} , Fig. 9), obtained from PCR-GLOBWB, with a combination of the Manning's formula (Manning et al., 1890) and Lacey's law formula (Lacey, 1930):

$$Riv_{bottom} = DEM - \left(\frac{n \times Q_{bkfl}^{0.5}}{4.8 \times Sl^{0.5}} \right)^{\frac{3}{5}} \quad (10)$$

Where n is the Manning roughness coefficient ($m^{-1/3}\ d^{-1}$) (Manning et al., 1890), assuming a rectangular channel. Q_{bkfl} is the long-term averaged discharge ($m^3\ d^{-1}$) calculated from Q_{av} , occurring every 1.5 years as a rule of thumb and Sl (-) is the channel longitudinal slope.

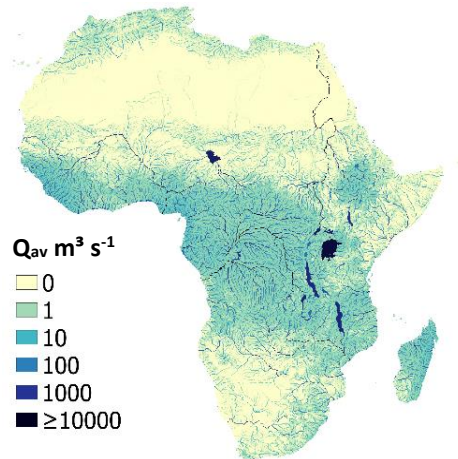


Fig. 9: Long-term average naturalized river discharge (Q_{av}), obtained from PCR-GLOBWB, used to calculate the channel dimensions that were passed on to MODFLOW.

The respective Riv_{head} was calculated as follows:

$$Riv_{head} = Riv_{bottom} + \left(\frac{n \times \overline{Q_{bkfl}^{0.5}}}{W_{riv} \times Sl^{0.5}} \right) \quad (11)$$

Where W_{riv} is the river width, approximated by the wetted perimeter (P_{bkfl}), calculated with the help of Lacey's law, as follows:

$$W_{riv} \approx P_{bkfl} = 4.8 \times Q_{bkfl}^{0.5} \quad (12)$$

With these channel dimensions, the interaction between groundwater and rivers ($W_{riv} \geq 10$) was implemented as follows:

$$Q_{riv} = \begin{cases} c \times (Riv_{head} - h) & \text{if } h > Riv_{bottom} \\ c \times (Riv_{head} - Riv_{bottom}) & \text{if } h \leq Riv_{bottom} \end{cases} \quad (13)$$

where Q_{riv} is the discharge between large rivers ($m^3 d^{-1}$) and the aquifer, h is the groundwater head (m) and c is a conductance ($m^2 d^{-1}$) calculated as follows:

$$c = \frac{1}{BRES} \times W_{riv} \times L_{riv} \quad (14)$$

with BRES as the bed resistance (d^{-1}) and L_{riv} as the river length (m) within one cell, approximated by the diagonal cell length.

Per definition, Q_{riv} was positive when rivers infiltrated into the groundwater ($Riv_{head} > h$) and negative when groundwater drained into the river ($Riv_{head} < h$).

Category 2 (smaller rivers)

For smaller rivers ($W_{riv} < 10$), the DRN package was used. In this case, no river depth was calculated but groundwater could leave the aquifer if h rose above the drainage elevation, which was set equal to the land surface (DEM). The interaction of groundwater and smaller rivers (Q_{dm}) was consequently implemented as follows:

$$Q_{dm} = \begin{cases} c \times (DEM - h) & \text{if } h > DEM \\ c \times 0 & \text{if } h \leq DEM \end{cases} \quad (15)$$

Where a negative Q_{dm} stands again for the groundwater drainage, but no positive Q_{dm} (river infiltration) occurred, as groundwater could only leave the system, not enter it.

Category 3 (smaller streams and springs higher up in the mountains)

As the last category, an additional drainage option was implemented to represent smaller streams and springs higher up in the mountains that were not covered by the 5' resolution. Here again, discharge could only leave the aquifer but not enter it and was therefore always indicated as a negative value. The drainage (Q_{SJ}) was implemented in form of an additional linear storage-outflow relationship:

$$Q_{SJ} = J \times S_{3,flp} \quad (16)$$

Where $S_{3,flp}$ (m) is the storage of groundwater above the surface elevation, calculated by PCR-GLOBWB, and J (d^{-1}) is a recession coefficient, calculated following to Kraijenhoff van de Leur (1958):

$$J = \frac{\pi T}{4S_s L^2} \quad (17)$$

Where T ($m^2 d^{-1}$) is the new transmissivity estimate, including regolith transmissivity from literature. S_s (-) is a storage coefficient for each hydrolithological class, according to Gleeson et al. (2014) and L (m)

is the average distance between rivers and streams, calculated from the drainage density from Schneider et al. (2017).

Finally, the overall ground- and surface water interactions (Q_b) in form of groundwater drainage (-) and river infiltration from larger rivers (+) were calculated via the sum of all three types of ground- and surface water interactions that were described above:

$$Q_b = Q_{riv} + Q_{drn} + Q_{SJ} \quad (18)$$

3.3.4 Recharge

Steady state recharge (Rch_{act} in $m\ d^{-1}$) was derived on a 5' resolution from the PCR-GLOBWB output as the long-term average over the years 1960-2000 (Fig. 10).

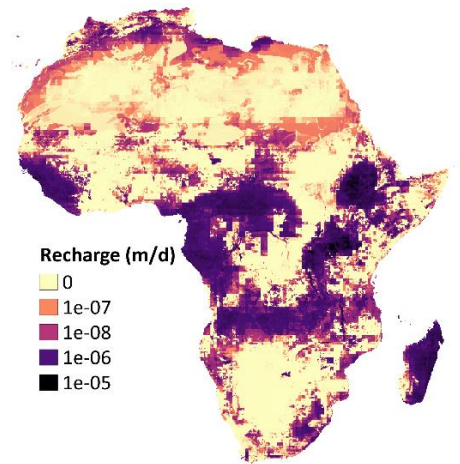


Fig. 10: Average daily groundwater recharge, calculated from PCR-GLOBWB, used to calculate input groundwater recharge that was passed on to MODFLOW.

MODFLOW internally transfers the input recharge (Rch_{inp} in $m\ d^{-1}$) into volumes ($m^3\ d^{-1}$) by multiplying it by the cell area. However, the MODFLOW cell area (A_{MF}) is in degrees, while the projected cell area (A_{cell}) was given in m^2 with a decreasing surface area per cell from the equator poleward. Therefore, the recharge passed on to MODFLOW was previously modified as follows:

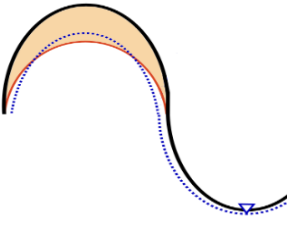
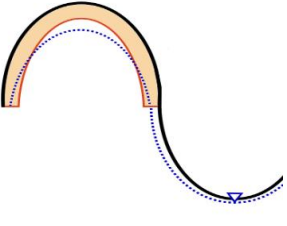
$$Rch_{inp} = Rch_{act} \times \frac{A_{cell}}{A_{MF}} \quad (19)$$

3.4 Sensitivity analysis

To assess the sensitivity of groundwater depth simulations to the integration of a regolith layer, the model was run with and without a regolith layer as a two- or one-layer simulation, respectively. Secondly, to test the sensitivity of simulations to the methodological structure of the regolith layer, the regolith scenario was varied between the topography scenario, the average scenario and the PWT scenario. Finally, to analyze the sensitivity of simulations to the transmissivity of regolith, the parametrization of regolith thickness (D) and permeability ($\log(k)$) were varied between their mean, lower and upper bound estimate from literature (Tab. 3). These three values for $\log(k)$ and for D were run in every possible constellation, resulting in 9 different transmissivity values, which were used to parameterize the three regolith scenarios. The only exception was the PWT scenario, where only $\log(k)$ was varied, while the original thickness (D_{PWT}) from Pelletier et al. (2016) was kept. Consequently, a

total of 22 different model runs, including a *No-Regolith* run, were conducted. For a better overview, all conducted model runs are displayed in (Tab. 3) and each constellation is assigned to a specific abbreviation that is used here on to refer to the specific model runs.

Tab. 3: All constellations of regolith parametrizations that were run in an extensive sensitivity analysis, varying either the regolith scenario, its thickness (D) or its permeability ($\log(k)$).

Number model run	Scenario	Thickness D (m)	Permeability $\log(k)$ (m^2)	Abbreviation
1	No-Regolith	-	-	<i>No-Regolith</i>
2	 Topography scenario	D _{min}	$\log(k)_{min}$	<i>Topography-D_{min}-log(k)_{min}</i>
3			$\log(k)_{mean}$	<i>Topography-D_{min}-log(k)_{mean}</i>
4			$\log(k)_{max}$	<i>Topography-D_{min}-log(k)_{mean}</i>
5		D _{mean}	$\log(k)_{min}$	<i>Topography-D_{mean}-log(k)_{min}</i>
6			$\log(k)_{mean}$	<i>Topography-D_{mean}-log(k)_{mean}</i>
7			$\log(k)_{max}$	<i>Topography-D_{mean}-log(k)_{max}</i>
8		D _{max}	$\log(k)_{min}$	<i>Topography-D_{max}-log(k)_{min}</i>
9			$\log(k)_{mean}$	<i>Topography-D_{max}-log(k)_{mean}</i>
10			$\log(k)_{max}$	<i>Topography-D_{max}-log(k)_{max}</i>
11	 Average scenario	D _{min}	$\log(k)_{min}$	<i>Average-D_{min}-log(k)_{min}</i>
12			$\log(k)_{mean}$	<i>Average-D_{min}-log(k)_{mean}</i>
13			$\log(k)_{max}$	<i>Average-D_{min}-log(k)_{max}</i>
14		D _{mean}	$\log(k)_{min}$	<i>Average-D_{mean}-log(k)_{min}</i>
15			$\log(k)_{mean}$	<i>Average-D_{mean}-log(k)_{mean}</i>
16			$\log(k)_{max}$	<i>Average-D_{mean}-log(k)_{max}</i>
17		D _{max}	$\log(k)_{min}$	<i>Average-D_{max}-log(k)_{min}</i>
18			$\log(k)_{mean}$	<i>Average-D_{max}-log(k)_{mean}</i>
19			$\log(k)_{max}$	<i>Average-D_{max}-log(k)_{max}</i>
20	PWT scenario	D _{PWT}	$\log(k)_{min}$	<i>PWT-log(k)_{min}</i>
21			$\log(k)_{mean}$	<i>PWT-log(k)_{mean}</i>
22			$\log(k)_{max}$	<i>PWT-log(k)_{max}</i>

Note: Indexed min, mean and max stand for the average lower limit, average and upper limit from literature values, respectively. PWT stands for the permanent water table scenario from Pelletier et al. (2016).

3.5 Validation

Simulated groundwater heads were validated against a dataset of groundwater heads that were compiled from observed groundwater depth data for Africa from Fan et al. (2013) (Fig. 7). From a physical perspective, groundwater heads rather than groundwater depths should be compared, as groundwater heads include the potential energy that is driving groundwater flow (Sutanudjaja et al., 2011). Therefore, simulated groundwater depth and the groundwater depth data from Fan et al. (2013) were transferred into groundwater heads. If two or more validation data points lay within one grid cell, their respective mean was calculated. Thus, a total of 431 groundwater head data points from Fan et al., 2013 was combined to 269 values assigned to the grid cell of their specific location from which 160 grid cells

were covered by regolith according to the estimation of this study. With an average depth to groundwater of 25 meters below ground level (mbgl), the validation data points were biased towards shallow groundwater depth. This bias can be explained by the fact that wells tend to be located in areas of shallow groundwater, where they are easy and inexpensive to maintain. Furthermore, validation data points were biased towards lowlands and shallower slopes with an average elevation of 310 meters above sea level (masl), while according to the DEM the average elevation level of Africa was 628 masl. As measure of validation, the coefficient of determination (R^2) was calculated and compared amongst different model runs.

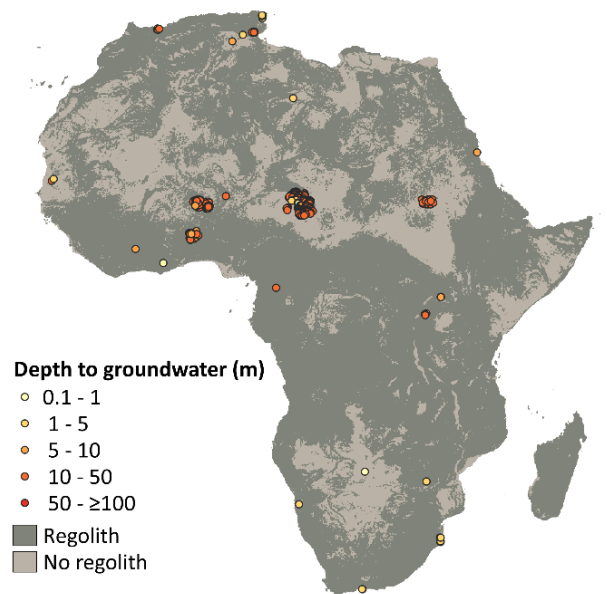


Fig. 11: Observed groundwater depth data from Fan et al. (2013) used for the model validation.

3.6 Software and programming language

PCRaster (version 4.1.0) was used as an interface to MODFLOW with all input datasets calculated and modified in the programming language python (version 2.7.13), with the help of the side packages *os* and *datetime*. All outputs came in form of a raster format that was further analyzed and visualized in QGIS (version 2.18.18) or with the programming language R (version: 3.4.3) and the R site packages: *sp*, *raster*, *RColorBrewer*, *rgdal*, *rasterVIS*, *rgeos* and *hydroGOF*.

All modelling codes and software used were freely accessible and open source.

4 Results

4.1 Regolith permeability and thickness in Africa – A literature review

Currently, regolith is only sparsely included into large-scale aquifer parametrizations and is still related to high uncertainties. To fill this gap, a literature review on regolith thickness and permeability was conducted. A total of 56 studies were found, located solely in sub-Saharan Africa, mainly within West and East Africa (Fig. 12). From the total number of studies, 33 studies included values of hydraulic conductivity, which were transformed to permeability and 39 studies reported direct values of regolith thickness. The confidence level for the studies found was mainly between 3 and 4 (medium to high confidence), while only 5 studies were classified as low confidence and 9 studies classified as highest confidence. The clear majority of data was obtained from field data, only three studies used calibrated models. Most frequent methods for hydraulic conductivity were vertical electrical soundings (VES) and pumping tests. To obtain data of regolith thickness, the analysis of borehole data was the most frequent method used. The complete database of regolith thickness and permeability including the respective confidence level, the country where the study was conducted, methods used, sample size and all references, are given in Appendix (Tab. S2).

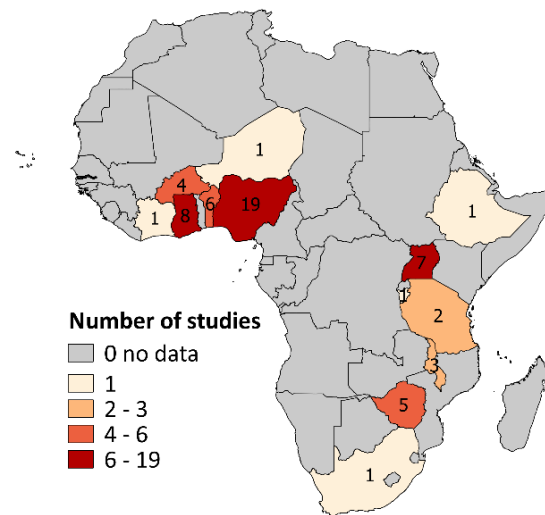


Fig. 12: Number of studies per African country that were found during the literature review.

The geometric mean for all permeability values ($\log(k)_{\text{mean}}$) derived from the literature was -12.37 ± 1.0 m², which is equivalent to a hydraulic conductivity (K) of 0.36 m d⁻¹. The geometric mean of lower limits ($\log(k)_{\text{min}}$) was -13.10 ± 0.9 m² (K: 0.07 m d⁻¹), the geometric mean of upper limits ($\log(k)_{\text{max}}$) was -11.77 ± 0.7 m² (K: 1.44 m d⁻¹) and the geometric mean from average values was -11.96 ± 0.4 m² (K: 0.93 m d⁻¹) (Fig. 13).

The arithmetic mean of all thickness values found in the literature was 27.0 ± 25.4 m. The arithmetic mean for all lower limits was 8.9 ± 9.0 m, for all upper limits it was 47.4 ± 28.9 m and for all average values it was 24.2 ± 11.7 m.

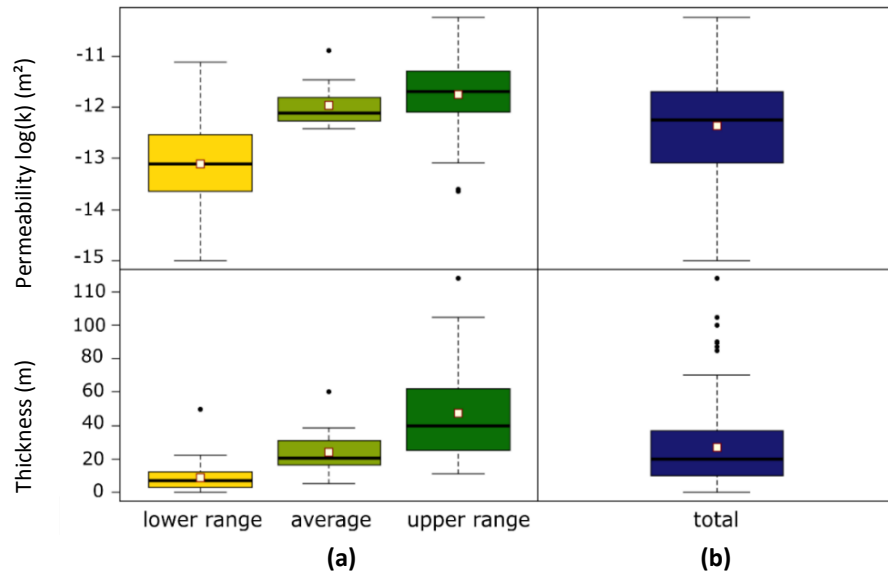


Fig. 13: Summarized regolith permeability and thickness values from the literature review for (a) all lower range, average and upper range values and (b) the total of all values. White squares show the respective geometric mean for regolith permeability or the arithmetic mean for regolith thickness.

4.2 Model parametrization – Regolith layer

With the aim to develop a new aquifer thickness estimate for Africa that includes both deep extensive aquifers and regolith, a sediment/crystalline layer and a regolith layer were developed. Both layers are displayed in Fig 14. The regolith layer shows the topography scenario, with thickest regolith at mountain ridges thinning towards valley bottoms and with the average thickness from all literature values (D_{mean}) applied in eq.8 (see methods 2.4.1). As the average scenario showed the same spatial distribution only without any variation in thickness it is not additionally displayed here. The permanent water tale scenario is depicted in the Pre-Analysis (chapter 2.1, Fig. 4, d).

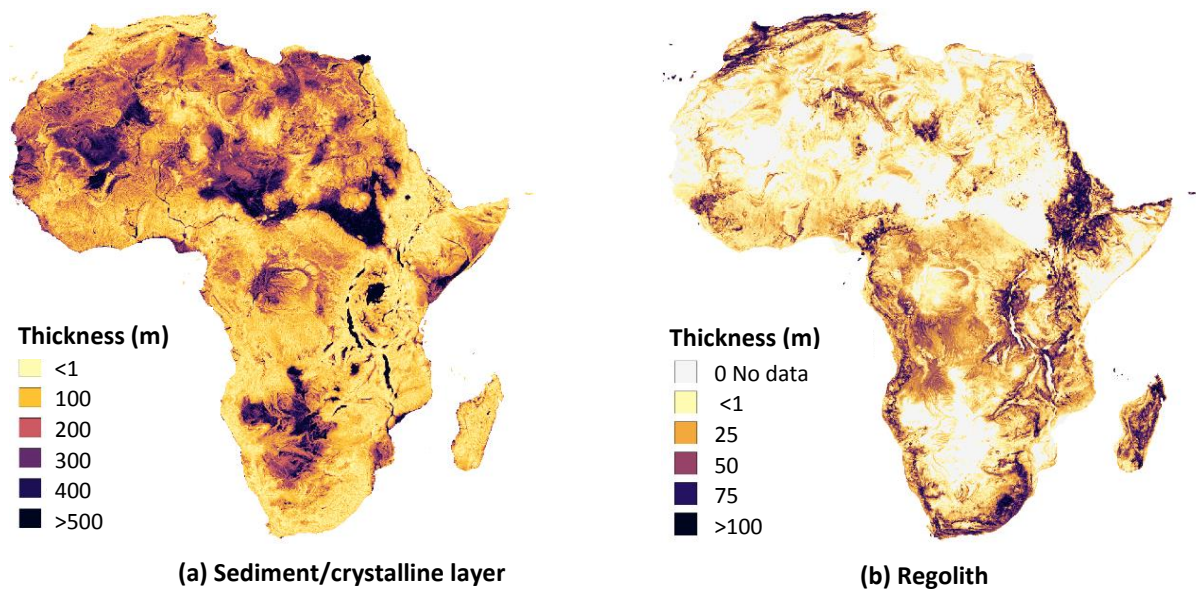


Fig. 14: Thickness of the two layers for the aquifer parametrization, with (a) the sediment/crystalline layer representing extensive deeper aquifer and crystalline basement underlying regolith and (b) the upper regolith layer, representing local regolith over crystalline basement, exemplified for the topography scenario with average thickness.

The sediment/crystalline layer (Fig. 14, a) covered 96.5% of Africa on a 30'' resolution. It had an average thickness of 150 m with its maximum at 1000 m and its minimum at 0.5 m. The clear majority (90%) of grid cells lay within a range of 6 – 521 m. Highest thickness was reached at Africa's large sedimentary basins such as the upper Nile basin, the Kalahari basin, the Chad basin and at the Taoudeni basin.

The regolith layer calculated according to the topography and the average scenario covered 53% of the African continent on a 30'' resolution (for the PWT scenario, see chapter 2.1). If all areas of higher permeable sediments and carbonates, mapped in GLHYMPS 2.0 were excluded, both scenarios covered 39% of the Africa continent. Furthermore, both scenarios covered approximately 70% of the crystalline, mapped in GLHYMPS and GLHYMPS 2.0 and they covered 44% and 71% of all mixed unconsolidated sediments mapped in GLHYMPS and GLHYMPS 2.0, respectively.

The average, minimum and maximum thickness for the regolith layer, calculated according to the topography scenario with D_{\min} , D_{mean} or D_{\max} (eq.8), can be observed in Tab. 4. The relative distribution of thickness for each specific regolith layer is shown in Fig. 15. The arithmetic mean and the standard variation (sd) did not vary more than 2 m from literature values, except for the sd of maximum regolith thickness, which was about twice as high as the sd from literature values. Thickness of the average scenario is not displayed as it was constant over the specific regolith layer, with D_{\min} : 9.1 m, D_{mean} : 26.5 m and D_{\max} : 49.3 m. The thickness distribution of the permanent water table (PWT) scenario is described and depicted in the Pre-Analysis (chapter 2.1, Fig. 4, d).

Tab. 4: Average regolith layer thickness with standard deviation and the absolute minimum and maximum regolith layer thickness of the topography scenario, calculated with average (D_{mean}), minimum (D_{\min}) and maximum thickness (D_{\max}) from literature.

Thickness	Thickness (m)		
	Min	Mean \pm sd	max
D_{\min}	0.1	9.1 \pm 8.0	89.0
D_{mean}	0.3	26.5 \pm 26.0	502.2
D_{\max}	0.5	49.3 \pm 52.1	1390.3

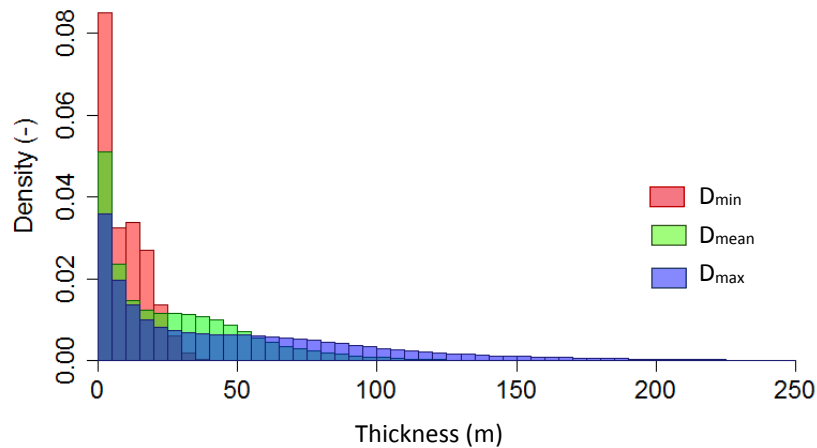


Fig. 15: Relative thickness distribution for the regolith layer that was calculated according to the topography scenario with minimum (D_{\min}), average (D_{mean}) and maximum thickness (D_{\max}).

Exemplified for the parametrization of the regolith layer $Topography-D_{mean}-log(k)_{mean}$ (comp. Tab. 3), transmissivity significantly increased for Africa in comparison to *No-Regolith*. This was especially true for sub-Saharan Africa in regions of crystalline basement aquifers, where no mixed unconsolidated sediments were mapped in GLHYMPS (Fig. 16). Averaged over the continent, the regolith layer transmissivity added a further $5.2 \text{ m}^2 \text{ d}^{-1}$ to the *No-Regolith* transmissivity estimate of $31.8 \text{ m}^2 \text{ d}^{-1}$. Consequently, the new average transmissivity was $37.0 \text{ m}^2 \text{ d}^{-1}$ including regolith. For the parametrization of $Average-D_{mean}-log(k)_{mean}$, average regolith transmissivity was $4.9 \text{ m}^2 \text{ d}^{-1}$, leading to a new average transmissivity of $36.7 \text{ m}^2 \text{ d}^{-1}$. Finally, the average transmissivity of the regolith layer for $PWT-D_{mean}-log(k)_{mean}$ was $3.1 \text{ m}^2 \text{ d}^{-1}$, leading to a new average transmissivity of $34.9 \text{ m}^2 \text{ d}^{-1}$.

As an example, only the transmissivity of the regolith layer $Topography-D_{mean}-log(k)_{mean}$ is depicted and a further transmissivity estimate for *No-Regolith* (Fig. 16). Maps of the average and the PWT scenario are shown in Appendix (Fig. S2); average transmissivity for all variations of regolith layer parametrizations are listed in Appendix 3 (Tab. S3).

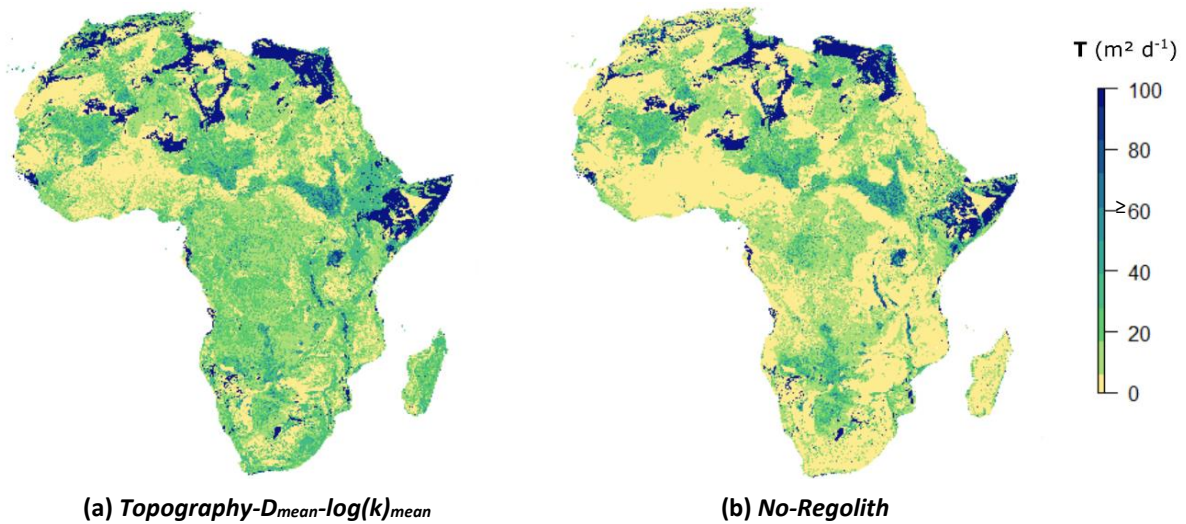


Fig. 16: Transmissivity over Africa where (a) includes a regolith layer that was calculated according to the topography scenario with average permeability and thickness from literature ($Topography-D_{mean}-log(k)_{mean}$), and where (b) was simulated without a regolith layer (*No-Regolith*).

4.3 Sensitivity Analysis

A sensitivity analysis was conducted to assess the sensitivity of simulated groundwater depth to the integration of the three regolith scenarios and their transmissivity (changes in D and $log(k)$) (Fig. 17). The overall sensitivity was low, with a coefficient of variation (CV) smaller than 0.15 at more than 99% of all grid cells. Furthermore, the sensitivity was strikingly similar for a change in the regolith layer scenario or a change in transmissivity with an average CV of 0.013 in both cases (Fig. 17). Therefore, neither the regolith layer scenario nor its transmissivity could be identified as a dominant driving force on the simulated groundwater depth. Solely the spatial variation of sensitivity changed slightly between changes in the regolith layer scenario and in its transmissivity: A change in the transmissivity led to relatively higher CVs in Sub-Saharan Africa, while a change in the regolith scenario led to relatively higher CVs in North Africa (Fig. 17). The highest sensitivity was found in areas of deep simulated groundwater tables (see. chapter 4.5 and comp. Fig. 7) and at higher elevations, where regolith made up a larger proportion of the total aquifer thickness than at lowlands (comp. Fig. 8).

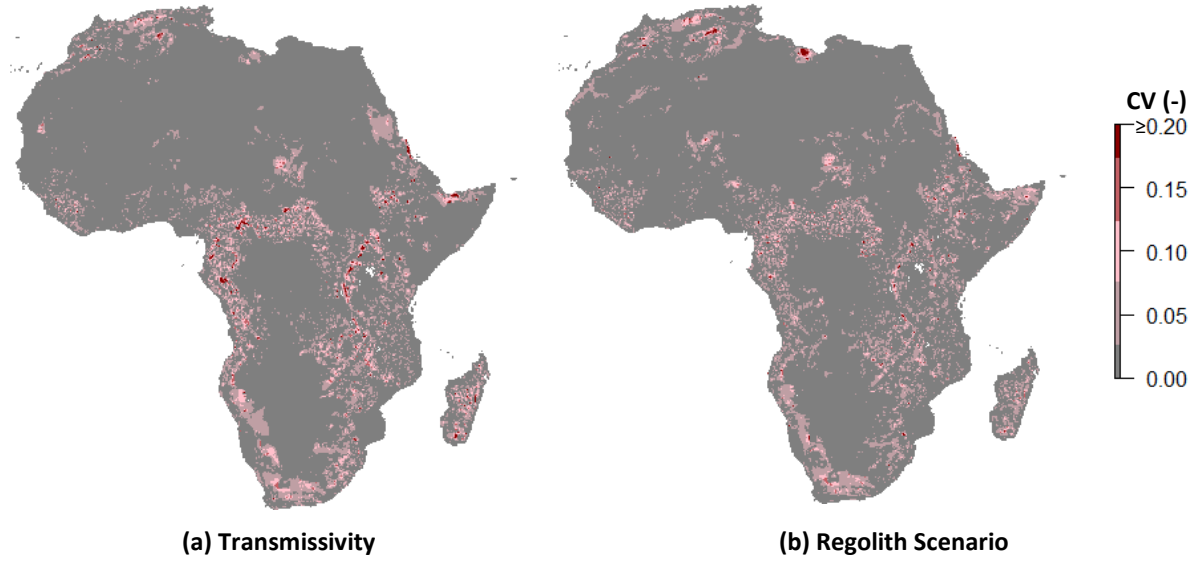


Fig. 17: Spatial distribution of the simulated groundwater depth sensitivity if (a) varying regolith transmissivity or (b) the regolith scenario (topography, average and permanent water table scenario). Sensitivity is expressed by the coefficient of variation (CV).

Although the overall sensitivity was low, changes in the groundwater table depth could still reach more than 100 m compared to the model run without regolith (Fig. 18). In most of the regions where regolith was added, depth to groundwater increased if including a higher permeable regolith layer, while only at some regions in the Sahara depth to groundwater decreased. In Fig. 18 the difference of simulated groundwater depth between *No-Regolith* and all model runs with a regolith layer are displayed. For the different scenarios of regolith (topography, average and PWT scenario), a variation in the magnitude of groundwater depth de- and increase and a slight change in their spatial distribution was noted. More pronounced however, were the de- and increases in simulated groundwater depth, which intensified at higher regolith transmissivities (higher D and/or $\log(k)$). The highest de- and increases in simulated groundwater table depth were found for *Topography- $D_{min}-\log(k)_{min}$* .

4.4 Validation of simulated groundwater heads

Simulated groundwater heads compared reasonably well to the observed groundwater heads with the R^2 varying between 0.919 – 0.930 (Tab.5). Groundwater heads simulated with *No-Regolith*, resulted in a R^2 of 0.928. Most of the groundwater head simulations that include a regolith layer, showed an equal or slightly higher R^2 . Still, 7 out of the 21 runs with regolith showed a lower fit than *No-Regolith*. The worst fit was found for *Topography- $D_{max}-\log(k)_{max}$* . The best model fit was found for *PWT- $\log(k)_{min}$* and *PWT- $\log(k)_{mean}$* .

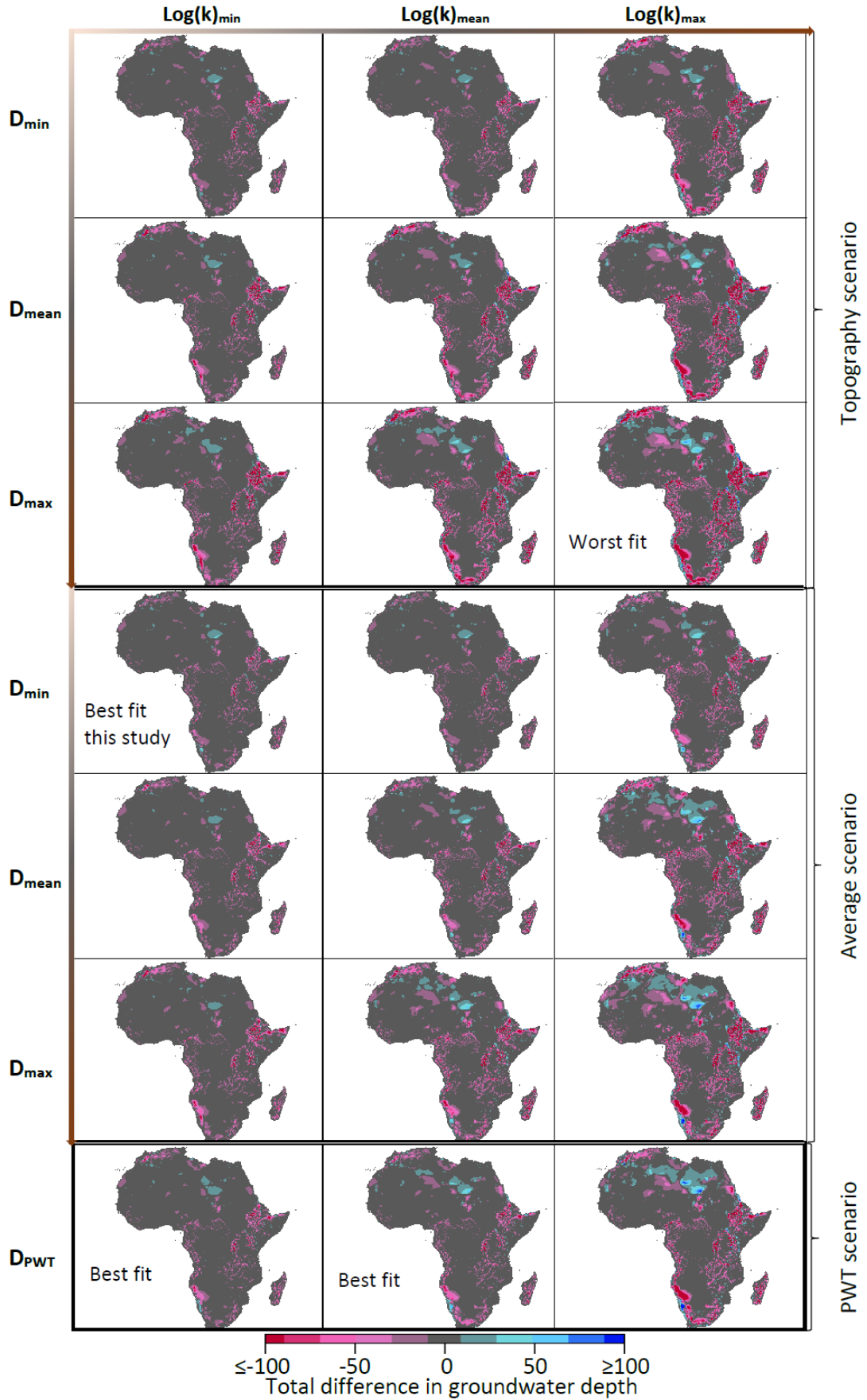


Fig. 18: De- and increase of groundwater depth (m) simulated with a regolith layer, compared to the simulation without a regolith layer (*No-Regolith*). PWT stands for the permanent water table, D stands for the average regolith thickness and $\log(k)$ for its permeability with their min, mean and max derived from literature values. Negative values (red) indicate deeper, positive values (blue) shallower groundwater depth than *No-Regolith*.

Tab. 5: Coefficient of determination (R^2) for the model validation of all regolith layer variations included into the simulation of groundwater heads for Africa. All model fits that were equal to the simulation without a regolith layer (*No-Regolith*) are printed in black, all better model fits are printed in blue and all poorer fits are printed in red.

Thickness	Permeability	R^2		
		Topography scenario	Average Scenario	PWT scenario
D_{\min}	$\log(k)_{\min}$	0.929	0.929	-
	$\log(k)_{\text{mean}}$	0.929	0.929	-
	$\log(k)_{\max}$	0.929	0.929	-
D_{mean}	$\log(k)_{\min}$	0.928	0.929	-
	$\log(k)_{\text{mean}}$	0.926	0.929	-
	$\log(k)_{\max}$	0.921	0.928	-
D_{\max}	$\log(k)_{\min}$	0.927	0.928	-
	$\log(k)_{\text{mean}}$	0.923	0.928	-
	$\log(k)_{\max}$	0.919	0.928	-
D_{PWT}	$\log(k)_{\min}$	-	-	0.930
	$\log(k)_{\text{mean}}$	-	-	0.930
	$\log(k)_{\max}$	-	-	0.927

Note: D is the average regolith thickness and $\log(k)$ is the average regolith permeability, with their min, mean and max derived from literature values. PWT is the permanent water table scenario, derived from Pelletier et al. (2016).

Overall, the R^2 for all model runs was similar, nevertheless, a tendency arose with better model fits for the average scenario and the PWT scenario with lower regolith transmissivities (D_{\min} and $\log(k)_{\min}$). Worse fits were generally found for the topography scenario and towards higher transmissivities (D_{\max} and $\log(k)_{\max}$).

Although the best model fit was found for the PWT scenario, the average scenario was chosen as the most promising scenario in this study. This was done under the rational that the differences of model fits between the average scenario and the PWT scenario were small (comp. Tab. 4) but the average scenario held the advantage of a considerably simpler calculation method. More specifically, the regolith parametrization *Average- D_{\min} - $\log(k)_{\min}$* was chosen, as the model fit for all regolith scenarios tended to get better at smaller transmissivities (D_{\min} and/or $\log(k)_{\min}$). Thus, the observed against the simulated groundwater heads for the most promising model run (*Average- D_{\min} - $\log(k)_{\min}$*) are displayed in Fig. 19. Model fit was slightly better for regions that were covered by the regolith layer, although an overall underestimation of groundwater heads became visible for all regions, which means that the groundwater depth was generally simulated too deep.

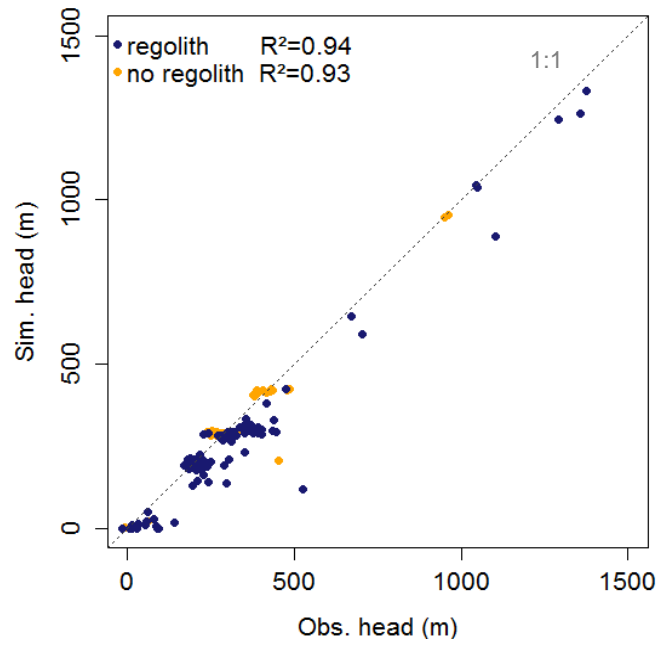


Fig. 19: Observed groundwater table heads against simulated ones from the most promising model run (*Average- D_{min} -log(k_{min})*), separated into regions covered by a regolith layer and regions without regolith coverage.

In Fig. 20 the spatial distribution of residuals (observed heads – simulated heads) is mapped. Positive residuals indicate that simulated heads were smaller than the observed ones. Consequently, groundwater table depth was generally simulated too deep. Negative residuals must be interpreted the other way around.

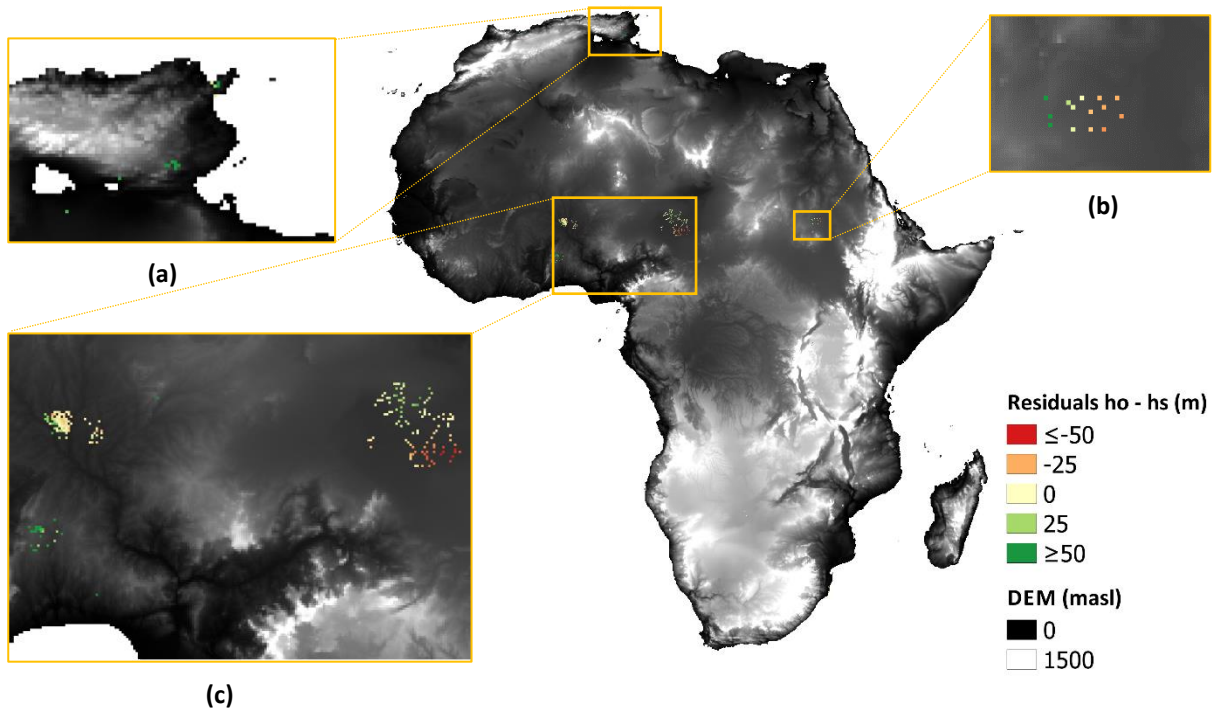


Fig. 20: Digital elevation map (DEM) of Africa with residuals (observed (h_o) - simulated heads (h_s)) for the groundwater head simulation according to the most promising model run (*Average- D_{min} -log(k_{min})*). Subfigures (a-c) are close-up maps of the regions with the highest frequencies of observation data points.

More than 90% of all residuals lay in a range between -36 m and 100 m with the median at 5 m (Fig. 21, a). Furthermore, there was a clear tendency of higher residuals at deeper observed groundwater tables, but only on a regional scale not on the continental scale (Fig. 21, b).

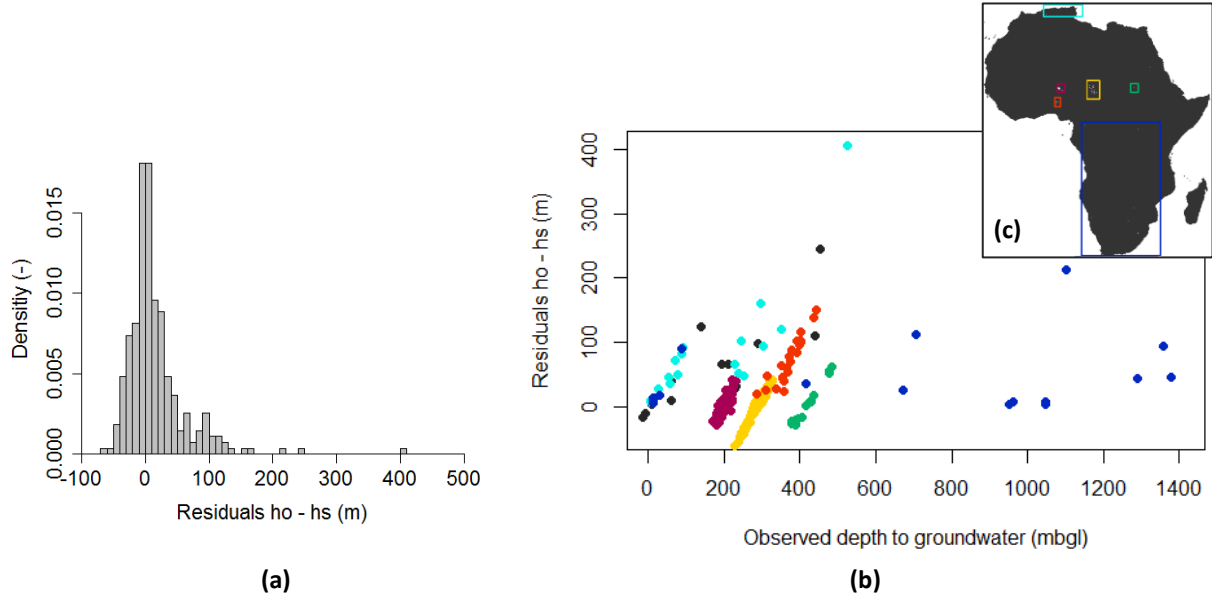


Fig. 21: Residuals (observed (ho) - simulated heads (hs)) for Africa, with (a) the relative distribution of residuals and (b) the residuals in dependency to observed groundwater depth, colored for their specific origin, which is marked in the Africa map at the top right corner (c).

In accordance to higher residuals at deeper groundwater tables, residuals tendentially increased at higher elevations, when the regolith layer was thicker and the sediment/crystalline thinner. On the contrary, depth to groundwater was only underestimated at locations with a thick sediment/crystalline layer, which held especially true around the Chad sedimentary basin (see Fig. 20, c).

4.5 Simulated groundwater depth and ground- and surface water interactions

In Fig. 22, the simulated depth to groundwater for the most promising model run (*Average- D_{min} -log(k)_{min}*) is shown. Most values lay in a range between 0.1 m and 100 m of depth. Shallow depth was found mainly at the large sedimentary basins with thick aquifers, deeper groundwater tables were found mainly in the desert regions of the Sahara and the Namib Desert and in mountainous regions in east Africa and at the Atlas Mountains. Depth increased slightly in comparison to *No-Regolith* (Fig. 23), with an average groundwater depth of 160.5 m for *Average- D_{min} -log(k)_{min}* and an average of 158.4 m for *No-Regolith*. Still, differences were small and the general pattern of the groundwater depth distribution if simulating with or without a regolith layer remained similar (Fig. 23). For this reason, no map of simulated groundwater depth without the integration of a regolith layer is shown, as no differences became visible.

In most areas covered by the regolith layer, groundwater tables were simulated deeper than the depth of regolith, hence, groundwater was located solely within the crystalline sediment layer. For the most promising model run, only 1% of all grid cells showed groundwater tables located within the regolith layer. The minimum percentage of water tables within regolith was found for the PWT scenario with $\log(k)_{max}$ with 0.03% (Appendix, Fig. S3). By far the greatest percentage of grid cells with groundwater tables located within the regolith layer was found for the average scenario, especially at high regolith thickness and low permeability. Consequently, the maximum of groundwater tables located within regolith was found for *Average- D_{max} -log(k)_{min}* with 25.1% (Appendix, Fig. S3).

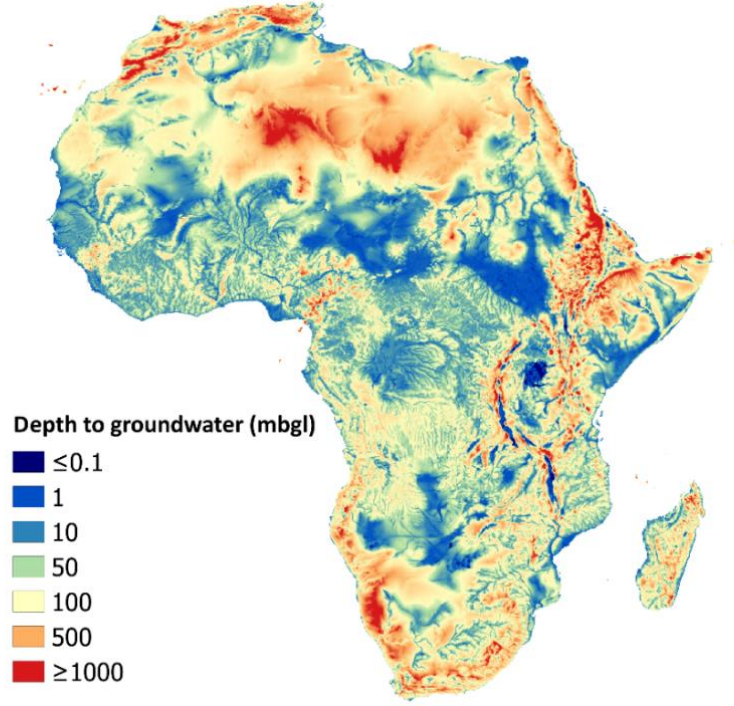


Fig. 22: Depth to groundwater in meters below the ground level (mbgl), simulated with the most promising regolith layer from this study ($Average-D_{min}-log(k)_{min}$) included into the aquifer parametrization.

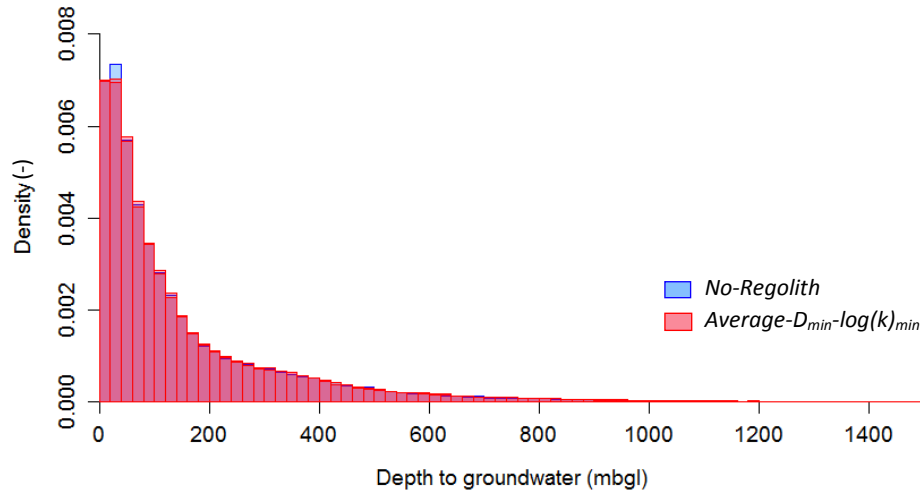


Fig. 23: Histogram of depth to groundwater for the model run that was simulated with the most promising regolith layer ($Average-D_{min}-log(k)_{min}$) and the one without a regolith layer (*No-Regolith*).

In Fig. 24, the simulated ground- and surface water interactions (Q_b) for the most promising model run ($Average-D_{min}-log(k)_{min}$) are depicted, showing either groundwater drainage (-) or river infiltration (+). With the increase in simulated groundwater depth, the grid cells effected by groundwater drainage or river infiltration decreased by 8.8% in comparison between the $Average-D_{min}-log(k)_{min}$ and *No-Regolith* (Fig. 24 and Fig. 25). This decrease mainly affected smaller drainage volumes in regions of high recharge (comp. Fig. 10). On the other hand, in the areas where groundwater drainage and river infiltration were still simulated, a shift towards higher drainage/infiltration volumes was noted with an average increase of 0.6% in groundwater drainage and an average increase of 1.7% in river infiltration.

Besides this general increase, the equilibrium also slightly changed towards a higher percentage of river infiltration than groundwater drainage, although most interactions were still dominated by groundwater drainage (Fig. 24 and Fig. 25).

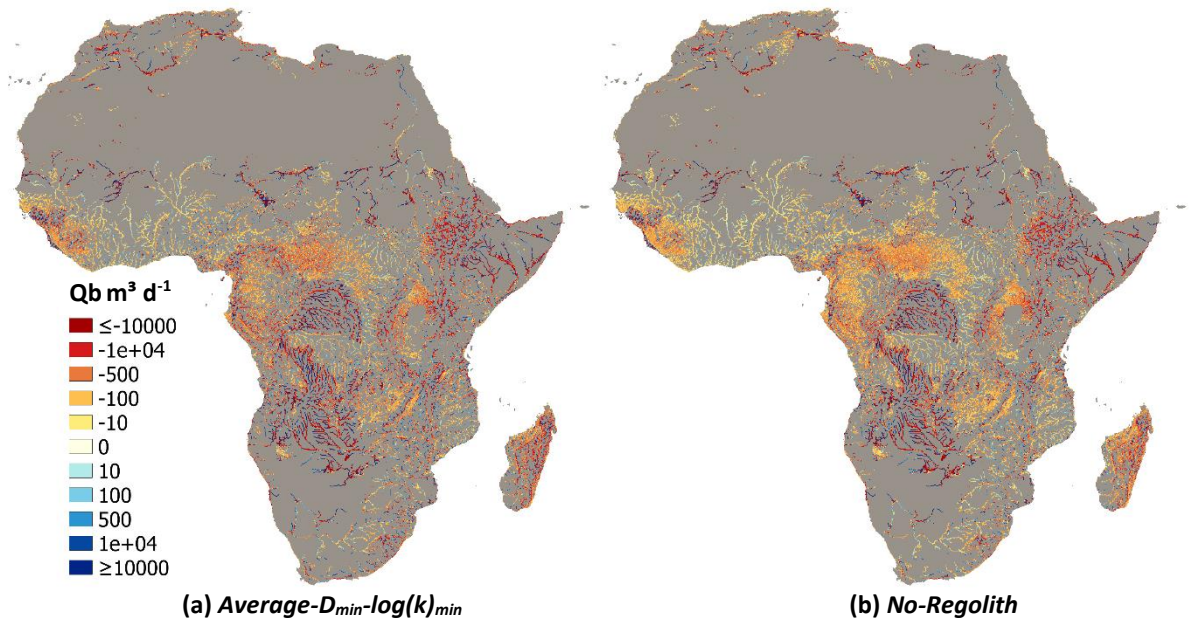


Fig. 24: Simulated groundwater drainage (Q_b negative) or river infiltration (Q_b positive), with (a) the simulation integrating the most promising regolith layer ($Average-D_{min}-log(k)_{min}$) and (b) the simulation without a regolith layer ($No-Regolith$).

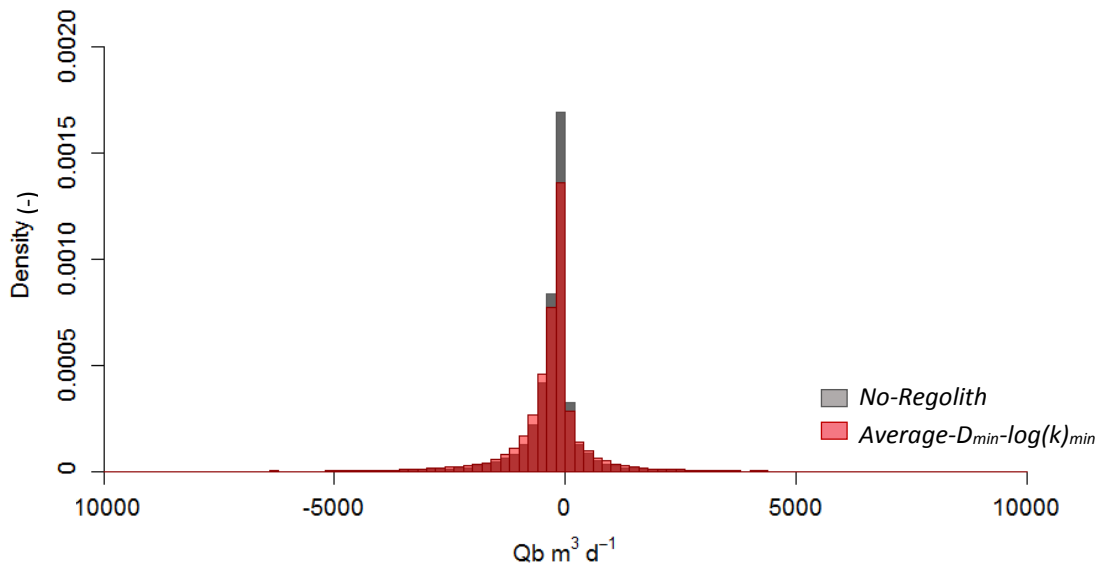


Fig. 25: Histogram of simulated groundwater drainage (Q_b negative) or river infiltration (Q_b positive) for simulations with the most promising regolith layer $Average-D_{min}-log(k)_{min}$ and without the integration of a regolith layer ($No-Regolith$).

5 Discussion

5.1 The global groundwater model PCR-GLOBWB-MODFLOW

The large-scale groundwater model PCR-GLBOWB-MODFLOW is an appropriate model choice if the aim is to simulate groundwater depth or groundwater drainage and river infiltration. It allows to implement two layers of different hydraulic properties, which were regolith and extensive deeper aquifers besides and underneath the regolith in this study. Therefore, the subdivision of aquifers on both the horizontal and the vertical extent are possible, hence it gives a closer reproduction of real world conditions. This horizontal subdivision of aquifers would not be possible with PCR-GLOBWB alone or with the global groundwater model from Fan et al. (2013) both holding the opportunity for only a one-layer groundwater store.

Further advantages are that MODFLOW enables lateral flow, the simulation of flow paths and the interaction between ground and surface water in form of groundwater drainage and river infiltration. In this study, lateral flow was enhanced by the higher permeability of regolith compared to crystalline basements. Moreover, ground- and surface water interactions decreased in their spatial extent but increased in total volumes (as further discussed in chapter 5.4). Both components, lateral flow and ground- and surface water interactions, are therefore relevant processes that should be included in large-scale groundwater modelling for Africa. Groundwater flow paths, as simulated by de Graaf et al. (2015), play only a minor role at crystalline basement aquifers in Africa, while they become important at the sedimentary basins and arid regions of Africa (de Graaf et al., 2015). Due to the focus on crystalline basement aquifers and regolith in this study, groundwater path flows were not analyzed, although their general importance for groundwater modelling in Africa is unquestioned.

However, as MODFLOW was coupled offline to PCR-GLOBWB in this study, the quality of simulated groundwater depth, groundwater drainage or river infiltration depends on the quality of the input data from PCR-GLOBWB (recharge and river discharge). Uncertainties in simulated groundwater recharge or river discharge transfer directly to the modelling results from MODFLOW. Furthermore, the dependency on PCR-GLOBWB inputs can be a disadvantage if these input datasets are provided at a coarser resolution compared to the desired model simulation, because resolution upscaling is inherently related to high uncertainties (Prudhomme et al., 2002).

Finally, running PCR-GLOBWBW-MODFLOW steady state, as done in this study, did not allow for the simulation of temporal changes over the year or with scenarios of decreasing water availability due to climate change and/or human interactions. However, this study allowed for a first estimate on the sensitivity of simulated groundwater depth, groundwater drainage and river infiltration to the integration and parametrization of regolith. Comparing simulated groundwater heads to observed ones furthermore allowed to select the best fitting set of parameters for regolith that can be used for the parametrization of future transient simulations and might also be applicable in other regions of the world. Thus, this study should be seen as an initial step towards integrating regolith into groundwater modelling for Africa and on the global scale.

5.2 Aquifer parametrization

All large-scale datasets on aquifer thickness and permeability that were compared in the pre-analysis (chapter 2) showed huge differences in the way they were compiled and in the range and spatial distribution of their data itself. This high variation made it mandatory to analyze and compare all up to date datasets with regard to the specific modelling goal, before choosing the most promising dataset, identifying possibilities for adaption, and using it for the final aquifer parametrization.

In this study, the algorithm from de Graaf et al. (2017, 2015) was chosen to calculate an extensive aquifer layer that covered both deep productive aquifers of sedimentary deposits and sediments and the crystalline basement underneath regolith - called sediment/crystalline layer. After an adaption towards Africa-specific aquifer thickness (eq. 5), the sediment/crystalline layer ranged mainly between 6-521 m of depth and therefore compared reasonably well to saturated aquifer thickness from Bonsor and MacDonald (2011) combined with the depth to bedrock from MacDonald et al. (2012) that ranged from <25 up to >500 m (Fig. 26). The average thickness of 150 m for the sediment/crystalline layer was clearly lower than the original thickness from de Graaf et al. (2017, 2015) and did therefore approximate towards the lower aquifer thickness from Shangguan et al. (2017) and Pelletier et al. (2016). Nevertheless, maps of MacDonald et al. (2012) and Bonsor and MacDonald (2011) clearly indicate a large proportion of aquifers deeper than 250 m (especially in North and South Africa), which was neither reached by the dataset from Pelletier et al. (2016) nor by Shangguan et al. (2017). Both datasets of aquifer thickness (Pelletier et al., 2016; Shangguan et al., 2017) are thus believed to underestimate the transmissivity of Africa's aquifers if used for the parametrization of groundwater models.

The spatial extent of the sediment/crystalline layer increased significantly in comparison to the aquifer thickness estimate from de Graaf et al. (2017, 2015). This is because the sediment/crystalline layer was calculated on a 30'' resolution, while the estimate from de Graaf et al. (2017, 2015) was calculated on a 5' resolution. The sediment/crystalline layer developed in this study is therefore considered suitable as extensive layer representing aquifers besides and underneath regolith.

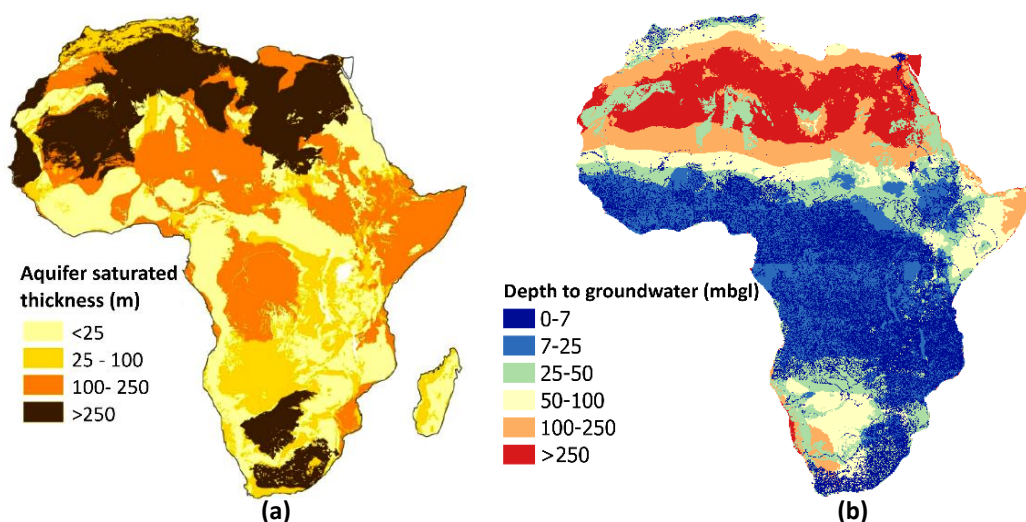


Fig. 26: Quantitative groundwater maps (a) of the aquifer saturated thickness from Bonsor and MacDonald et al. (2011) and (b) of the estimated depth to groundwater in meters below the ground level (mbgl) from MacDonald et al. (2012) (maps derived from the British geological survey © NERC 2011).

The GLHYMPS dataset, used to parametrize the permeability of the sediment/crystalline layer was the only available permeability dataset for extensive and deeper aquifers represented by the sediment/crystalline layer and was thus the only option. The new version GLHYMPS 2.0 characterized an upper layer permeability, excluding regolith, and was thus not suitable for the specific focus of this study (see chapter 2.3). Regarding the first research question, it is thus argued that aquifer thickness from de Graaf et al. (2017, 2015) with further adaptations towards Africa's aquifer characteristics and a higher resolution (30''), together with the permeability from GLHYMPS, are currently the most reliable parameters for deep extensive aquifers of Africa (represented by the sediment/crystalline layer).

5.2.1 Regolith layer

Three different regolith scenarios were tested in this study: (1) the topography scenario, (2) the average scenario (see chapter 3.3.1 for both) and (3) the permanent water table (PWT) scenario (see chapter 2.2). Both, the topography and the average scenario were developed in this study, while the PWT scenario was developed by Pelletier et al. (2016).

For the parametrization of the regolith scenarios a literature review on regolith thickness (D) and permeability ($\log(k)$) was conducted. This literature review consisted of 56 studies, which is approximately one third of the 152 studies compiled by MacDonald et al. (2012) for the creation of quantitative groundwater maps of Africa. As the literature review of this study only focused on regolith and not on the whole continent like the one from MacDonald et al. (2012), the number of studies is considered to be appropriate for a reliable first estimate of regolith hydraulic properties. Furthermore, it is the most extensive compilation of regolith thickness and permeability until today.

Nevertheless, large parts of sub-Saharan Africa were still not covered by the studies found during the literature review, especially in South and Central Africa (comp. Fig. 12). These gaps also include the regions that were mapped as lateritic soils in the GLHYMPS dataset from Gleeson et al. (2014). Although, no studies could be found, the occurrence of regolith underneath of lateritic soils is highly probable, as lateritic soils indicate strong weathering processes. Consequently, these regions were covered by the regolith layer in all three regolith scenarios.

Nonetheless, D and $\log(k)$ estimates, derived through the literature review, were judged as appropriate by hydrogeology experts from the IGE (personal communication, Grenoble, May 2018). The derived estimates are, therefore, assumed to represent reasonably accurate regolith parameters that can be extrapolated over the continent.

Based on the literature review, a lower bound regolith thickness estimate (D_{\min}) and average thickness (D_{mean}) and an upper bound thickness estimate (D_{\max}) were calculated. These parameters were inserted into eq. 8 for the calculation of the topography scenario or assumed as constant thickness for the average scenario. Due to the constant thickness in the average scenario, however, the standard variation (sd) from literature was not represented in this scenario. On the contrary, in the topography scenario the sd was accurately matched if inserting D_{\min} and D_{mean} into eq.8 but not if inserting D_{\max} . In this case, the calculated thickness reached unrealistically high values (>1000 m, comp. Tab. 4), which is not in accordance to the maximum thickness of regolith in any of the studies found. To illustrate, the highest regolith thickness found was 128 m in Burundi, by Bakundukize et al. (2016).

As the calculation method of the topography scenario was kept very simple, it might lag further controlling factors, such as the erosion at steep slopes for example (Braun et al., 2016). Future studies that strike to address this shortcoming, while keeping the approach simple, could limit the regolith thickness to a maximum thickness value as proposed by Strudley et al. (2006) (for example 128 m) to exclude unrealistically high values.

The PWT scenario was the only regolith scenario tested that was not developed in this study, but developed by Pelletier et al. (2016). However, this regolith layer was subjected to great uncertainties. For example, the very high values of >50 m in the desert regions were an artefact of very deep water tables in these regions. Weathering is in fact enhanced in the unsaturated zone, hence the permanent water table can limit regolith thickness (Braun et al., 2016; Holbrook et al., 2014). Nevertheless, the method of purely limiting regolith to the permanent water table neglects the fact that the availability of water that percolates through the unsaturated zone is a driving factor for the weathering process (Braun et al., 2016; Graham et al., 2010) and that this water is naturally limited in arid regions. On the other

hand, regolith in the non-arid regions was estimated very thin compared to results from the literature review (e.g. Aizebeokhai and Oyeyemi, 2018; Muchingami et al., 2012; Taylor and Howard, 2000). Average regolith thickness from the literature suggests approximately two times higher average regolith thickness in these non-arid regions of sub-Saharan Africa. This very thin regolith estimate can be attributed to the equilibrium water table depth from Fan et al. (2013) that was taken as a proxy for the permanent water table and further divided by two to account for shallow water tables that were not captured by the 30'' resolution. This approach has three drawbacks: (1) the equilibrium water table is generally higher than the permanent water table thus if regolith thickness is limited to the equilibrium water table it is estimated too thin. (2) The equilibrium water table of Fan et al. (2013) is biased towards shallower water tables, an observation that becomes especially visible in comparison to the map of depth to groundwater from MacDonald et al. (2012) (see chapter 5.3.3). (3) The division of groundwater depth by two was mainly justified by the fact that, with this, the average regolith thickness fits the reported values of regolith thickness between 10-40m (Pelletier et al., 2016). The average of estimated regolith thickness was however, strongly influenced by the thicker regolith estimates in arid regions, while in the regions where regolith is commonly reported, regolith thickness did not match that range. Besides the great uncertainties, the PWT scenario was the first available estimation on regolith thickness a global scale. It is therefore advisable to test it hydrologically to understand its possible impact on groundwater simulations, which are discussed in chapter 5.3.

The regolith layer from the topography and the average scenario covered 53% of Africa and the PWT scenario covered 47%. All three regolith layer scenarios were, therefore, too large compared to reports of an approximate regolith coverage of 40% over Africa (MacDonald and Davies, 2000; Vouillamoz et al., 2015). If subtracting all regions that were reclassified from mixed unconsolidated towards higher permeable sediments in GLHYMPS 2.0, the coverage was 39% and therefore clearly better. This indicates that the integration of GLHYMPS 2.0 holds further potential to the improvement of Africa's aquifer parametrization that was not yet assessed by this study.

The regolith transmissivity calculated for all three scenarios with the average regolith thickness and permeability from literature (D_{mean} and $\log(k)_{\text{mean}}$) lay between $3.9 - 5.2 \text{ m}^2 \text{ d}^{-1}$. These transmissivity values compare well to local studies on regolith transmissivity that reported $4.8 \text{ m}^2 \text{ d}^{-1}$ in Uganda (Taylor and Howard, 2000) or $4.3 \text{ m}^2 \text{ d}^{-1}$ in Nigeria (Tijani et al., 2015).

5.3 Impact of regolith parametrization on simulated groundwater depth

5.3.1 Sensitivity

It was hypothesized in this study that the simulation of groundwater depth is highly sensitive to the integration of regolith. This hypothesis, however, could be rejected as the overall coefficient of variation (CV), which was calculated as a measure of sensitivity, was low. Highest sensitivities rarely exceeded a CV of 0.15. This finding is in accordance to a previous sensitivity analysis from de Graaf et al. (2015) on a global scale, who found low overall sensitivity if varying the hydraulic conductivity, the aquifer thickness or the recharge for one single aquifer layer. In Africa, the CV from de Graaf et al. (2015) reached up to 1 in the Saharan desert and was generally highest in regions that are not covered by regolith. Therefore, these regions could not show any sensitivity in this study, as only the regolith parametrization was tested.

The higher sensitivity of groundwater depth at higher elevations found in this study can be explained by the fact, that estimated regolith contributed a higher proportion to the total aquifer thickness in these areas. This holds especially true for the topography scenario (comp. Fig. 18), as it was calculated inversely proportional to the sediment/crystalline layer. It therefore contributed even stronger to the total

aquifer thickness at high elevations. Importantly, at all model runs the highest changes in simulated groundwater depth coincided with deep groundwater tables. Changes in deep groundwater tables, however, play only a minor role for environmental cycles and hand pump abstractions as they generally do not reach deep groundwater. This indicates that the impact of the regolith parametrization on simulated groundwater depth is highest where its impact is of minor relevance.

Generally, the sensitivity analysis showed that the simulated depth to groundwater increased for most regions of Africa, if integrating a regolith layer. This pattern can be explained by the higher transmissivity of regolith that enhances the vertical and lateral flow of groundwater. Consequently, groundwater tables were simulated the deepest, where regolith transmissivity was the highest. Nevertheless, the comparison of simulated groundwater heads to observed ones showed a systematic underestimation of groundwater heads, meaning that groundwater depth was generally simulated too deep in all model runs. However, a more permeable regolith layer leads to the simulation of even deeper groundwater tables, indicating that its integration into the model parametrization might not improve the simulation of groundwater depth as it was hypothesized in this study.

5.3.2 Validation

In general, all simulations of groundwater heads compared well to the observed data with only a small variation in the coefficient of determination (R^2) comparing observed against simulated heads. This held true for all model runs of different regolith parametrizations and even when excluding the regolith layer (comp. Tab. 5). Therefore, also the second hypothesis of a clear improvement in the model outcome with the integration of regolith was rejected. All simulations of groundwater heads could compete with the R^2 from de Graaf et al. (2015) that lay in-between 0.86 for global mountain ranges and 0.94 for global sediment basins. However, no regolith scenario from this study was able to surpass an R^2 of 0.94. Residuals spread around zero (comp. Fig. 21), confirming the generally good model fit. However, the residuals also reflected the clustered pattern of the observed data points, which increased with increasing observed groundwater depth on the regional scale (comp. Fig. 21). Still, an increase of residuals with increasing groundwater depth indicates that the general pattern of groundwater heads was matched by the simulation, even on the regional scale.

Although the second hypothesis of a clear improvement in modelling outcomes was rejected, a slight improvement in the simulation of groundwater heads, compared to the simulation without regolith, was possible. The results (chapter 4.4) show that simulated groundwater heads compared better to observed heads when the transmissivity of regolith was relatively low (D_{\min} and/or $\log(k)_{\min}$) and when either the permanent water table or the average scenario was applied. The topography scenario however, showed the worst model fits with most of the simulations being worse than the one for *No-Regolith*.

There are two possible explanations for the trend of better model fits with a lower regolith transmissivity: (1) the average transmissivity from the compiled studies was estimated too high, hence there was a bias in the observed regolith thickness and/or permeability towards thicker and more permeable regolith at the sampled bore wells. This is plausible as regolith forms an important aquifer, hence most bore wells are sited where regolith is thicker, and wells are filtered at deeper zones where regolith tends to be more permeable (comp. Fig. 3). The second explanation is that (2) the underlying crystalline, which was parametrized by the permeability from GLHYMPS (Gleeson et al., 2014) was estimated too high, hence the overall aquifer permeability was estimated too high. This is especially plausible in areas where the permeability of mixed unconsolidated sediments for lateritic soils was mapped in an attempt to characterize regolith. Hence, the permeability of the underlying layer, where permeability from GLHYMPS was assigned to, is not representative for underlying crystalline, but rather for the overlaying regolith. In this context, it should be noted that the $\log(k)_{\min}$ of -13.1 m^2 is very close to the permeability

for mixed unconsolidated sediments in GLHYMPS of -13.0 m^2 . As best model fits were found if assigning $\log(k)_{\min}$ to the regolith layer, it can be assumed that the permeability in GLHYMPS for lateritic soils has been already a good approximation. However, this estimate from GLHYMPS is not suitable for the parametrization of underlying deeper crystalline basement permeability.

The topography scenario, as previously discussed, reached very high regolith thickness at mountain ridges. Mountain ridges are, however, the regions where water tables were anyway simulated very deep and the residuals show that here the overestimation of water table depth was the most pronounced. A very thick regolith layer leads to a relatively strong increase in transmissivity and an even deeper simulation of water tables. This, most likely, is the explanation for the lower R^2 for simulations from the topography scenario.

The PWT scenario showed thickest regolith in areas of deep water tables. However, in these regions regolith thickness often reached the pre-defined limit of 50 m and got disconnected from the permanent water table. In this case, groundwater was located far beneath the regolith layer. The impact of the regolith parametrization of the PWT scenario on simulated groundwater depth is thus smallest where its thickness is greatest. On the contrary, in the tropics where groundwater is shallow and more likely to be influenced by regolith, regolith thickness was estimated relatively thin, around 10 m (similar to D_{\min} of 9.1 m). The impact of the PWT scenario on simulated groundwater depth was, thus, small compared to the other scenarios with a higher regolith thickness in areas of shallow groundwater (D_{mean} and D_{max}). The impact of the average scenario with D_{\min} , however, was also small, as it had a similarly small regolith thickness as the PWT scenario in areas of shallow groundwater. Therefore, the PWT scenario and the average scenario with D_{\min} showed very similar modelling outcomes.

Both, the average and the PWT scenario had the highest R^2 , especially if combined with $\log(k)_{\min}$. The average scenario however, was by far the simplest approach. Furthermore, by simply assuming a constant average regolith thickness, the uncertainties of a methodological structure that was based on one single predictor such as the permanent water table or topography, which is certainly not the only driving factor for regolith thickness (e.g. Braun et al., 2016; Wright, 1992), were avoided. Therefore, acknowledging the fact that regolith formation is a complex and regionally variable process (Braun et al., 2016) that is still not fully understood, an average regolith thickness might be the most robust approach considering today's knowledge. Regarding the second research question of this study, it is thus argued that the most promising regolith estimate for groundwater modelling is an average thickness of approximately 10 m and a permeability of -13.1 m^2 that are applied constantly over crystalline basement aquifers in Africa.

Groundwater depth vs. regolith depth

Nevertheless, discussing the variation in model fits, one should not forget that overall all, simulations showed a high R^2 and that differences were small. The main explanation for this is probably that, to a great extent, the simulated groundwater table fell below the regolith layer at all simulations. Hence, the groundwater flow was no longer influenced by the regolith parametrization but only by the parametrization of the underlying sediment/crystalline layer that was the same for all simulations. This pattern was most pronounced for the PWT scenario where as good as all grid cells showed groundwater tables below regolith (99.97%). This can be explained by the fact that the PWT scenario explicitly assumed the regolith thickness to be limited to the groundwater table. Moreover, groundwater tables used to calculate this layer were biased towards shallow groundwater (see above), hence, groundwater tables were located below regolith. As topography and the permanent water table are closely related parameters (comp. Fig. 8), the same logic also applies for the topography scenario (only less pronounced). Although the average scenario with D_{\min} did neither follow the permanent water table nor

the topography, its regolith thickness was still thinner than the one from the PWT scenario. Consequently, regolith from the average scenario with D_{\min} was too shallow to reach groundwater. The only exception were the average scenarios with D_{mean} and D_{\max} , where up to a quarter of regolith held groundwater. In this case the regolith thickness neither followed the groundwater table nor was it too thin to reach the simulated groundwater depth. Consequently, groundwater was stored within regolith at regions where the groundwater table was shallower than average regolith thickness. This held true especially for the simulations with $\log(k)_{\min}$, because with a lower permeability, groundwater percolates slower through the regolith.

It is commonly reported that regolith serves as an important aquifer (e.g. Foster, 2012; Holbrook et al., 2014; Lachassagne et al., 2011), therefore groundwater must be located within the regolith, hence most simulations still do not correctly simulate real world conditions. Taken this into account, again the average scenario performed best.

Reflection on model validation

Apart from good and worse model fits, it is crucial to consider the uncertainties in the observed data that was used for the model validation. In this study, only a very sparse validation dataset of groundwater heads (transferred from observed groundwater depth) was used, with only a few hundred data points over the whole continent (compared to a total of $> 1,500,000$ observation points globally, Fan et al., 2013). Furthermore, data points were heavily clustered within a few regions around $10\text{-}15^\circ$ latitude (comp. Fig. 11). Although roughly half of the data points were covered by the estimated regolith layers, they were not located in the regions of deep groundwater tables that showed higher sensitivity to the integration of a regolith layer. The greatest impact of the integration of regolith was therefore not covered by the validation data and consequently not assessed. In conclusion, validation results should not be overestimated but only be used for a rough initial estimate on model performance. Furthermore, simulated groundwater heads assumed natural conditions, excluding all artificial abstraction. The observed groundwater heads, however, reflected real world conditions and were likely influenced by abstractions. Thus, observed groundwater heads were smaller (groundwater depth was higher) than under natural conditions. Consequently, the underestimation of groundwater heads (overestimation of depth) from simulations, as discussed above, might have been even higher than assessed by the comparison of observed versus simulated heads.

An additional point to consider when looking at the quality of the validation, is the comparison with groundwater heads instead of groundwater depth. It is common sense in large-scale groundwater modelling to validate with groundwater heads (e.g. Henriksen et al., 2003; House et al., 2016; Sutanudjaja et al., 2011; Wada et al., 2016). The reasoning behind this is that heads measure the potential energy that is driving groundwater flow and that heads are therefore physically more meaningful (Sutanudjaja et al., 2011). In field however, only groundwater depth is measured and therefore the more direct variable to validate. On the contrary, groundwater heads are subtracted from a common digital elevation model (DEM) and typically lead to a higher R^2 than simulated against observed depth. Nonetheless, for the comparison of the suitability of different regolith parametrizations amongst each other, the validation with groundwater heads is believed to be appropriate and the better option regarding groundwater flow. Still, one should keep in mind that the comparison between observed and simulated groundwater heads in this study might have led to higher R^2 's than a comparison with groundwater depth.

5.3.3 Simulated groundwater depth

With the argumentation that (1) differences between all model runs were small, (2) the average scenario was the simplest approach with lower uncertainties and (3) simulated groundwater heads compared better to observed ones when using a low regolith transmissivity, the regolith layer *Average- D_{min} - $\log(k)_{min}$* (see. Tab. 3) was chosen as the most promising approach for parameterizing regolith. Consequently, results in simulated groundwater depth and ground- and surface water interactions from this regolith parametrization are discussed in more detail:

The magnitude and spatial distribution of simulated groundwater depth was highly similar to the one simulated by de Graaf et al. (2017) (Fig. 27). If divided into the groundwater depth-ranges from MacDonald et al. (2012) no difference became visible, neither on the map nor on at the histogram (Fig 27, a and b). Again, this underlines the small impact of integrating a regolith layer, which led to the rejection of the second hypothesis. At both simulations, modelled via PCR-GLOBWB-MODFLOW, the groundwater table was mainly controlled by (1) the ocean, (2) topography and (3) groundwater recharge, which is explained in the following:

On the continental scale, the ocean was the main driving force for groundwater depth. Shallow groundwater occurred all along the coastline and expanded inland in regions of low elevations, as can be observed at the southern coast of Somalia or around Senegal (comp. Fig. 22), for example. At areas of high elevations close to the coastline (e.g. South Africa, at the Atlas Mountains in Morocco or Algeria) this effect was overlain by the topographic influence. Topography mainly controlled the inland water table depth leading to shallow groundwater in areas of low elevations (e.g. upper Nile basin and Chad basin) and deep groundwater at high elevations (e.g. Atlas Mountains, Ethiopian Highlands). However, recharge could dominate over the topographic influence if recharge was low. This effect is most visible in the Sahara where extremely low recharge led to groundwater tables more than 1000m deep although the elevation was mainly low (comp. Fig. 7 and Fig 22), which would have led to shallow ground water levels if topography would have been the main driving force. On the contrary, at regions of high groundwater recharge *and* a high elevation, the topography influence dominated, leading to deep water tables, as can be observed at the Ethiopian Highlands. On the contrary, MacDonald et al. (2012) mapped shallow groundwater in the Ethiopian Highlands, accounting for a high density of local groundwater tables that were not captured by the simulation with PCR-GLOBWB-MODFLOW.

The general comparison of estimated depth to groundwater between the main available approaches published until today (de Graaf et al., 2017; Fan et al., 2013; MacDonald et al., 2012) revealed great differences. As discussed before, this study was similar to the estimate from de Graaf et al. (2017). The depth to groundwater estimate from Fan et al. (2013) in contrast, estimated clearly shallower groundwater tables over the whole continent. The general pattern was similar as the driving factors on groundwater depth were the same (ocean, topography and recharge), but as only soil permeability, decreasing with depth, was included as aquifer parametrization and no ground- and surface water interactions were implemented, the model lacks important hydro(geo)logical input and is thus biased towards shallower groundwater. In comparison to the observed data (Fig. 27, in grey), the estimate from Fan et al. (2013) was too shallow while the estimate from this study and the study from de Graaf et al. (2017) were too deep. However, under the aspect that the validation dataset did not cover desert and regions of very deep water tables, the estimate from this study and from de Graaf et al. (2017) are believed to be more reliable.

A good reference for Africa's groundwater depth is the estimate from MacDonald et al. (2012) because it was based on real data and expert knowledge. Although being rather coarse and not made for the simulation of future changes in water availability (due to climate change and human interactions), it is

believed to give the most reliable estimate of real groundwater depth on a continental scale until today. According to their estimate, groundwater tables in arid regions, especially the Sahara, were clearly better met by the groundwater depth estimations from PCR-GLOBWB-MODFLOW, while in sub-Saharan Africa, groundwater tables were still simulated too deep and therefore the estimate from Fan et al. (2013) appears to be the better one. This might be attributed to the fact that local water tables at high elevations were still not accurately captured by the simulations of this study, as discussed already above for the Ethiopian Highlands, or that the drainage level was estimated too deep with current surface water estimates. Future studies might be able to address the shortcoming of limited computational power in this study by further resolution upscaling, which would enable to include higher levels of detail, hence capture a higher percentage of local aquifers.

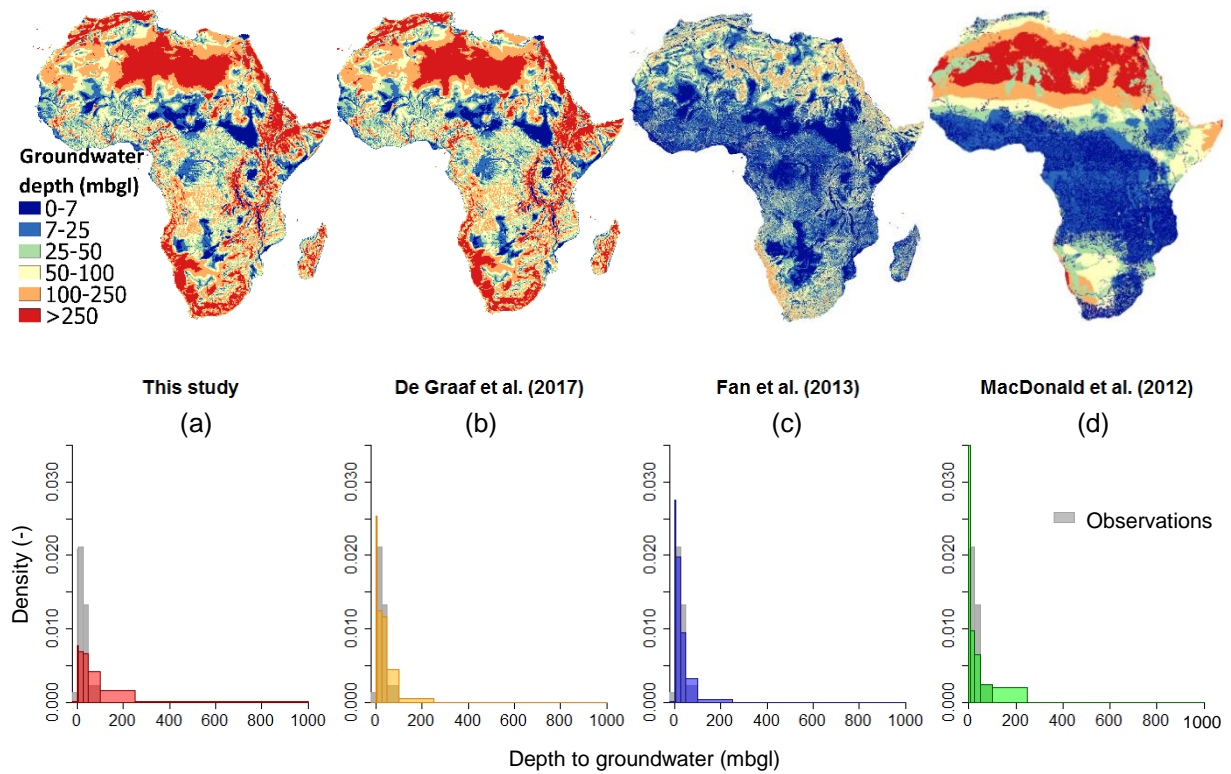


Fig. 27: Maps and histograms of estimated depth to groundwater from (a) this study, (b) the study from de Graaf et al. (2017), (c) the study from Fan et al. (2013) and the study from MacDonald et al. (2012). All estimates were classified according to the groundwater depth ranges from MacDonald et al. (2012) in meters below ground level (mbgl). Observed groundwater depth data, compiled by Fan et al. (2013), is displayed in grey in the background of the histograms.

Finally, it can be stated that the differences in estimated groundwater depth are highly depended on how they were compiled (de Graaf et al., 2017; Fan et al., 2013; MacDonald et al., 2012) while the integration of regolith is of minor importance in the face of continent wide groundwater depth estimates.

5.4 Simulated groundwater drainage and river infiltration

While the integration of regolith seems to be of minor importance for simulated groundwater depth in Africa, changes in the simulated ground- and surface water interaction were slightly more pronounced. Importantly, they occurred at shallow water tables and are thus of higher relevance for humans and environmental cycles. The changes were that areas affected by ground- and surface water interactions decreased with the integration of regolith. However, in areas that still showed ground- and surface water

interaction after the integration of a regolith layer, groundwater drainage (-) or river infiltration (+) increased (comp. Fig. 26). The decrease in affected areas can be explained by the slight increase in groundwater depth, as ground- and surface water interactions are highly sensitive to even small changes at shallow groundwater tables. With an increased groundwater depth, more areas get disconnected from rivers and streams, meaning that neither the river supports the groundwater anymore, nor does the groundwater support the river with baseflow. The intensification of existing interactions can be explained by the higher permeability of regolith that enhanced vertical flow from rivers to groundwater and the other way around.

The important point in the changes in ground- and surface water interactions with the integration of regolith is that they occurred only at shallow groundwater. While deep groundwater is anyway disconnected from surface water at deeper groundwater tables, changes at shallow groundwater can have severe impacts on the environment (Giordano, 2009) and the accessibility for hand pumps, which are extensively used in sub-Saharan Africa (Foster, 2012; MacDonald and Davies, 2000). However, no validation was possible, as this would have required a long-term and wide spread dataset on river baseflows. Such a dataset, however, did not exist for Africa and it remains unclear whether the simulated ground- and surface water interactions were simulated better or even worse with the tested regolith parametrization.

Nevertheless, the change in ground- and surface water interactions was probably the most striking one, with most implications for the interpretation of groundwater availability for humans and environmental cycles. It should therefore be a target of future studies focus on this issue and find possibilities to validate the interactions of ground- and surface water, especially in sub-Saharan Africa. Additionally, transient simulation would allow to reveal more details of the dynamics of ground- and surface water interactions than the steady state simulations of this study. For example, the effect on baseflow during dry seasons could be simulated as well as scenarios of human induced water abstractions. Based on the results of the steady state simulations of this study, it is expected that the integration of a regolith layer at transient simulations should consequently reveal: (1) a higher risk of rivers falling dry during droughts, (2) a higher risk of depletion due to human induced water abstractions, and (3) a faster groundwater recovery during rainy periods.

6 Conclusion and Outlook

This study presents a promising option to simulate Africa's groundwater resources with PCR-GLOBWB-MODFLOW and a modified and improved aquifer parametrization based on an extensive literature review. The improved parametrization consists of two separate layers that were passed on to MODFLOW. One layer represents extensive and deep aquifers and was called sediment/crystalline layer in this study as it covers the aquifer characteristics besides and below regolith. The thickness of this layer was calculated on a 30'' resolution with the algorithm from de Graaf et al. (2015, 2017) and further adapted with the help of maps from MacDonald et al. (2012). The assigned permeability was taken from GLHYMPS. The second layer represents regolith overlying crystalline bedrock. The most promising results for the regolith parametrization were a constant thickness (average scenario) of approximately 10 m and a permeability of approximately -13.1 m^2 , which were both the lower bound estimates from literature.

In general, the sensitivity of simulated groundwater depth to the integration and parametrization of regolith was low and most pronounced at areas of deeper groundwater tables where a change in groundwater depth is of minor relevance for environmental cycles and for handpump abstraction. Also, the changes in simulated groundwater depth between different regolith scenarios were marginal, leading to the conclusion that complex approaches to simulate regolith might be overrated, while a simple approach of applying an average regolith thickness might already be sufficient and even be subject to lower uncertainties.

For none of the tested parametrizations a clear improvement in model performance through the integration of regolith hydraulic properties could be confirmed. However, this result should not be overinterpreted due to the sparse and clustered groundwater depth data used for validation. Nevertheless, changes in groundwater depth remained clearly higher between different studies compared to the changes caused by the integration of regolith within one hydrological model (PCR-GLOBWB-MODFLOW). This indicates that regolith is not one of the major driving factors for current model uncertainties over Africa.

Nevertheless, changes in ground- and surface water interactions through the integration of regolith hydraulic parameters were more pronounced than for the simulated groundwater depth. Importantly, these changes occurred at shallow groundwater tables with mayor importance for environmental cycles and handpump abstractions. However, these changes could not be validated due to a lack of datasets that compile river baseflow for Africa. Future studies that aim (1) to validate findings on ground- and surface water interactions in Africa and (2) to give a better insight into the model performance with or without regolith will thus require a consistent and extensive dataset on river baseflows. It would be highly interesting to investigate whether the here adopted 'best' regolith parametrization that was validated with simulated groundwater heads, could be confirmed by a validation of ground- and surface water interactions.

As a further outlook, future studies should conduct transient simulations of groundwater depth, groundwater drainage and river infiltration, integrating the new parametrization developed in this study. Transient simulations would give further insights into the impacts of the regolith parametrization on groundwater abstraction, decreasing recharge with climate change and groundwater recovery during rainy seasons. However, for transient simulations with integrated regolith, a storage coefficient for the regolith layer is required which was not compiled in this study, as it is not needed for steady state simulations. Future studies that aim to simulate Africa's groundwater resources transiently should thus

compile a regolith-specific storage coefficient, for example from regolith porosity values in the literature, as done in this study for regolith thickness and permeability.

Another interesting research focus would be the hydrological testing of permeability estimates from GLHYMPS 2.0, via integrating GLHYMPS 2.0 into a model's parametrization. In this context, an upper thickness layer would be required that enables to integrate both regolith and upper unconsolidated sediments adequately. Results in this study indicate that the separation between higher permeable sediments from GLHYMPS 2.0 and regolith layers from this study might lead to a better estimate of the spatial extent of regolith. A combination of the new regolith estimates from this study and an updated permeability for unconsolidated sediments would thus be a promising. This could further improve the model parametrization and hence the simulation of Africa's groundwater resources.

The model outcome might be further enhanced through resolution upscaling towards hyper resolution modelling. Unfortunately, the simulation at hyper resolution was not possible in this study due to a lack in computational power. However, the preceding aquifer parametrization was conducted on 30'' (hyper resolution) which improved the aquifer coverage and integrated an additional degree of details. Running PCR-GLOBWB-MODFLOW on a 30'' resolution would thus be the consequent next step to improve simulations of Africa's groundwater resources. Nonetheless, also the groundwater recharge and river discharge from PCR-GLOBWB would be needed on a hyper resolution to ensure the quality of simulations.

Finally, the new regolith parametrization should also be tested outside of Africa, in other regions where regolith forms a significant part of local aquifers, such as Scandinavia, India or Australia. This study could not assess the full potential of regolith impacts on large-scale groundwater modelling, due to insufficient validation data on groundwater heads and a lack in validation data on ground- and surface water interactions. Nevertheless, the developed parametrization is the first hydrologically tested aquifer parametrization that includes regolith on a large scale. Testing and adapting the presented parametrization also in other regions of the world that potentially hold more validation data, could, in the long run, potentially improve the parametrization of large-scale groundwater models on a global scale.

References

- Aizebeokhai, A.P., Oyeyemi, K.D., 2018. Geoelectrical characterisation of basement aquifers: the case of Iberekodo, southwestern Nigeria. *Hydrogeol. J.* 26, 651–664.
- Akanmu, T.O., Adewumi, A.J., 2016. Geophysical Characterization of Aquifer Parameters within Basement Complex Rocks Using Electrical Sounding Data from the Polytechnic, Ibandan, Southwestern Nigeria. *Int. J. Sci. Res. Knowl.* 112–126. <https://doi.org/10.12983/ijrsrk-2016-p0112-0126>
- Bakundukize, C., Mtoni, Y., Martens, K., Van Camp, M., Walraevens, K., 2016. Poor understanding of the hydrogeological structure is a main cause of hand-dug wells failure in developing countries: A case study of a Precambrian basement aquifer in Bugesera region (Burundi). *J. Afr. Earth Sci.* 121, 180–199.
- Bala, A.E., Edivie, O.M., Byami, J., 2011. Borehole depth and regolith aquifer hydraulic characteristics of bedrock types in Kano area, Northern Nigeria. *Afr. J. Environ. Sci. Technol.* 5, 228–237.
- Bierkens, M.F., Bell, V.A., Burek, P., Chaney, N., Condon, L.E., David, C.H., de Roo, A., Döll, P., Drost, N., Famiglietti, J.S., 2015. Hyper-resolution global hydrological modelling: What is next? Everywhere and locally relevant. *Hydrol Process* 29, 310–320.
- Bonsor, H.C., MacDonald, A.M., 2011. An initial estimate of depth to groundwater across Africa. British Geological Survey Open Rep. OR/11/067.
- Börker, J., Hartmann, J., Amann, T., Romero-Mujalli, G., 2018. Terrestrial sediments of the earth: development of a global unconsolidated sediments map database (GUM). *Geochem. Geophys. Geosystems* 19, 997–1024.
- Braun, J., Mercier, J., Guillocheau, F., Robin, C., 2016. A simple model for regolith formation by chemical weathering. *J. Geophys. Res. Earth Surf.* 121, 2140–2171.
- Braune, E., Xu, Y., 2010. The role of ground water in Sub-Saharan Africa. *Groundwater* 48, 229–238.
- Burney, J.A., Naylor, R.L., 2012. Smallholder Irrigation as a Poverty Alleviation Tool in Sub-Saharan Africa. *World Dev.* 40, 110–123. <https://doi.org/10.1016/j.worlddev.2011.05.007>
- Chilton, P.J., Foster, S.S.D., 1995. Hydrogeological characterisation and water-supply potential of basement aquifers in tropical Africa. *Hydrogeol. J.* 3, 36–49.
- Chilton, P.J., Smith-Carington, A.K., 1984. Characteristics of the weathered basement aquifer in Malawi in relation to rural water supplies. *IAHS Press.* 144, 57–72.
- Courtois, N., Lachassagne, P., Wyns, R., Blanchin, R., Bougairé, F.D., Somé, S., Tapsoba, A., 2010. Large-Scale Mapping of Hard-Rock Aquifer Properties Applied to Burkina Faso. *Groundwater* 48, 269–283.
- Da Costa, M.L., da Silva Cruz, G., de Almeida, H.D.F., Poellmann, H., 2014. On the geology, mineralogy and geochemistry of the bauxite-bearing regolith in the lower Amazon basin: Evidence of genetic relationships. *J. Geochem. Explor.* 146, 58–74.
- Dai, A., 2013. Increasing drought under global warming in observations and models. *Nat. Clim. Change* 3, 52.
- De Graaf, I.E., van Beek, L.P., Gleeson, T., Moosdorf, N., Schmitz, O., Sutanudjaja, E.H., Bierkens, M.F., 2017. A global-scale two-layer transient groundwater model: Development and application to groundwater depletion. *Adv. Water Resour.* 102, 53–67.
- De Graaf, I.E.M., Sutanudjaja, E.H., van Beek, L.P.H., Bierkens, M.F.P., 2015. A high-resolution global-scale groundwater model. *Hydrol. Earth Syst. Sci.* 19, 823–837.
- Dewandel, B., Lachassagne, P., Wyns, R., Maréchal, J.C., Krishnamurthy, N.S., 2006. A generalized 3-D geological and hydrogeological conceptual model of granite aquifers controlled by single or multiphase weathering. *J. Hydrol.* 330, 260–284.
- Deyassa, G., Kebede, S., Ayenew, T., Kidane, T., 2014. Crystalline basement aquifers of Ethiopia: their genesis, classification and aquifer properties. *J. Afr. Earth Sci.* 100, 191–202.
- Dregne, H.E., 2011. *Soils of arid regions*. Elsevier. Amsterdam.
- Dürr, H.H., Meybeck, M., Dürr, S.H., 2005. Lithologic composition of the Earth's continental surfaces derived from a new digital map emphasizing riverine material transfer. *Glob. Biogeochem. Cycles* 19.
- Fan, Y., Li, H., Miguez-Macho, G., 2013. Global patterns of groundwater table depth. *Science* 339, 940–943.

- Foster, S., 2012. Hard-rock aquifers in tropical regions: using science to inform development and management policy. *Hydrogeol. J.* 20, 659–672.
- Giordano, M., 2009. Global groundwater? Issues and solutions. *Annu. Rev. Environ. Resour.* 34, 153–178.
- Gleeson, T., Moosdorf, N., Hartmann, J., Beek, L.P.H., 2014. A glimpse beneath earth's surface: GLobal HYdrogeology MaPS (GLHYMPS) of permeability and porosity. *Geophys. Res. Lett.* 41, 3891–3898.
- Gleeson, T., Smith, L., Moosdorf, N., Hartmann, J., Dürr, H.H., Manning, A.H., van Beek, L.P., Jellinek, A.M., 2011. Mapping permeability over the surface of the Earth. *Geophys. Res. Lett.* 38.
- Gleick, P.H., 2003. Global Freshwater Resources: Soft-Path Solutions for the 21st Century. *Science* 302, 1524–1528. <https://doi.org/10.1126/science.1089967>
- Graham, R.C., Rossi, A.M., Hubbert, K.R., 2010. Rock to regolith conversion: Producing hospitable substrates for terrestrial ecosystems. *GSA Today* 20, 5. <https://doi.org/10.1130/GSAT57A.1>
- Harbaugh, A.W., Banta, E.R., Hill, M.C., McDonald, M.G., 2000. MODFLOW-2000, The U. S. Geological Survey Modular Ground-Water Model-User Guide to Modularization Concepts and the Ground-Water Flow Process. Open-File Rep. U Geol. Surv. 134.
- Hartmann, J., Moosdorf, N., 2012. The new global lithological map database GLiM: A representation of rock properties at the Earth surface. *Geochem. Geophys. Geosystems* 13.
- Henriksen, H.J., Trolborg, L., Nyegaard, P., Sonnenborg, T.O., Refsgaard, J.C., Madsen, B., 2003. Methodology for construction, calibration and validation of a national hydrological model for Denmark. *J. Hydrol.* 280, 52–71.
- Holbrook, W.S., Riebe, C.S., Elwaseif, M., L. Hayes, J., Basler-Reeder, K., L. Harry, D., Malazian, A., Dosseto, A., C. Hartsough, P., W. Hopmans, J., 2014. Geophysical constraints on deep weathering and water storage potential in the Southern Sierra Critical Zone Observatory. *Earth Surf. Process. Landf.* 39, 366–380. <https://doi.org/10.1002/esp.3502>
- House, A.R., Thompson, J.R., Sorensen, J.P.R., Roberts, C., Acreman, M.C., 2016. Modelling groundwater/surface water interaction in a managed riparian chalk valley wetland. *Hydrol. Process.* 30, 447–462.
- Huscroft, J., Gleeson, T., Hartmann, J., Börker, J., 2018. Compiling and mapping global permeability of the unconsolidated and consolidated Earth: GLobal HYdrogeology MaPS 2.0 (GLHYMPS 2.0). *Geophys. Res. Lett.* 45, 1897–1904.
- IPCC, 2014. Mitigation of Climate Change. Contribution of Working Group III to the Fifth Assessment Report of the Intergovernmental Panel on Climate Change. Camb. Univ. Press Camb. UK N. Y. NY.
- IPCC, 2007. The Fourth Assessment Report of the Intergovernmental Panel on Climate Change. Geneva Switz.
- Karlsson, C.S.J., Jamali, I.A., Earon, R., Olofsson, B., Mörtberg, U., 2014. Comparison of methods for predicting regolith thickness in previously glaciated terrain, Stockholm, Sweden. *Geoderma* 226, 116–129.
- Kraijenhoff Van De Leur, D.A., 1958. A study of non-steady groundwater flow with special reference to a reservoir coefficient. *Ing.* 70, 87–94.
- Lacey, G., 1930. Stable channels in alluvium. Minutes of the Proceedings of the Institution of Civil Engineers. Thomas Telford-ICE Virtual Library, pp. 259–292.
- Lachassagne, P., Wyns, R., Dewandel, B., 2011. The fracture permeability of hard rock aquifers is due neither to tectonics, nor to unloading, but to weathering processes. *Terra Nova* 23, 145–161.
- MacDonald, A.M., Bonsor, H.C., Dochartaigh, B.É.Ó., Taylor, R.G., 2012. Quantitative maps of groundwater resources in Africa. *Environ. Res. Lett.* 7, 024009.
- MacDonald, A.M., Davies, J., 2000. A brief review of groundwater for rural water supply in sub-Saharan Africa. BGS Technical Report WC/00/33
- Manning, R., Griffith, J.P., Pigot, T.F., Vernon-Harcourt, L.F., 1890. On the flow of water in open channels and pipes. Institution of Civil Engineers of Ireland. 20, 161–207
- McDonald, M.G., Harbaugh, A.W., 1988. A modular three-dimensional finite-difference ground-water flow model. US Geological Survey Reston, VA. Washington D.C.
- Miguez-Macho, G., Fan, Y., 2012. The role of groundwater in the Amazon water cycle: 2. Influence on seasonal soil moisture and evapotranspiration. *J. Geophys. Res. Atmospheres* 117, D15114. <https://doi.org/10.1029/2012JD017540>

- Muchingami, I., Hlatywayo, D.J., Nel, J.M., Chuma, C., 2012. Electrical resistivity survey for groundwater investigations and shallow subsurface evaluation of the basaltic-greenstone formation of the urban Bulawayo aquifer. *Phys. Chem. Earth Parts ABC* 50, 44–51.
- Ok, T., Kanae, S., 2006. Global hydrological cycles and world water resources. *science* 313, 1068–1072.
- Parsekian, A.D., Singha, K., Minsley, B.J., Holbrook, W.S., Slater, L., 2015. Multiscale geophysical imaging of the critical zone. *Rev. Geophys.* 53, 1–26.
- Pavelic, P., Villholth, K.G., Shu, Y., Rebelo, L.-M., Smakhtin, V., 2013. Smallholder groundwater irrigation in Sub-Saharan Africa: country-level estimates of development potential. *Water Int.* 38, 392–407.
- Pavich, M.J., Leo, G.W., Obermeier, S.F., Estabrook, J.R., 1989. Investigations of the characteristics, origin, and residence time of the upland residual mantle of the Piedmont of Fairfax County, Virginia. 1352, 58.
- Pelletier, J.D., Broxton, P.D., Hazenberg, P., Zeng, X., Troch, P.A., Niu, G.-Y., Williams, Z., Brunke, M.A., Gochis, D., 2016. A gridded global data set of soil, intact regolith, and sedimentary deposit thicknesses for regional and global land surface modeling. *J. Adv. Model. Earth Syst.* 8, 41–65.
- Prudhomme, C., Reynard, N., Crooks, S., 2002. Downscaling of global climate models for flood frequency analysis: where are we now? *Hydrol. Process.* 16, 1137–1150.
- Rempe, D.M., Dietrich, W.E., 2014. A bottom-up control on fresh-bedrock topography under landscapes. *Proc. Natl. Acad. Sci.* 111, 6576–6581.
- Ruddock, E.C., 1967. Residual soils of the Kumasi District in Ghana. *Geotechnique* 17, 359–377.
- Schaller, M.F., Fan, Y., 2009. River basins as groundwater exporters and importers: Implications for water cycle and climate modeling. *J. Geophys. Res. Atmospheres* 114.
- Schneider, A., Jost, A., Coulon, C., Silvestre, M., Théry, S., Ducharne, A., 2017. Global-scale river network extraction based on high-resolution topography and constrained by lithology, climate, slope, and observed drainage density. *Geophys. Res. Lett.* 44, 2773–2781.
- Shangguan, W., Hengl, T., Mendes de Jesus, J., Yuan, H., Dai, Y., 2017. Mapping the global depth to bedrock for land surface modeling. *J. Adv. Model. Earth Syst.* 9, 65–88.
- St. Clair, J., Moon, S., Holbrook, W.S., Perron, J.T., Riebe, C.S., Martel, S.J., Carr, B., Harman, C., Singha, K., 2015. Geophysical imaging reveals topographic stress control of bedrock weathering. *Science* 350, 534–538.
- Strudley, M.W., Murray, A.B., Haff, P.K., 2006. Regolith thickness instability and the formation of tors in arid environments. *J. Geophys. Res. Earth Surf.* 111.
- Sutanudjaja, E.H., Beek, R. van, Wanders, N., Wada, Y., Bosmans, J.H., Drost, N., Ent, R.J., de Graaf, I.E., Hoch, J.M., Jong, K. de, 2018. PCR-GLOBWB 2: a 5 arcmin global hydrological and water resources model. *Geosci. Model Dev.* 11, 2429–2453.
- Sutanudjaja, E.H., van Beek, L.P., de Jong, S.M., van Geer, F.C., Bierkens, M.F.P., 2011. Large-scale groundwater modeling using global datasets: a test case for the Rhine-Meuse basin. *Hydrol. Earth Syst. Sci.* 15, 2913–2935.
- Taylor, R., Howard, K., 2000. A tectono-geomorphic model of the hydrogeology of deeply weathered crystalline rock: evidence from Uganda. *Hydrogeol. J.* 8, 279–294.
- Tessema, A., Nzotta, U., Chirenje, E., 2014. Assessment of Groundwater Potential in Fractured Hard Rocks around Vryburg, North West Province, South Africa. *Water Res. Comm. Pretoria WRC Rep.* 13.
- Thomas, M.F., 1966. Some geomorphological implications of deep weathering patterns in crystalline rocks in Nigeria. *Trans. Inst. Br. Geogr.* 173–193.
- Thornthwaite, C.W., 1948. An approach toward a rational classification of climate. *Geogr. Rev.* 38, 55–94.
- Tijani, M.N., Alich, A.U., Seybatou, D., 2015. Characterization of weathered basement aquifers: implication for groundwater recharge. *Energy Sources Part Recovery Util. Environ. Eff.* 37, 1853–1860.
- Tindimugaya, C., 1995. Regolith importance in groundwater development, in: WEDC Conference. Water, Engineering and Development Centre, pp. 281–283.
- Van Beek, L.P., Bierkens, M.F., 2009. The global hydrological model PCR-GLOBWB: conceptualization, parameterization and verification. *Utrecht Univ. Utrecht Neth.*

- Van Beek, L.P., Wada, Y., Bierkens, M.F., 2011. Global monthly water stress: 1. Water balance and water availability. *Water Resour. Res.* 47.
- Villholth, K.G., 2013. Groundwater irrigation for smallholders in Sub-Saharan Africa—a synthesis of current knowledge to guide sustainable outcomes. *Water Int.* 38, 369–391.
- Vörösmarty, C.J., Douglas, E.M., Green, P.A., Revenga, C., 2005. Geospatial indicators of emerging water stress: an application to Africa. *AMBIO J. Hum. Environ.* 34, 230–236.
- Vouillamoz, J.-M., Lawson, F.M.A., Yalo, N., Descloitres, M., 2015. Groundwater in hard rocks of Benin: Regional storage and buffer capacity in the face of change. *J. Hydrol.* 520, 379–386.
- Wada, Y., de Graaf, I.E., van Beek, L.P., 2016. High-resolution modeling of human and climate impacts on global water resources. *J. Adv. Model. Earth Syst.* 8, 735–763.
- Wilford, J.R., Searle, R., Thomas, M., Pagendam, D., Grundy, M.J., 2016. A regolith depth map of the Australian continent. *Geoderma* 266, 1–13.
- World Health Organization, UNICEF, 2017. Progress on drinking water, sanitation and hygiene: 2017 update and SDG baselines.
- Wright, E.P., 1992. The hydrogeology of crystalline basement aquifers in Africa. *Geol. Soc. Lond. Spec. Publ.* 66, 1–27.

Appendix

Supplement to chapter 3

Tab. S 1: Confidence levels and their respective criteria, assigned to studies of regolith thickness and permeability in Africa

Confidence level	Confidence criteria
5 Very High	<ul style="list-style-type: none"> - Study published within the last 10 years (from 2018 backwards) - Methods are explained in detail - Methods for permeability: pump tests (sample size ≥ 50) or electric resistivity measurement (sample size ≥ 10) or broad scale assessment on hydrogeologic reports (>100) - Methods for thickness: borewell data and/or drilling logs (sample size ≥ 50) or broad scale assessment on hydrogeologic reports (>100) - Peer reviewed journal
4 High	<ul style="list-style-type: none"> - Methods explained (pump test, slug test, resistivity, borewells or drill logs) - More than 20 wells or more than 5 transects - Conference paper - Standard paper > 200 citations
3 Medium	<ul style="list-style-type: none"> - Methods explained or values reported with explanation - Hydrological models - Technical report or dissertation
2 Low	<ul style="list-style-type: none"> - Methods not properly explained - Reported values properly cited - Regolith parameters estimated from figure if methods are accurately explained - Not peer reviewed journal
1 Very low	<ul style="list-style-type: none"> - Minor errors in units, etc. - Regolith only implicitly linked to values - Values estimated from figure - No explanation of methods

Tab. S 2: Database of regolith thickness and permeability in Africa including the source of data, the respective confidence level, the country where the study was conducted, methods used and sample size.

Source	permeability (m ²)			Thickness (m)			confidence level	country	methods	sample size
	min	mean	max	min	mean	max				
Abdulahi and Udensi 2008		-12.2					1	Nigeria	VES	60
Abdulrahman et al. 2016				1.4	11.0		4	Nigeria	VES	13
Adepelumi et al. 2006	-11.8	-11.8	-10.2				2	Nigeria	BH, DR, VLF -	

Aizebeokhai and Oyeyemi 2018				8.6	13.1	18.1	4	Nigeria	VES, ER	7
Akanmu and Adewumi 2016	-12.7	-11.5	-10.7	1.2	9.8	21.0	5	Nigeria	VES, ER	15
Alle et al 2017				10.0	38.5	64.0	4	Benin	m, ER	7
Armand 1987							5	Ghana	BH, PT	111
Asante-Annor and Ewusi 2011	-13.6	-12.3	-11.5	3.0		128	5	Burundi	VES, PT	41
Bakundukize et al. 2016							5	Nigeria	BH, PT	259
Bala et al. 2011	-13.6	-12.4	-11.5	20.0		50.0	3	Uganda	VES, ER	20
Batte et al. 2008	-13.9	-12.2	-11.5	1.0	15.2	30.0	3	Niger	BH	-
Carrier et al. 2008				12.0	23.0	33.0	4	Ghana	BH	13
Chilton and Foster 1993	-13.2		-12.2	13.0		22.0	4	Malawi; Zimba	PT, Lit	-
Chilton and Smith-Carrington 1984	-13.2		-11.8				3	Malawi ,Zimba	PT, BH	2
Courtois et al. 2010				0.1	23.0	105	5	Burkina Faso	BH	14645
Deyassa et al. 2014	-13.2		-11.2	10.0	38.3	90.0	2	Ethiopia	BH	1643
Dodds n.d.	-14.9		-11.9				1	Tanzania	ST	-
Edet and Okereke 2004		-12.1		3.8	38.0	89.5	4	Nigeria	BH, ER	90
Edet 2018	-14.1						3	Nigeria	Lit	5
El-Fahem 2008				3.0	19.1	47.0	3	Benin	BH, PT	-
Engalenc 1978	-12.5		-11.9				1	Burkina Faso	-	-
Fass 2004	-14.2		-13.6				3	Benin	PT	1
Forkuor et al. 2013				15.0		30.0	5	Ghana	BH	790
Foster 2012	-12.9		-11.6				3	tropical Africa	Lit	-
Gaspá et al. 2004	-12.5		-11.5	3.0	29.5	62.0	3	north Uganda	Lit	-
Hamidu et al. 2013	-13.3		-11.3				2	Nigeria	PT	25
Hector 2014	-14.6	-12.4	-11.7				3	Benin	MRS, ER	11
Holland and Witthüser 2011				15.0		50.0	4	South Africa	PT	>2500
Jacquín and Seygona 2004				3.0	16.2	30.0	1	Benin	-	-
Jayeoba and Oladunjoye 2015				3.2	5.5	13.1	4	Nigeria	ER	6
Jika and Mamah 2014	-13.1		-11.7	13.0	30.8	40.0	2	Nigeria	VLF, ER	-
Kortasi and Quansah 2004				11.1	20.5	51.2	3	Ghana	BH	-
Martin 2006	-12.6		-11.6				4	Ghana	BH	26000
Muchingami et al. 2012		-12.2			34.0		3	Zimbabwe	ER, VES	4
Muiuane 1999		-11.8		3.0		13.4	2	Nigeria	VES, ER, Lit	-
Nkotagu 1996	-12.0		-11.0	50.0	60.0	100	1	Taanzania	Lit	-
Nyende e al. 2013	-15.0		-11.0	5.5		35.0	3	Uganda	PT	8
Nyenje et al. 2013	-12.5		-11.5				3	Uganda	Lit	-
Olaniyan et al. 2010	-12.5			5.0	16.2	36.0	4	Nigeria	BH	91
Olayinka et al. 1999				0.1	19.2	70.0	3	Nigeria	VES, BH	179
Oluwafemi 2012				2.0	20.0	84.9	4	Nigeria	VES, VLF	14
Owen et al. 2007	-12.3		-11.7				4	Zimbabwe	ER	12
Owoade 1995	-12.9	-11.8	-11.1	2.0	16.0	45.0	3	Nigeria	PT	24
Owor 2010	-14.2		-13.4				4	Uganda	BH, VES, ER	37
Robins 1996	-13.2		-11.8	15.0		30.0	2	Malawi	BH	-
Sam 2013	-13.2		-11.9				3	Ghana; Burkina Faso, Uganda, Zimbabwe	Lit	-
Soro et al. 2017				22.0	37.6	49.0		Burkina Faso	ER	30

Sunmonu et al. 2012	-11.1	-10.9	-10.7	4.4	21.1	2	Nigeria	VES	10	
Taylor and Howard 2000	-13.3		-12.1	11.0	23.0	4	Uganda	PT, ST	40	
Tessema et al. 2014				1.7	12.2	46.2	5	Nigeria	BH	31
Tijani et al. 2010	-13.9		-12.2	12.1	87.0	5	Nigeria	BH	21	
Unicef 2009					24.5	4	Ivory coast	BH	-	
Vouillamoz et al. 2015				10.0	25.0	5	Benin	MRS	38	
Wright 1992			-12.2			4	Malawi, Zimbabwe	PT	>319	
Yidana et al. 2014	-12.4		-11.3	7.0	22.0	3	Ghana	m	-	
Yidana et al. 2015	-11.7		-11.6		25.0	3	Ghana	m, BH	-	

Note: BH: Borehole/well, PT: Pumping test, ST: Slug test, ER: electrical resistivity sounding, VES: vertical electrical sounding, MRS: magnetic resonance sounding, VLF: very low frequency survey, DR: direct current dipole-dipole resistivity, Lit: Literature review, m: calibrated model

References - Regolith permeability and thickness in Africa

- Abdulahi, N.K., Udensi, E.E., 2008. Vertical electrical sounding applied to hydrogeologic and engineering investigations: A case study of Kaduna polytechnic staff quarters. *Niger. J. Phys.* 20, 175–188.
- Abdulrahman, A., Shehu, A.D., Ibrahim, S., 2015. Using vertical electrical sounding for a groundwater potential map of ATBU Yelwa Campus, Bauchi, Nigeria. *JOLORN.* 17, 11-21.
- Adepelumi, A.A., Yi, M.-J., Kim, J.-H., Ako, B.D., Son, J.S., 2006. Integration of surface geophysical methods for fracture detection in crystalline bedrocks of southwestern Nigeria. *Hydrogeol. J.* 14, 1284–1306.
- Aizebeokhai, A.P., Oyeyemi, K.D., 2018. Geoelectrical characterisation of basement aquifers: the case of Iberekodo, southwestern Nigeria. *Hydrogeol. J.* 26, 651–664.
- Akanmu, T.O., Adewumi, A.J., 2016. Geophysical Characterization of Aquifer Parameters within Basement Complex Rocks Using Electrical Sounding Data from the Polytechnic, Ibandan, Southwestern Nigeria. *Int. J. Sci. Res. Knowl.* 112–126. <https://doi.org/10.12983/ijrsk-2016-p0112-0126>
- Alle, I.C., Descloitres, M., Vouillamoz, J.-M., Yalo, N., Lawson, F.M.A., Adihou, C., 2017. Why 1D electrical resistivity techniques can results in inaccurate siting of boreholes in hard rock aquifers and why electrical resistivity tomography must be preferred: the example of Benin, West Africa. *J. Afr. Earth Sci.* 139, 341–353.
- Armand, C., 1987. Actualisation de l'atlas des eaux souterraines du Niger. *Rapp. BRGM* 87.
- Asante-Annor, A., Ewusi, A., 2016. Hydrogeological Properties of the Rocks in Adansi Mining Area, Ghana. *Ghana Min. J.* 16, 31–39.
- Bakundukize, C., Mtoni, Y., Martens, K., van Camp, M., Walraevens, K., 2016. Poor understanding of the hydrogeological structure is a main cause of hand-dug wells failure in developing countries: A case study of a Precambrian basement aquifer in Bugesera region (Burundi). *J. Afr. Earth Sci.* 121, 180–199.
- Bala, A.E., Edivie, O.M., Byami, J., 2011. Borehole depth and regolith aquifer hydraulic characteristics of bedrock types in Kano area, Northern Nigeria. *Afr. J. Environ. Sci. Technol.* 5, 228–237.
- Batte, A.G., Muwanga, A., Sigrist, P.W., Owor, M., 2008. Vertical electrical sounding as an exploration technique to improve on the certainty of groundwater yield in the fractured crystalline basement aquifers of eastern Uganda. *Hydrogeol. J.* 16, 1683–1693.
- Carrier, M.-A., Lefebvre, R., Racicot, J., Asare, E.B., 2008. Groundwater recharge assessment in northern Ghana using soil moisture balance and chloride mass balance. *GeoEdmonton* 8, 1437–1444.
- Chilton, P.J., Foster, S.S.D., 1995. Hydrogeological characterisation and water-supply potential of basement aquifers in tropical Africa. *Hydrogeol. J.* 3, 36–49.
- Chilton, P.J., Smith-Carington, A.K., 1984. Characteristics of the weathered basement aquifer in Malawi in relation to rural water supplies. *IAHS Press.* 144, 57-72.

- Courtois, N., Lachassagne, P., Wyns, R., Blanchin, R., Bougaïré, F.D., Somé, S., Tapsoba, A., 2010. Large-Scale Mapping of Hard-Rock Aquifer Properties Applied to Burkina Faso. *Groundwater* 48, 269–283.
- Deyassa, G., Kebede, S., Ayenew, T., Kidane, T., 2014. Crystalline basement aquifers of Ethiopia: their genesis, classification and aquifer properties. *J. Afr. Earth Sci.* 100, 191–202.
- Dodds, J., Hall J., n.d. Groundwater Management Planning at an East African Gold Mine.
- Edet, A., 2018. Seasonal and spatio-temporal patterns, evolution and quality of groundwater in Cross River State, Nigeria: implications for groundwater management. *Sustain. Water Resour. Manag.* 1–21.
- Edet, A., Okereke, C., 2005. Hydrogeological and hydrochemical character of the regolith aquifer, northern Obudu Plateau, southern Nigeria. *Hydrogeol. J.* 13, 391–415.
- El-Fahem, T., 2008. Hydrogeological conceptualisation of a tropical river catchment in a crystalline basement area and transfer into a numerical groundwater flow model-Case study for the Upper Ouémé catchment in Benin (Doctoral dissertation, Allem. Univ. Bonn).
- Engalenc, C., 2009. Le patrimoine rural crée de l'emploi, Equal Départ France: réflexions et actions d'un réseau, in: *Landscape and Rural Heritage, Proc. of the Sixth Meeting of the Workshops of the Council of Europe for the Implementation of the European Landscape Convention* (Sibiu, Romania, 20-21 Sept 2007), European Spatial Planning and Landscape.
- Fass, T., 2004. Hydrogeologie im Aguima Einzugsgebiet in Benin/Westafrica (Doctoral dissertation, Allem. Univ. Bonn).
- Forkuor, G., Pavelic, P., Asare, E., Obuobie, E., 2013. Modelling potential areas of groundwater development for agriculture in northern Ghana using GIS/RS. *Hydrol. Sci. J.* 58, 437–451.
- Foster, S., 2012. Hard-rock aquifers in tropical regions: using science to inform development and management policy. *Hydrogeol. J.* 20, 659–672.
- Gaspá, M.M., Flynn, R., Zwahlem, F., Taylor, R., 2004. Use of Hydrochemical, Microbiological and Physical Monitoring to determine Contamination Mechanisms of Spring Water Discharge from a deeply weathered Regolith aquifer (Doctoral dissertation, University of Neuchâtel, Switzerland).
- Hamidu, H., Bala, A.E., Ikpokonte, A.E., 2013. Assessment Of Groundwater Potentials Of The Crystalline Aquifers Using Hydraulic Propertiesfor Gidanwaya Town And Its Environs, Southern Parts Of Kaduna State, North Western Nigeria. *Assessment* 3.
- Hector, B., 2014. Caractérisation hydrogéophysique multi-échelles et dynamique des stocks d'eau souterrains d'un bassin versant en zone soudanienne de socle: apport de la gravimétrie. Strasbourg (Doctoral dissertation, Straßbourg).
- Holland, M., Witthüser, K.T., 2011. Evaluation of geologic and geomorphologic influences on borehole productivity in crystalline bedrock aquifers of Limpopo Province, South Africa. *Hydrogeol. J.* 19, 1065–1083.
- Jacquin, F., Seygona, Z.Y., 2004. Contribution à l'étude du fonctionnement hydrodynamique des aquifères du bassin versant de la Donga. ORE AMMACATCH IRD Cotonou Bénin.
- Jayeoba, A., Oladunjoye, M.A., 2015. 2-D Electrical Resistivity Tomography for Groundwater Exploration in Hard Rock Terrain. *Int. J. Sci. Technol.* 4.
- Jika, H.T., Mamah, L.I., 2014. Application Of Electromagnetic Method And Electrical Resistivity Sounding In Hydrogeological Studies, A Case Study Of Vandeikya Area, Central Nigeria. *Int. J. Sci. Technol. Res.* 3, 179–190.
- Kortatsi, B.K., Quansah, J., 2004. Assessment of groundwater potential in the Sunyai and techiman areas of Ghana for urban water supply. *West Afr. J. Appl. Ecol.* 5.
- Martin, N., 2006. Development of a water balance for the Atankwidi catchment, West Africa: A case study of groundwater recharge in a semi-arid climate. Cuvillier. (Doctoral dissertaion, University of Göttingen).
- Muchingami, I., Hlatywayo, D.J., Nel, J.M., Chuma, C., 2012. Electrical resistivity survey for groundwater investigations and shallow subsurface evaluation of the basaltic-greenstone formation of the urban Bulawayo aquifer. *Phys. Chem. Earth Parts ABC* 50, 44–51.
- Muiuane, E., 1999. Hydrogeophysics of Tropical Africa: Recent advances and perspectives (Doctoral dissertation, Uppsala University).
- Nkotagu, H., 1996. Application of environmental isotopes to groundwater recharge studies in a semi-arid fractured crystalline basement area of Dodoma, Tanzania. *J. Afr. Earth Sci.* 22, 443–457.

- Nyende, J., Van, T.G., Vermeulen, D., 2013. Conceptual and Numerical Model Development for Groundwater Resources Management in a Regolith-Fractured-Basement Aquifer System. *J Earth Sci Clim Change* 4, 2.
- Nyenje, P.M., Foppen, J.W., Uhlenbrook, S., Lutterodt, G., 2014. Using hydrochemical tracers to assess impacts of unsewered urban catchments on hydrochemistry and nutrients in groundwater. *Hydrol. Process.* 28, 5860–5878. <https://doi.org/10.1002/hyp.10070>
- Olaniyan, I.O., Agunwamba, J.C., Ademiluyi, J.O., 2010. Assessment of aquifer characteristics in relation to rural water supply in part of Northern Nigeria. *Researcher* 2, 22–27.
- Olayinka, A.I., Abimbola, A.F., Isibor, R.A., Rafiu, A.R., 1999. A geoelectrical-hydrogeochemical investigation of shallow groundwater occurrence in Ibadan, southwestern Nigeria. *Environ. Geol.* 37, 31–39.
- Oluwafemi, O., 2012. The role of geophysics in the investigation of waste disposal site in Ikare-Akoko area, southwestern Nigeria. *Int. J. Sci. Emerg. Technol.* 4.
- Owen, R., Maziti, A., Dahlin, T., 2007. The relationship between regional stress field, fracture orientation and depth of weathering and implications for groundwater prospecting in crystalline rocks. *Hydrogeol. J.* 15, 1231–1238.
- Owoade, A., 1995. The potential for minimizing drawdowns in groundwater wells in tropical aquifers. *J. Afr. Earth Sci.* 20, 289–293.
- Owor, M., 2010. Groundwater-surface water interactions on deeply weathered surfaces of low relief in the Upper Nile Basin of Uganda. UCL (Doctoral dissertation, University College London).
- Robins, N.S., 1996. Malawi Community Schools Project review and recommendations on the most appropriate and cost-effective means of providing safe water points. BGS Technical Report WC/96/36C
- Sam, F., 2014. The assessment of potential impacts of open cast gold mining on the regional groundwater flow system in hard rock environments: with special reference to Ghana. University of Birmingham (Doctoral dissertation, University of Birmingham).
- Soro, D.D., Koïta, M., Biaou, C.A., Outoumbe, E., Vouillamoz, J.-M., Yacouba, H., Guérin, R., 2017. Geophysical demonstration of the absence of correlation between lineaments and hydrogeologically useful fractures: case study of the Sanon hard rock aquifer (central northern Burkina Faso). *J. Afr. Earth Sci.* 129, 842–852.
- Sunmonu, L.A., Adagunodo, T.A., Olafisoye, E.R., Oladejo, O.P., 2012. The groundwater potential evaluation at industrial estate Ogbomoso, Southwestern Nigeria. *RMZ–Materials Geoenvironment* 59, 363–390.
- Taylor, R., Howard, K., 2000. A tectono-geomorphic model of the hydrogeology of deeply weathered crystalline rock: evidence from Uganda. *Hydrogeol. J.* 8, 279–294.
- Tessema, A., Nzotta, U., Chirenje, E., 2014. Assessment of Groundwater Potential in Fractured Hard Rocks around Vryburg, North West Province, South Africa. *Water Res. Comm. Pretoria WRC Rep.* 13.
- Tijani, M.N., Alich, A.U., Seybatou, D., 2015. Characterization of weathered basement aquifers: implication for groundwater recharge. *Energy Sources Part Recovery Util. Environ. Eff.* 37, 1853–1860.
- Unicef, 2010. Etude De Faisabilite Des Forages Manuels Identification Des Zones Potentiellement Favorables, Rep. Republique Mali Mali.
- Vouillamoz, J.M., Tossa, A.Y.A., Chatenoux, B., Kpegli, K.A.R., 2015. Propriétés des aquifères de socle du Bénin: analyse multi-variables et multi-échelles des paramètres de contrôle Properties of Benin hard rock aquifers: multivariables and multiscale analysis of controlling parameters. *Aquifères Socle Point Sur Concepts Appl Opérationnelles» Roche-Sur-Yon.*
- Wright, E.P., 1992. The hydrogeology of crystalline basement aquifers in Africa. *Geol. Soc. Lond. Spec. Publ.* 66, 1–27.
- Yidana, S.M., Alo, C., Addai, M.O., Fynn, O.F., Essel, S.K., 2015. Numerical analysis of groundwater flow and potential in parts of a crystalline aquifer system in Northern Ghana. *Int. J. Environ. Sci. Technol.* 12, 3805–3818.
- Yidana, S.M., Fynn, O.F., Chegbele, L.P., Loh, Y., Obeng, M.A., 2014. Analysis of recharge and groundwater flow in parts of a weathered aquifer system in Northern Ghana. *J. Appl. Water Eng. Res.* 2, 91–104.

0.01	0.02	0.02	0.02	0.01
0.02	0.04	0.04	0.04	0.02
0.02	0.04	0.40	0.04	0.02
0.02	0.04	0.04	0.04	0.02
0.01	0.02	0.02	0.02	0.01

Fig. S 1: Matrix of weights, created for the purpose of this study to smooth aquifer thickness.

Supplement to chapter 4

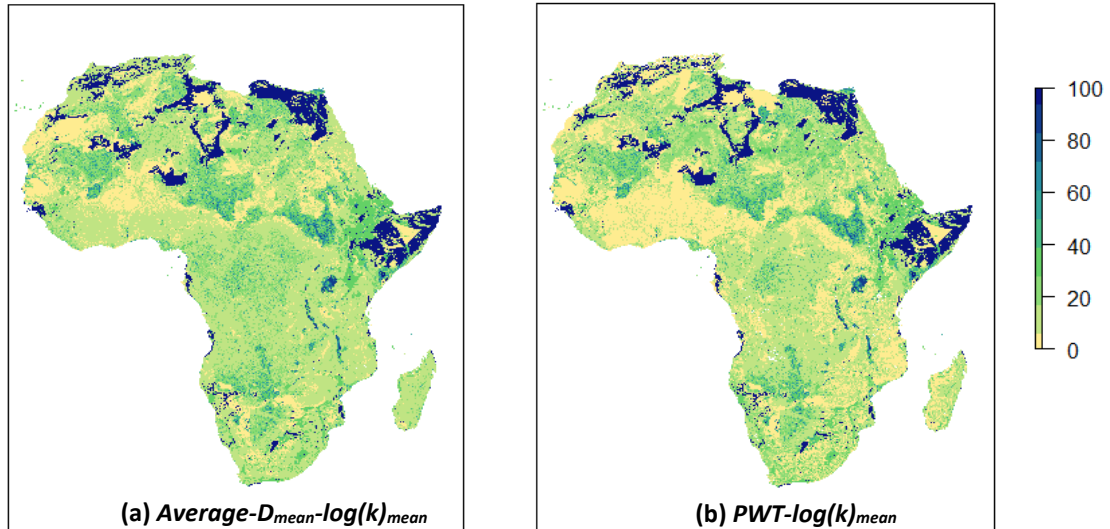


Fig. S 2: Transmissivity over Africa simulated with an additional regolith layer that was calculated according to (a) the average scenario with average transmissivity from literature (*Average-D_{mean}-log(k)_{mean}*) and (b) the permanent water table scenario with average permeability from literature (*PWT-log(k)_{mean}*).

Tab. S 3: Average transmissivity (T) over Africa for all tested regolith layers alone, combined with the underlying sediment/crystalline layer and the relative increase through the integration of the respective Regolith layer.

Regolith layer parametrization	T_{Regolith}	T_{new}	$T_{\text{No-Regolith}}$	T - increase
		(m ² d ⁻¹)		(%)
<i>Topography-D_{min}-log(k)_{min}</i>	0.2	31.9	31.8	0.6
<i>Topography-D_{min}-log(k)_{mean}</i>	1.8	33.6	31.8	5.7
<i>Topography-D_{min}-log(k)_{max}</i>	7.8	39.6	31.8	24.5
<i>Topography-D_{mean}-log(k)_{min}</i>	0.5	32.3	31.8	1.6
<i>Topography-D_{mean}-log(k)_{mean}</i>	5.2	37.0	31.8	16.4

<i>Topography-D_{mean}-log(k)_{max}</i>	22.7	54.6	31.8	71.4
<i>Topography-D_{max}-log(k)_{min}</i>	1.0	32.9	31.8	3.1
<i>Topography-D_{max}-log(k)_{mean}</i>	9.7	41.5	31.8	30.5
<i>Topography-D_{max}-log(k)_{max}</i>	42.3	74.1	31.8	133.0
<i>Average-D_{min}-log(k)_{min}</i>	0.2	32.0	31.8	0.6
<i>Average-D_{min}-log(k)_{mean}</i>	1.7	33.5	31.8	5.3
<i>Average-D_{min}-log(k)_{max}</i>	7.3	39.1	31.8	23.0
<i>Average-D_{mean}-log(k)_{min}</i>	0.5	32.3	31.8	1.6
<i>Average-D_{mean}-log(k)_{mean}</i>	4.9	36.7	31.8	15.4
<i>Average-D_{mean}-log(k)_{max}</i>	21.1	52.9	31.8	66.4
<i>Average-D_{max}-log(k)_{min}</i>	0.9	32.7	31.8	2.8
<i>Average-D_{max}-log(k)_{mean}</i>	9.1	40.9	31.8	28.6
<i>Average-D_{max}-log(k)_{max}</i>	39.3	71.1	31.8	123.6
<i>PWT-log(k)_{min}</i>	0.4	32.2	31.8	1.3
<i>PWT-log(k)_{mean}</i>	3.1	34.9	31.8	9.7
<i>PWT-log(k)_{max}</i>	14.0	45.9	31.8	44.0

Note: Indexed *Regolith* stands for the respective regolith layer alone, *new* for the overall aquifer parametrization including the regolith layer and *No-Regolith* for a one-layer aquifer parametrization without regolith.

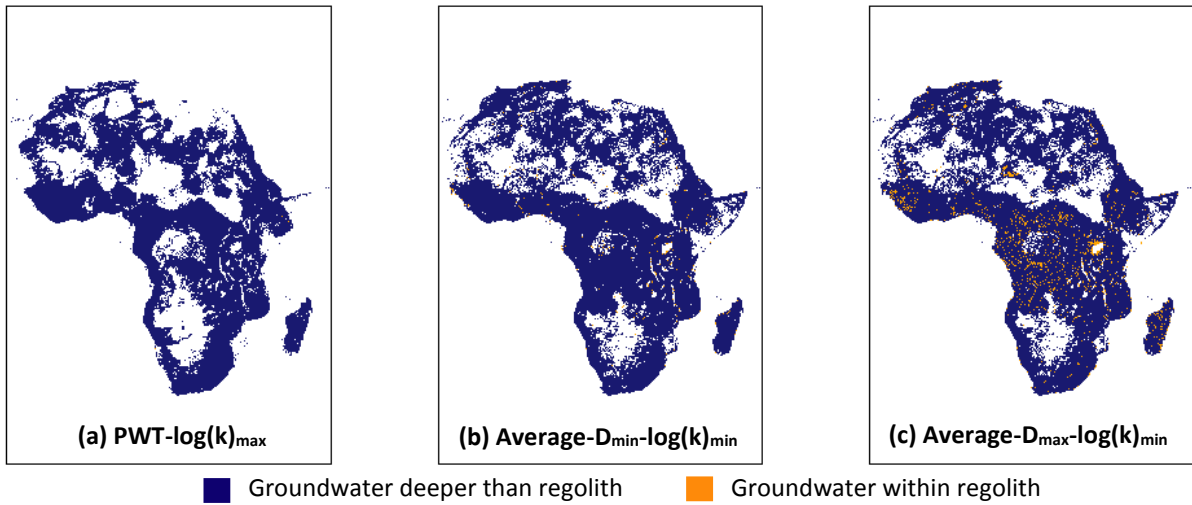


Fig. S 3: Proportion of regolith that was simulated to hold groundwater and of regolith where groundwater was simulated below the regolith layer.

List of abbreviations

Name	Unit	Abbreviation
Acceleration due to gravity on earth	(m s ⁻²)	g
Actual recharge	(m d ⁻¹)	Rch _{act}
Aquifer thickness	(m)	D
Average distance between rivers and streams	(m)	L

Average of lower limit regolith permeability from the literature review	(m ²)	log(k) _{min}
Average of lower limit regolith thickness from the literature review	(m)	D _{min}
Average of upper limit regolith permeability from the literature review	(m ²)	log(k) _{max}
Average of upper limit regolith thickness from the literature review	(m)	D _{max}
Average regolith permeability from the literature review	(m ²)	log(k) _{mean}
Average regolith thickness from the literature review	(m)	D _{mean}
Bankfull river discharge	(m ³ d ⁻¹)	Q _{bkfl}
Bed resistance	(d ⁻¹)	BRES
Channel longitudinal slope		SI
Coarse grained		c.g.
Coefficient of determination		R ²
Coefficient of variation		CV
Conductance	(m ² d ⁻¹)	c
Difference between surface and floodplain elevation	(m)	F()
Digital elevation model	(m)	DEM
Fine grained		f.g.
Fluid density	(kg m ⁻³)	ρ
Fluid viscosity	(kg m ⁻¹ s ⁻¹)	μ
Global hydrogeology maps	(m ²)	GLHYMPS
Global lithological map		GLiM
Global unconsolidated sediments map	(m ²)	GUM
Groundwater drainage, smaller streams and springs in the mountains	(m ³ d ⁻¹)	Q _{SI}
Groundwater drainage and river infiltration, total	(m ³ d ⁻¹)	Q _b
Groundwater drainage and river infiltration, large rivers	(m ³ d ⁻¹)	Q _{riv}
Groundwater drainage, small rivers	(m ³ d ⁻¹)	Q _{drn}
Hydraulic conductivity	(m d ⁻¹)	K
Internation Sientific Indexing		ISI
Inverse of the standard normal distribution		G ⁻¹ ()
Long-term averaged naturalized river discharge	(m ³ d ⁻¹)	Q _{av}
Manning roughness coefficient	(m ^{-1/3} d ⁻¹)	n
MODFLOW cell area	(°)	A _{MF}
Observed groundwater head	(m)	h _o
PCRaster global water balance		PCR-GLOBWB
Permanent water table scenario		PWT
Permeability	(m ²)	log(k)
potentiometric groundwater head	(m)	h
Projected grid cell area	(m ²)	A _{cell}
Recession coefficient	(d ⁻¹)	J
Recharge passed on to MODFLOW	(m d ⁻¹)	Rch _{inp}
River bottom	(m)	Riv _{bottom}
River head	(m)	Riv _{head}
River length	(m)	L _{riv}
River width	(m)	W _{riv}
Second version of global hydrogeology maps	(m ²)	GLHYMPS 2.0
Sedimentary is siliciclastic		sil.
Simulated groundwater head	(m)	h _s

Specific storage	(m)	S_s
Storage of groundwater above the surface elevation	(m)	$S_{3,flp}$
Time	(d)	t
Transmissivity	($m^2 d^{-1}$)	T
United States		U.S.
United States Geological Survey		USGS
United States Geological Survey modular hydrological model		MODFLOW
Vertical electrical soundings		VES
Volumetric groundwater flux	($m^3 d^{-1}$)	Q
Wetted perimeter at bankfull discharge	(m)	P_{bkfl}
Z-score		$Z()$

Ehrenwörtliche Erklärung

Hiermit erkläre ich, dass die Arbeit selbständig und nur unter Verwendung der angegebenen Hilfsmittel angefertigt wurde.

Freiburg i. Br., 12.08.2018